15. T. Von Karman and S.S. Penner, *Selected Combustion Problems, Fundamentals and Aeronautical Applications*, Scientific Publications, London, 1954, 5-41.
16. A.G. Gaydon and H.G. Wolfhard, *Proc. Roy Soc.* (*London*), 1949. Ser. A. 196: 105-113.
17. C. Tanford, *Third Symposium on Combustion, Flames and Explosion Phenomena*, Williams and Wilkins (Baltimore), 1949, 140-146.
C. Tanford, and R.N. Pease, *J. Chem. Phys.*, 1947, 15: 861-865.
C. Tanford, *J. Chem. Phys.*, 1947, 15: 433-439.
18. J.O. Hirschfelder, C.F. Curtiss and D.E. Campbell, *Fourth Symposium (International) on Combustion*, Williams and Wilkins, Baltimore, 1953, 190-211.
J.O. Hirschfelder, and C.F. Curtiss, *Third Symposium on Combustion, Flames and Explosion Phenomena*, Williams and Wilkins, Baltimore, 1949, 121-127.

# 10

# DETERMINATION OF BURNING VELOCITIES

Laminar burning velocity is as characteristic of a combustible mixture as the specific heat and thermal conductivity. It is considered an important tool for the understanding of several technical combustion processes. Studies in combustion are conducted in terms of laminar burning velocity, minimum ignition energy, flammability limits, and quenching distance. These have been verified as the fundamental properties of the combustible mixtures.

The aim of laminar flame research is a complete knowledge of the chemical kinetics of flame reactions. The science of combustion kinetics is not yet so developed as to be able to predict combustion reaction rates in advance. The most important result of laminar flame research is that the burning velocity is directly proportional to the square-root of the reaction rate constant which is almost unmeasurable by any other technique. Laminar flame studies also find their application in the turbulent combustion, flame stabilization, etc.

Unfortunately, the burning velocity of a combustible mixture cannot be measured directly. In this chapter we shall review the various methods of measuring burning velocity and the equations for calculating this property as proposed by several investigators.

## 10.1 DEFINITION OF BURNING VELOCITY

Burning velocity, commonly symbolized by $S_u$ (also referred to as laminar burning velocity, flame velocity or normal combustion velocity), is defined as the linear velocity of the flame front normal to itself and relative to the unburned gas. This definition refers to an infinite plane flame, i.e., the velocity is determined at some point beyond the influence of the flame,

More generally, burning velocity is defined as the volume of unburned gas consumed per unit time divided by the area of the flame front in which that volume is consumed.

According to Linnett[1], it is difficult to define the term burning velocity in a rigorous manner to fit any geometry of flame surface, and no definition free from all possible objections can be formulated. In general, the differences in the values of the burning velocities measured by different techniques can be reduced, and the results can be made to approximate the true burning velocity for a plane flame, if the volume flow rate of the unburned gas is divided by an area measured as near the low temperature of the flame as possible.

As per definition, burning velocity appears to be a simple parameter, but because of the practical difficulty in obtaining an infinite plane flame, it is difficult to measure it accurately. If the definition is applied to other flame shapes, the accurate measurement of the flame front surface area and/or the exact location of the flame front poses a problem. The values of burning velocity obtained by different workers using different techniques gave a wide variation in view of the difficulties stated above.

Andrews and Bradley[2] have suggested some correction factors for each of the methods of measuring burning velocity. These correction factors are obtained on the basis of theoretical considerations and give a common agreeable value of the burning velocity. We shall briefly discuss the criteria for each correction factor while describing the methods.

## 10.2 METHODS OF OBSERVING FLAME FRONT

The area of the flame front in a system will depend upon the particular surface that is observed and measured. The various methods of locating the flame front are discussed below.

### *Direct Photography*

Direct photography of the luminous zone has been used most frequently. The unburned gas side of this zone is taken as the location of the flame front which corresponds to the maximum temperature zone.

### *Schlieren Photography*

This gives the zone where the density gradient is a maximum or where the temperature gradient is most steep.



### *Shadow Photography*

Shadow photography is a rather difficult and some workers have shown this method to be unreliable and its use is not recommended. The outer black band is called the shadowgraph. The outer edge is not sharp but is coincident with the schlieren edge. The inner edge of the shadowgraph is quite sharp but it is a function of the distance between the photographic plate and the flame.

For a conical flame on a cylindrical burner, the relative positions of the three reaction zones as observed by different techniques, are shown in Fig. 10.1. There is universal agreement that schlieren photography gives the most accurate location of the reaction zone.

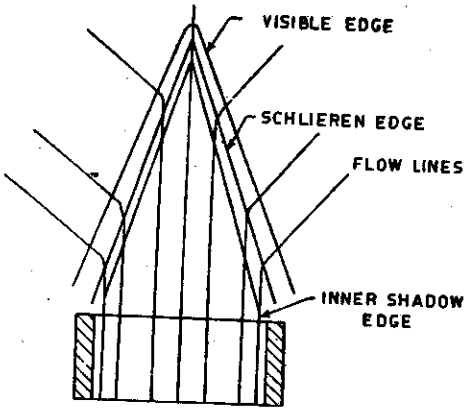


**Fig. 10.1 Comparison of luminous, schlieren, and shadow cones of a laminar flame (With permission of the Combustion Institute, from *Fourth Symposium (International) on Combustion*, 1953, p. 38).**

### *Particle Track Method*

This is used where very small non-volatile, non-reactive, and non-catalytic particles are observed floating in the combustible mixture and which are illuminated by an external source of light or by the flame itself. Pyrex, aluminium oxide ($Al_2O_3$), and magnesium oxide (MgO) particles are generally considered best for flame studies.

### *Ionization Gap Technique*

This is applied to non-stationary flames, e.g., flames which move in closed vessels or tubes which give time for travel of the flame front between two fixed points.

*Interferometry*

Gas density is a function of temperature. The measurement of density difference is easily possible by using an interferometer where a beam of light is split in two parts. The phase difference is obtained between the two beams, one passing through the flame and the other through the standard atmosphere. The resulting interference pattern can be interpreted quantitatively in terms of density.

*Temperature Measurement*

By the measurement of temperature with the help of micro-thermocouples, the location of reaction zone can be obtained. A contour map of various temperatures can be drawn for stationary flames.

Another difficulty arises in the accurate measurement of gas flow velocity. The total mass or volume flow can be measured quite accurately with the help of orifice flow meters, particle track method or micro-pitot tube measurement. Hot wire anemometery is suitable for local velocity measurements. For stationary flames, the particle track method gives accurate values of the magnitude and direction of gas flow, while hot wire anemometry is recommended for double flame kernels.

## 10.3 METHODS OF MEASURING BURNING VELOCITY

The methods of measuring burning velocity may be divided into two parts:

1. Methods using stationary flames.
2. Methods using non-stationary flames.

The methods using stationary flames employ burners of various shapes. Some common types in use are:

(i) Flat flame burner
(ii) Cylindrical burner
(iii) Slot burner.

The methods using non-stationary flames are:

(i) Tube methods
(ii) Constant pressure bomb method
(iii) Constant volume bomb method
(iv) Double flame kernel method.

A summary of the important methods of measuring laminar burning velocity is given in the Chart 1 on p. 210.

### Flat Flame Burner Method

Egerton and Powling[3] first constructed a flat flame burner as shown in



Fig. (10.2). The basic design of the burner used is still the same. A button shaped, i.e., a flat flame is obtained above the burner matrix. This shape

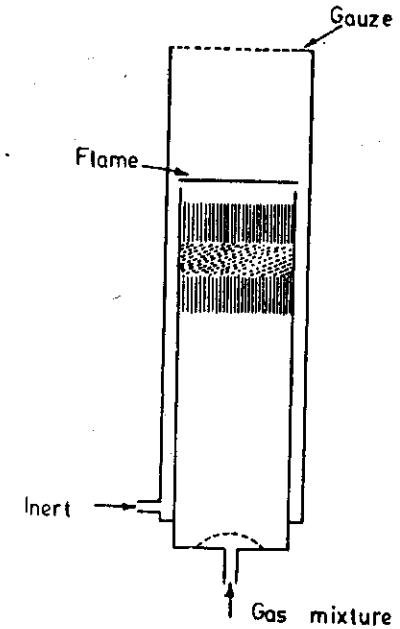


**Fig. 10.2 Flat flame burner (With permission of Pergamon Press, from J. Surugue (Ed.), *Experimental Methods in Combustion Research*, 1981, p. 15).**

is possible because of the constant velocity profile above the matrix. The limitation of this method is that a flat flame is obtained only for very low burning velocity mixtures, i.e., $S_u$ values of the order of 15-20 cm/s. This method is useful for measuring burning velocity of limit mixtures.

The source of error is that the edges of flame are not sharp. Thus there can be some argument about the correct diameter of the flame. Particle tracks have shown that some unburned mixture can escape due to the divergence of flow. There is also a loss of heat to the matrix which reduces the burning velocity. Due to the initial pre-heating of the mixture by the matrix, the temperature of the unburned gas is raised. The above two effects will try to compensate the error. As most of the literature on burning velocities deals with stoichiometric or maximum burning velocity mixtures, the results of flat flame burners which are generally for rich or lean mixtures cannot be compared with the data of other methods. Nevertheless, the flat flame is an ideal flame for the study of slow burning mixtures.

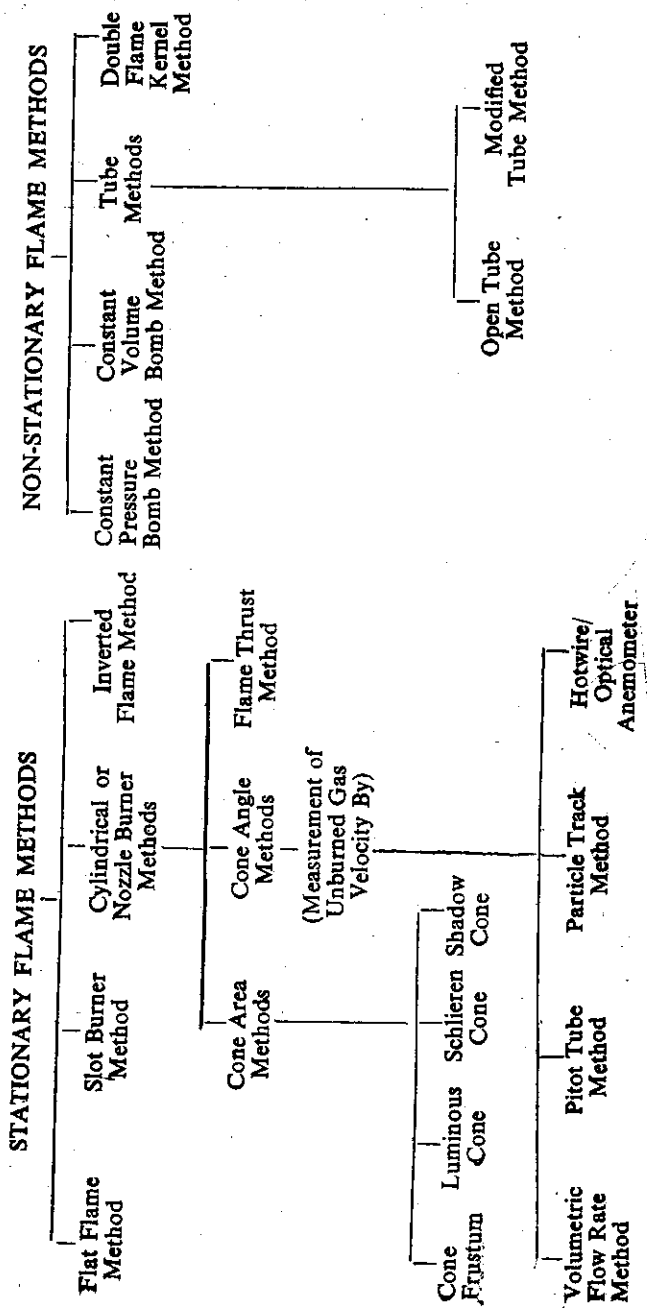


**Chart 1 Important methods of measuring laminar burning velocity.**



### Circular Tube, Nozzle and Slot Burner Methods

If a premixed mixture of fuel and air is passed through a cylindrical tube within certain velocities depending upon the air/fuel ratio and type of fuel, a stable flame is formed at the open end of the tube. Such burners are the simple bunsen burners. If the flow of mixture is laminar, a blue luminous conical flame front is observed, unless the mixture is very rich. Gouy[1] and Michelson[4] were the first to use this conical flame front to measure the burning velocity. They divided the volume flow rate of the unburned mixture by the area of the conical flame using the visible cone and assuming it to be a right circular cone with its base equal to the tube diameter. However, there will be an error in the calculated value because of the following reasons:

1. The cone produced will not be conical because the flow distribution across the tube is parabolic in nature with zero velocity at the burner wall to a maximum at the axis.
2. Due to preheating, the zone layer of measurable thickness, the inner cone is rounded off at the top, and at the base, the flame is a bit lifted and widened. This widening is approximately equal to the thickness of the preheating zone which is inversely proportional to flame velocity, varying from 0.5 mm for the methane-air mixture to about 0.05 mm for the hydrogen-air mixture. This thickness, being fixed, changes the flame velocity calculated on different diameter burners, the error being greater for small burners.
3. The burning velocity is assumed to be uniform along the entire flame front, while in actual practice, the value is quite low near the burner rim due to the quenching effect of burner walls and quite high at the tip due to excessive preheating of the mixture. Lewis and Von Elbe[5] obtained the variation of burning velocity across a cylindrical tube burner as shown in Fig. 10.3.
4. As a conical flame is obtained due to the concave curvature of the flame, the incoming cold mixture receives more heat than it would from a plane flame front. This increases the value of the burning velocity as its definition is for a plane flame front.
5. The location of the flame front is taken from the visible cone, while in actual practice the flame front is said to be located where the heating of cold stream starts. Thus the actual flame front will be located inside the visible cone.
6. It is assumed that only the premixed mixture enters the flame and no air enters from the atmosphere.

In spite of the above difficulties, the burner method is used quite extensively because the apparatus is simple, flexible, and the various parameters such as initial temperature, pressure, mixture composition, etc. can be controlled easily. The burners are modified and the measuring technique improved to remove a few sources of error, but it is still not

possible to get an ideal flame or the correct burning velocity from cylindrical burners.

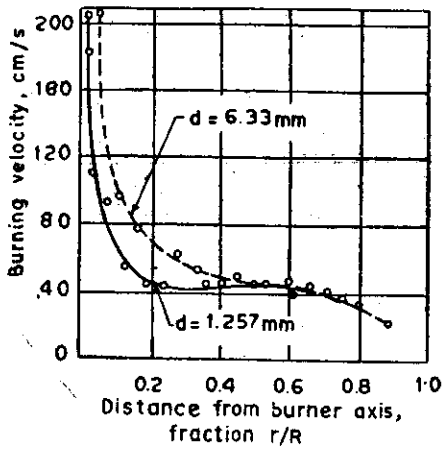


**Fig. 10.3 Variation of burning velocity across a cylindrical tube burner.**

The first difficulty can be somewhat removed by using a shaped nozzle such as the Mache-Hebra nozzle, or even a sharp-edged orifice with an area reduction greater than four. Such nozzles give uniform velocity distribution across the burner, except in very thin boundary layer zones near the rim. However, this uniform flow at the burner outlet again tries to become parabolic as the distance from the burner top increases, but at a small height above the burner port it can be safely said to be uniform. This results in a straight-edged cone along most of the flame front.

The second and third difficulties can be best removed if we take a frustum of the cone leaving the tip and base, i.e., measuring the area and flow across radii $r_1$ to $r_2$. Between these radii, we shall get a straight edge of right circular cone without errors in the flow and burning velocity at the tip and base. The difficulty with this partial area method is that there can be no accurate test to check that the area chosen is free from the tip and base effects. Also, the redistribution of the burned gas flow due to the pressure field set up by the flame makes it difficult to calculate the exact volume flowing through the area of the frustum. By using a large diameter burner the above difficulties can be minimized. However, by increasing the diameter the Reynolds number also increases, thus changing the flow from laminar to turbulent. For most hydrocarbons and for carbonmonoxide-air mixtures with flame velocities of about 30 to 80 cm/s, a burner diameter of 7 to 8 mm is found to be quite suitable. For acetylene-air and hydrogen-air mixtures, a burner with a diameter of 2 to 3 mm becomes necessary. With large diameter burners either the flow will become turbulent or the flame will flash back.



Regarding the fourth difficulty, i.e., of the flame curvature, Babkin et al.[6] have shown that curvature effects are quite important up to a radius of curvature of 3 mm. Thus, for 7 to 8 mm diameter burners with gradually reducing diameter of flame with height, the curvature effect will change the burning velocity. The effect will be quite appreciable for burners of 2 to 3 mm diameter as is essential for fast burning mixtures. Thus it is difficult to remove the curvature effects with a cylindrical burner. But this effect can be removed by using a rectangular slot burner instead of a circular one. By using a long (length at least three times the width) rectangular nozzle with constant velocity profile, a flat-sided inverted V-flame can be obtained, thus removing any curvature effects. However, the instability and wrinkling of flames occurs in slot burners making the measurement a bit complicated. Uberoi et al.[7] developed a two-dimensional flame on two small electrically heated ceramic tubes positioned along the edges of a rectangular port. This minimized the quenching effect and the flame approached a theoretical model. So far the slot burners have not been studied well enough to replace conventional cylindrical burners.

The fifth difficulty regarding the location of the flame front can be solved by using schlieren photography as the schlieren edge is found to be quite near the zone where the heating starts. It is better still to locate this cold gas zone by means of particle tracking, but proper care should be taken in choosing the right type, amount, and size of particles.

### *Methods for Calculating Flame Area and Burning Velocity*

Gouy first defined the burning velocity as

$$S_u = \frac{V_{f1}}{A_F} \tag{10.1}$$

where $V_{f1}$=volume flow rate of the unburned mixture consumed

$A_F$=flame front surface area.

Using a conventional cylindrical burner, different methods can be adopted to calculate the burning velocity. A few of these are as follows:

### Burner Methods

*(a) Total Area Method*

Assuming the cone to be right circular with base diameter equal to tube diameter (Fig. 10.4(a)) the burning velocity is given by

$$S_u = \frac{V_{f1}}{A_F} = \frac{U_{0,m}\, A_{\text{tube}}}{A_F} \tag{10.2}$$

where $U_{0,m}$=space mean velocity of approach flow in the tube, cm/s

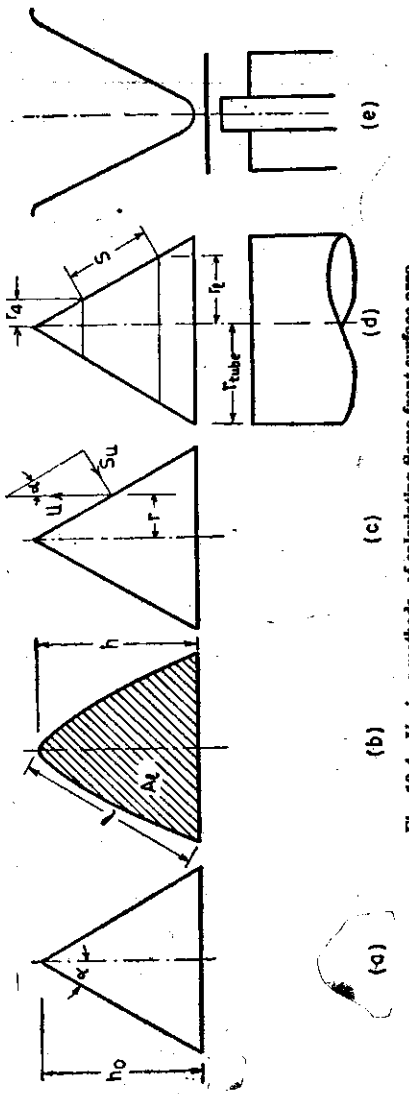


Fig. 10.4 Various methods of calculating flame front surface area.



$S_u$=burning velocity, cm/s

$V_{f1}$=volume flow rate, cm³/s

$A_F$=surface area of the cone, cm²

$A_{tube}$=cross-sectional area of the tube, cm²

$$A_F=r_{tube}^2\sqrt{r_{tube}^2+h^2}$$

where $h$=height of the cone, cm.

*(b) Total Area Method: Cone with Convex Edges (Fig. 10.4(b))*

Another good approximation for the area of the cone not having straight edges can be obtained by using the cross-sectional area of the cone as obtained by its image on a photographic plate or on any plane and calculating the area of surface as:

$$A_F=\frac{\pi A_1 l}{h} \tag{10.3}$$

where $A_1$=cross-sectional area of the cone, cm²

$A_F$=total surface area of the cone, cm²

$l$=slant height of the cone, cm

$h$=height of the cone, cm.

The cross-sectional area of the cone can be best determined by dividing the cone into a large number of segments or with the help of a planimeter. Few workers prefer to take the actual diameter of the cone instead of the tube diameter and apply method (a) or (c) for calculating the flame surface area.

*(c) Angle Method*

If the cone is assumed to be a straight-edged right circular cone (Fig. 10.4(c)), then the flame velocity can be computed by measuring the semi-cone angle between the direction of flow and the burning surface. This obviates the need for measuring or calculating the area of the flame surface, and the error due to the uncertain location of the flame zone is reduced. The burning velocity can be given by:

$$S_u=U_0 \sin\alpha \tag{10.4}$$

For a Poiseuille flow

$$U_0=\frac{2\,V_{f1}\left(r_{tube}^2-r^2\right)}{r_{tube}^4}$$

or

$$U_0=\frac{U_{0,m}\left(r_{tube}^2-r^2\right)}{r_{tube}^2} \tag{10.5}$$

where $U_0$=local approach velocity

$r$=radial distance from the tube axis to flame surface.

It is found that due to the cone not being a straight one, it is best to calculate the angle by drawing a tangent to the flame surface at a distance 0.707 $r_{tube}$ from the cone axis.

*(d) The Frustum Area Method (Fig. 10.4(d))*

As already explained, to remove the errors due to tip and base effects the frustum area method is used sometimes. The burning velocity for Poiseuile flow is expressed as:

$$S_u = \frac{2\,U_{0,m}\,(r_l - r_u)\left[1 - \dfrac{r_l^2 - r_u^2}{2\,r_{tube}^2}\right]}{S} \qquad (10.6)$$

where $r_u$ and $r_l$ are the radii of the upper and lower faces of the frustum and $S$ is the slant height of the frustum as shown in Fig. 10.4(d).

*(e) Inverted Flame Method*

A V-shaped flame was first produced by Gross[8] by stabilizing the flame on the tip of an axially mounted wire (Fig. 10.4(e)). This inverted flame reduced the base and tip effects of quenching and excessive heating. Gross calculated the burning velocity by taking the measurement of pressures and temperatures of flames and applying the equation of conservation of momentum across the plane.

Of the five methods discussed above, the total area method, using schlieren photographs and a nozzle burner, is the one most extensively used and gives good reproducible results. If it is assumed that the location of flame front corresponds to the cold gas cone, where the preheating of mixture starts, then there will be appreciable difference in the areas obtained by either schlieren or direct photography.

Figure 10.5(b) represents the relative position and shape of the two flame fronts. If the optically observed flame front is located at a distance

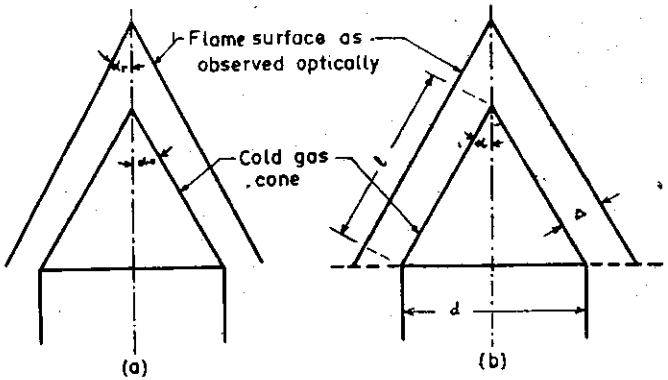


**Fig. 10.5 Relative position and shape of optically observed flame front and cold gas cone (With permission of Academic Press, from B. Lewis and G. Von Elbe, *Combustion and Flame*, p. 139).**



from the cold gas cone (Fig. 10.5(a)), then we can calculate the difference in the cone areas. Fristrom[9] assumed the two fronts to be parallel, i.e., the angle $\alpha$ to be the same for both cones. With this simple assumption the area ratio, i.e., of the optically observed cone $a_r$ to that of the cold gas cone $a_0$ will be written as:

$$\frac{a_r}{a_0} = 1 + \frac{\Delta}{l\tan\alpha} + \frac{\Delta\tan\alpha}{l} + \frac{2\,\Delta}{d\cos\alpha} + \frac{2\Delta^2}{l\,d\sin\alpha} + \frac{2\Delta^2\tan\alpha}{l\,d\cos\alpha} \qquad (10.7)$$

For a mixture of fuel and air with approximately 45 cm/s burning velocity on a 10 mm diameter burner, the ratio $a_r/a_0$ turns out to be 1.11 and 1.21 if the flame is observed by schlieren and luminous photography, respectively. Thus, if a flame is observed by schlieren photograph and the total area method is used to calculate $S_u$, the corrected value of the burning velocity is obtained by multiplying the factor 1.11. Similarly, if a luminous record is used with the total area method, the value of $S_u$ should be multiplied by the factor 1.21 to get the corrected value of $S_u$. It should be remembered that the above factors are for a particular value of burning velocity and burner diameter.

## Cylindrical Tube Method

Mallard and Le Chatelier[10] were the first to use the cylindrical tube method for the measurement of flame speed. They filled the mixture of fuel and air in a tube closed at one end and ignited the mixture at the open end. The flame travelled in the tube and its propagation was photographed. The flame speed was calculated by measuring the time taken by the flame to travel between two fixed points at a known distance. But the flame speed thus obtained was not the burning velocity because they did not consider the area of the flame front.

Later, Coward and Hartwell[11] not only measured the speed of propagation of the flame front in the tube but also calculated the flame area by taking the instantaneous photograph of the flame front at different angles. The rate of propagation of a flame in a tube can be obtained by either one of the methods given below:

1. By placing two ionization gaps, recording the movement of the flame front on a rotating drum, and calculating the flame speed with the help of the slope of the distance-time curve obtained.
2. By placing two photocells at some known distance and measuring the time between two pulses obtained on an oscilloscope.
3. By using high speed photography.

The tube method has the following drawbacks:

(i) Due to the quenching effect of the walls of the tube, the burning velocity is reduced.

(ii) Due to the convection current in the vertical tube, the rate of flame propagation is increased if the mixture is ignited at the bottom and

reduced if it is ignited at the top. If the tube is kept horizontal, the flame becomes hook-shaped and non-symmetrical along the axis, thus making it more difficult to get the exact area of the flame front.

(iii) Due to the reflected pressure waves produced by the movement of the flame front, the flame changes its shape while propagating.

(iv) The control of initial pressure and temperature is more difficult than in the burner method. The method can be conveniently used at atmospheric conditions.

A major advantage of the tube method is that the effect of the surrounding atmosphere due to diffusion is not present as in the case of the burner method. Also, the quantity of fuel required is very small as compared to the burner system. A few of the difficulties mentioned above have been overcome by using modified techniques. To overcome the effect of quenching by the tube walls, the burning velocity is calculated on various tube diameters. By increasing the tube diameter, a higher value of burning velocity is obtained. The value of the burning velocity can be extrapolated to an infinite tube diameter, thus nullifying the effect of wall quenching. However, with the increase in diameter, the flow of the unburned gas may become turbulent and may change the burning velocity. Care should be taken, therefore, to ensure that the burning velocity obtained is a laminar one.

To minimize the effect of convection, a horizontal tube is used instead of a vertical one. To obtain a stable shape of the flame, the tube length was reduced by Gerstein[12] and a small orifice was placed at the closed end of the tube and a large orifice was placed at the ingition end Guenoche et al.[13] measured the speed of gas flow in the unburned zone by measuring the rate of growth of a soap bubble through the orifice at the unburned end. It was found that the gas flow at the unburned end varies directly with the flame speed. The two orifices result in reduced presure waves reflected by the ends and a stable flame shape is thus obtained.

The Gouy's formula is again used to calculate the burning velocity. For a closed end tube and the mixture ignited at the open end, the equation for burning velocity will be written as:

$$S_u = \frac{a}{A} S_s \tag{10.8}$$

where $a$=area of cross-section of the tube

$A$=area of flame surface

$S_s$=flame speed, i.e., velocity of flame with reference to the tube.

As the unburned gas is stationary, the burning velocity obtained will be true. However, as with the closed end tube, the oscillations set in. Therefore, for a tube with an orifice at the further end, the burning velocity will be expressed as:

$$S_u = \frac{a}{A} (S_s - S_g) \tag{10.9}$$



where $S_g$ is the unburned mean gas velocity in the tube as measured from the growth of the soap bubble.

The measurement of the flame surface area, $A$ is a difficult task and may result in serious error in the value of the burning velocity. Henderson and Hill[14] have shown that some calculation may overestimate the area by as much as 20%. A simplified equation for calculating $A$ with the assumption that the flame is symmetrical and semi-ellipsoid is

$$A = \frac{2\pi (r_{cir}\, r_{ins} + r_{ins}\, r_{tube} + r_{cir}\, r_{tube})}{3} \tag{10.10}$$

where $r_{cir}$=radius of the circumscribed circle about the projected flame image, cm

$r_{ins}$=radius of the inscribed circle, cm.

Sometimes the area is calculated assuming the flame to be semi-spherical in shape. Another error is due to the wall quenching effect. If we assume that the burning velocity, $S_u$ is reduced in the thickness $l$ near the wall and the flame front is inclined at an angles $\alpha$ to the wall as shown in Fig. 10.6, the diameter of the unquenched mixture will then be $(d-2l)$ where $d$ is the diameter of the tube. The area of the flame front in this unquenched diameter will be

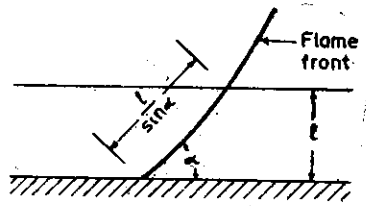


Fig. 10.6 Wall quenching effect on flame front (With permission of the Combustion Institute, from *Combustion and Flame*, 1972, 18: 141).

$$\{A - l\pi(d-\tfrac{1}{2})/\sin\alpha\} \tag{10.11}$$

With this modification, Eq. (10.8) becomes

$$S_u = \frac{\pi}{4} \frac{(d-2l)^2 S_s}{\{A - \pi l(d-\frac{1}{2}) \sin\alpha\}} \tag{10.12}$$

while Eq. (10.9) becomes

$$S_u = \frac{\pi}{4} \frac{(d-2l)^2 (S_s - S_g \mid a^2 - l^2 - 2al \mid /a^2)}{A - l(d-\frac{1}{2})/\sin\alpha} \tag{10.13}$$

Now, with a quenching distance of 0.085 cm for the methane-air flame in a 2.5 cm diameter tube, the approximate value of $\sin\alpha$ is 0.2 and the flame area is approximately 12.6 cm$^2$. The value of $S_u$ from Eq. (10.12) is 1.17 times that given by Eq. (10.8), and the value of $S_u$ from Eq. (10.13) yields a value 16% higher, i.e., 1.16 times than that given by Eq. (10.9). Thus a correction factor of 1.16 is obtained, considering the quenching effect for the methane-air flame. This correction factor improves the average burning velocity calculated along the cross-section of the tube to the true burning velocity. Laffitte and Combourieu[15] have concluded that the tube method is the best for mixtures which have burning velocities up to 80 cm/s. With slow burning mixtures the error increases, faster burning velocities result in unstable flame shapes, and the effect of turbulence increases the values of burning velocity.

**Constant Pressure Bomb Method (Soap Bubble Technique)**

The main disadvantage of the tube method is that the calculation of the exact flame area is difficult because of the unsymmetrical shape of the flame. The problem can be solved if we can obtain a flame of simple geometry. It is quite difficult to obtain a plane combustion wave for high velocity mixtures. The next simplest shape is a sphere. If a mixture is ignited by means of a spark, a spherical flame front propagates through the mixture and changes its shape to the shape of the vessel in which the mixture is enclosed. If the vessel is also spherical, the flame front will propagate in a spherical form up to the vessel wall. In a rigid vessel, the pressure and temperature of the unburned mixture will increase continuously as the flame will propagate, but if the container is elastic, then the expansion of the vessel will allow a flame front to move at constant pressure.

Stevens[16] and Fiock[17] developed this technique of measuring the burning velocity in a constant pressure elastic spherical vessel. A soap bubble is blown with the help of a combustible mixture which is ignited by means of spark at its centre. The soap bubble acts as a constant pressure bomb since the soap film can expand without any stress. The pressure of the mixture inside the bubble is the same as the outside ambient atmosphere. The rate of growth of the flame diameter is recorded on a rotating drum camera. Either direct or schlieren photography can be used. The slope of the V-shaped figure will give the rate of propagation of the flame front with reference to the laboratory frame of coordinates. The burning velocity can be calculated by using the equations derived later.

The main advantages of the soap bubble technique are that it requires a small amount of fuel, the shape of the flame front is spherical, the diffusion of the mixture to ambient atmosphere is less than in the open burner method, and exact mathematical analysis and calculations are possible.

The main disadvantages and difficulties are:

1. As the soap bubble always contains some liquid, the vapour of the liquid can mix with the combustible mixture and alter the value of burning velocity. The effect is more serious if water acts as an inhibitor or a catalyst.
2. The diffusion of the mixture through the soap bubble is possible and it can lead to serious error.
3. If the mixture is slow burning, then due to convection a non-spherical flame may develop.
4. At high velocities of expansion, the inertia of the bubble becomes important and a non-isotropic flame front is observed.
5. After the mixture has been burnt, it becomes quite difficult to measure the final diameter of the soap bubble.
6. A small quenching effect of spark electrodes and the bubble surface is present.



The first problem is substantially reduced by using a special glycerin-soap solution which has a very low vapour pressure at atmospheric temperature and pressure. The diffusion and vapour pressure effects are also eliminated by using transparent latex rubber balloons. If the time of ignition from the formation of the bubble is quite low and the diffusion coefficient of the mixture and ambient atmospheric pressure is also low, then the glycerol-soap bubble gives quite reliable and accurate values. Normally it takes 5 to 10 s to fire a mixture from the formation of the bubble. The diffusion will have a substantial effect in the case of $H_2$, He, and $CO_2$, but other gases do not diffuse much during this short period.

A spherical flame is obtained if the mixture is fast burning. However, a very fast burning mixture will set up a pressure field across the flame front which cannot be ignored and the assumption of constant pressure will become invalid. Flame thickness also affects results, and therefore, for a slow burning mixture this cannot be neglected. This method is found suitable for moderately fast mixtures only.

The measurement of the final flame size is still the main problem which leads to error. This is further aggravated by the appearance of cubes of diameter in the final expression for $S_u$. Thus a small error is cubed. After the combustion wave has propagated through the mixture, the burned gases expand. Therefore, the propagation rate of the recorded flame front will not be the true burning velocity. Assuming negligible flame thickness, the relationship between the burning velocity $S_u$ and flame speed $S_s$ can be easily derived as:

$$S_u \rho_0 = S_s \bar{\rho}_b \tag{10.14}$$

where $\rho_0$ = unburned gas density at the initial condition and

$\bar{\rho}_b$ = mean density of the burned gas

or $$S_u = \frac{\bar{\rho}_b}{\rho_0} S_s$$

where $$S_s = \frac{dr_b}{dt} \tag{10.15}$$

and $r_b$ is the radius of the boundary of burned gas.

$$\frac{\rho_b}{\rho_0} = E = \frac{V_f}{V_0} \tag{10.16}$$

where $E$ = the expansion ratio

$V$ = volume of mixture in the soap bubble.

The suffixes $f$ and 0 indicate the final and initial stages respectively. For a spherical bubble

$$E = \left(\frac{r_f}{r_0}\right)^3$$

$$S_u = \left(\frac{r_f}{r_0}\right)^3 S_s \tag{10.17}$$

In this equation the value of $r_0$ can be measured easily and $S_s$ can be obtained from the flame record. But due to after-burning, it is quite difficult to ascertain the final radius $r_f$. The boundaries of the soap bubble are also usually not clear in the photograph. To avoid this difficulty, few workers have assumed the final temperature to be the ideal adiabatic burned gas temperature, and calculated the final radius. However, in practice the final temperature is less than the ideal adiabatic temperature due to heat losses. Dixon-Lewis and Wilson[18], assuming that the temperature profile of the flame in a closed vessel is the same as in the burner method, found for the methane-air mixture with $r_b=2.5$ that

$$\frac{\rho_b}{\rho_u}=1.22\,\frac{T_u}{T_b} \tag{10.18}$$

where $T_u$ and $T_b$ are the unburned and burned gas temperatures respectively. Thus the value of $S_u$ calculated should be multiplied by 1.22 to get the exact value of burning velocity. The value of the correction factor increases with the increased thickness of flame front, i.e., with decreasing flame velocity. Thus for richer and leaner mixtures, the correction factor will have higher values.

### Constant Volume Bomb Method

This method is one of the most accurate and versatile methods because the control on various parameters, e.g., initial temperature, pressure, mixture strength, etc., is the easiest to manage in this method. However, due to its complex apparatus, measuring techniques, and mathematical equations, this method is not used as much as it should be.

In the constant volume bomb method, a spherical rigid glass or metallic vessel is filled with a combustible mixture which is then ignited by a controlled spark. Either the increase in pressure with time is recorded on an oscilloscope with the help of a pressure transducer and oscillograph record camera or a photographic flame record is obtained on a rotating drum camera. As the spherical combustion wave propagates through the mixture, the temperature and pressure of the unburned gas are also increased. However, the expansion of gas is not possible because of the rigid vessel. This method is found to be most suitable for fast burning mixtures and is recommended by Lewis and Von Elbe and others as a standard method against which the validity of other methods may be tested. To repeat, the main advantages are:

1. It requires only a small quantity of the fuel.
2. Mixture composition, initial pressure, temperature, and humidity can be easily controlled. Thus the effect of any one parameter on the burning velocity can be best studied by this method.
3. From a single flame record, several values of the burning velocity at different initial pressures and temperatures can be obtained.



4. For a large diameter bomb, the flame approaches the ideal one-dimensional flame with no interaction surface.
5. The method is self-corroborative.

The main disadvantages of the constant volume bomb apparatus are that it is quite expensive and complex. It needs lengthy and tedious calculations. The initial setting and adjustment of the apparatus for getting a spherical flame takes a long time. Even a slight change in the spark gap or the ignition energy may lead to non-spherical flame propagation. For slow burning mixtures, due to convective rise of hot gases, the shape of the flame front is not truly spherical. This difficulty is somewhat removed if we use the pressure record for the calculation of $S_u$ instead of the flame record.

Though in the constant volume bomb method the total volume of the mixture remains constant during the entire combustion process, the gas mixture cannot be said to be stationary during the period of flame propagation. As the flame front moves outwards from the centre of the sphere, the pressure inside the vessel increases continuously due to the expansion of the burned charge. This results in compression of the unburned charge which moves radially towards the sphere walls. But as the flame approaches the vessel walls, the expansion of gas near the walls takes place due to the burning of the charge. This results in gas flow towards the centre of the sphere. Because of this compression and expansion which take place during flame propagation the gas near the centre initially expands from its initial pressure. The same expanded gas is ultimately brought back to its initial volume, but the compression at the end is at a much higher pressure. Thus the energy lost during expansion is always less than the energy gained during compression, resulting in a gain of energy with the products being heated up in the end. Near the walls, the reverse takes place, i.e., the gas is compressed at a lower pressure and expanded at a higher pressure. The gas near the walls, therefore, looses, its energy and is cooled down. This results in a temperature difference from the centre of the sphere to the walls of the vessel. The difference in temperature may be of the order of several hundred degrees celsius.

Because of this changing pressure and temperature during flame propagation at every point, the initial condition at every point for the flame becomes different. Therefore, at every point the value of burning velocity, $S_u$ is different. This makes it very difficult to propose a single equation for the calculation of burning velocity. Burning velocity can be calculated either by using only the pressure record or the photographic record or flame propagation or both. The curve of pressure rise versus time may be obtained by using a sensitive pressure pick up—an oscilloscope instrumentation equipped with oscillograph record camera. A rotating drum camera may be used for the continuous recording of the flame growth with time.

Usually the calculation of burning velocity is limited to the pre-pressure, i.e., the period when only a small fraction of the charge is burned giving rise to pressure $P/P_i \leqslant 1.1$, i.e., there is only about 10 per cent rise in pressure during this period. The pressure may be, therefore, assumed to be constant and the equation used in the soap bubble technique for calculating $S_u$ may be applied. However, to utilize the full advantage of the constant volume method, more comprehensive and complicated equations have been used.

The basic assumptions in the derivation of burning velocity equations are:

1. The flame propagates spherically and isotropically.
2. The flame front is a surface of discontinuity across which the change from the unburned to burned state takes place. This implies that the thickness of the flame front is negligible or the mass fraction burning at any instant is negligible in comparison to the burned or the unburned charge. This is not true during the initial and final stages of propagation.

Because of the complex nature of the equation for burning velocity, various workers have proposed different forms of equations considering one or the other simplifying assumption. The equation can be derived either in terms of the unburned or burned charge. These two equations should yield the same value of burning velocity. But the value of $S_u$ is found to differ. This may be due to the systematic and other inherent errors in observation. A combined form of the equation will give better results.

Assuming that the mass fraction of the charge burned $n$ is given by

$$n=\frac{P-P_i}{P_e-P_i} \tag{10.19}$$

Lewis and Von Elbe[19] obtained the following equation:

$$S_u=\frac{R^3}{3r_b^2}\cdot\frac{\rho_i}{\rho_u}\cdot\frac{dn}{dt} \tag{10.20}$$

where $r_b=R\,[\,1-(1-n)\,\rho_i/\rho_u]^{1/3}$ (10.21)

Fiock and Marvin[20] derived two forms of burning velocity equations, viz.,

$$S_u=S_s-\frac{R^3-r_b^3}{3r_b^2\,\gamma_u\,p}\cdot\frac{dp}{dt} \tag{10.22}$$

and

$$S_b=\frac{1}{E}\left[S_s+\frac{r_s}{3r_b\,p}\cdot\frac{dp}{dt}\right] \tag{10.23}$$

The former equation is based on the properties of the unburned gas, while the latter is based on the properties of the burned gas in addition to the unburned gas properties.



Manton, Von Elbe, and Lewis[21] showed that the value of $S_u$ can be calculated by using the slope of flame radius-time record in conjunction with the thermodynamically computed value of the peak pressure $P_e$ reached after combustion. The following equation was derived:

$$S_u=\frac{dr_b/dt}{1+\{(P_e/P)-1\}/\gamma_u} \tag{10.24}$$

where $R$=radius of spherical vessel
$r$=flame radius at any instant of time
$\rho$=density
$N$=mass fraction of the charge burned
$\gamma$=ratio of specific heats
$P$=absolute pressure
$t$=time
$E$=expansion ratio and subscripts $u$ and $b$ indicate unburned and burned gas states
$S$ indicates spatial
$i$ indicates initial condition of unburned gas
$e$ indicates final condition of burned gas.

Equation (10.24) is valid for $n \leqslant 0.01$.

Eschenbach and Agnew[22] have proposed equations for the calculation of burning velocity from pressure-time and radius-time records of explosions in spherical vessels. They have shown that the use of conventional equations for the determination of burning velocities of fast-burning mixtures can lead to errors because of the effects due to the finite velocity of the propagation of pressure waves. This influence is shown to be appreciable whenever the spatial velocity of the flame front is greater than one-tenth of the velocity of sound in the unburned gas. They have also developed equations which allow for the effects of a non-uniform pressure distribution. Grumer, Cook, and Kubala[23] have shown that the value of mass fraction burned can be reduced to:

$$n=\frac{P-P_i}{P_i\,\gamma_u\,(E_i-1)} \tag{10.25}$$

where $P \leqslant 1.1\,P_i$ and $E_i\,(=m_{bi}\,T_{bi}/m_i\,T_i)$ is the expansion ratio for constant pressure burning at $P_i$ and $T_i$, and $m$ is number of moles. They claim that this equation enables $n$ to be calculated more reliably and accurately than from the Lewis and Von Elbe Eq. 10.19.

O' Donovan and Rallis[24] have derived the relation

$$n=\frac{P-P_i\,(T_u/T_i)}{P_e\,(T_b/T_e)-P_i\,(T_u/T_i)} \tag{10.26}$$

claimed to be valid throughout the process of combustion

where

$$T_u/T_i=\left(\frac{P}{P_i}\right)^{(\gamma_u-1)/\gamma_u} \tag{10.27}$$

$T_b$=mean temperature of the burned gas at time $t$

$T_e$=mean temperature of the burned gas at end of combustion.

Babkin, V'yun and Kozachenko[6] have determined the burning velocity over the initial section of the flame travel in a constant-volume bomb by using the ratio of the spatial velocity to the expansion ratio. The equation is:

$$S_u=\frac{S_u}{E_i} \tag{a}$$

where

$$E_i=\frac{\Sigma m_b\, T_b\, P_e}{\Sigma m_e\, T_e\, P_i} \tag{b}$$

The value of $E_i$ can be computed either thermodynamically or experimentally. They have shown that a linear relation exists between the coefficient of expansion and the relative end pressure:

$$E_i=a+b\,(P_e/P_i) \tag{c}$$

where $a$ and $b$ are the coefficients which are weakly dependent on the composition and state of the mixture. Their numerical calculations for the combustion process following constant pressure and volume for a wide range of mixture composition and other variables have shown that the relationship can be represented by the simple approximate formula:

$$E_i=0.85\,P_e/P_i \tag{d}$$

The maximum deviation of the coefficient of expansion ($E_i$) determined theoretically and by Eq. (d) is reported to be less than 6 per cent. The coefficient 0.85 shows that the ratio of the adiabatic flame temperature to the mean temperature of the combustion products at constant volume is an almost constant quantity, and since

$$\Sigma m_b \simeq \Sigma m_e$$
$$T_b/T_e \simeq 0.85 \tag{e}$$

The value of $S_u$ can thus be determined solely from the experimental data by using Eqs. (a) and (d).

Rallis[25] has derived three separate burning velocity equations referred to as the unburned gas, burned gas, and combined equations respectively.

*Unburned Gas Equation*

$$S_u=\left(\frac{\beta}{\beta'}\right)\left[\frac{dr_b}{dt}-\frac{R^3-r_b^3}{3r_b^2}\,\frac{d\beta}{dt}\right] \tag{10.28}$$

*Burned Gas Equation*

$$S_u=\left(\frac{\alpha}{\beta'}\right)\left[\frac{dr_b}{dt}+\frac{r_b}{3\alpha}\,\frac{d\alpha}{dt}\right] \tag{10.29}$$

*Combined Equation*

$$S_u=\frac{\alpha\beta}{\beta'}\left[\frac{dr_b}{dt}+\frac{r_b\beta\,(1-\alpha)}{3\alpha\,(\beta-\alpha)}\,\frac{d(\alpha/\beta)}{dt}\right] \tag{10.30}$$



where $\alpha$=ratio of the mean density of the burned gas to the initial density of mixture ($\bar{\rho}_b/\rho_i$)

$\beta$=ratio of the mean density of the unburned gas to the initial density of the mixture ($\bar{\rho}_u/\rho_i$)

$\beta'$=ratio of the unburned gas density immediately ahead of the flame front to the initial density of mixture ($\rho_u/\rho_i$).

In general, it should be unnecessary to calculate the mean values of the burned gas, temperatures, pressures, and molecular weight. Values immediately behind the flame front, calculated on the basis of chemical equilibrium in the region, may then be used in place of the mean values without causing significant error in $\alpha$. If the spatial velocity of the flame front is not very high, $\bar{\rho}_u=\rho_u$ (i.e., $\beta=\beta'$). Also, for the constant pressure experiments it can be shown for relatively slow flames, $\bar{\rho}_u=\rho_u$. Obviously, for $\beta=\beta'$, Eqs. (10.28) and (10.29) will reduce to:

$$S_u=\left[\frac{dr_b}{dt}-\frac{R^3-r_b^3}{3\,P\,\gamma_u\,r_b^2}\,\frac{dP}{dt}\right] \tag{10.31}$$

and

$$S_u=\frac{\rho_i}{\rho_u}\left[\alpha\,\frac{dr_b}{dt}+\frac{r_b}{3}\cdot\frac{d\alpha}{dP}\cdot\frac{dP}{dt}\right] \tag{10.32}$$

respectively.

Rallis and Tremeer[56] have developed another equation following the analysis on the lines given in Reference (8). The equation is:

$$S_u=\frac{\rho_i}{\rho_u}\left[\alpha\,\frac{dr_b}{dt}+\frac{r_b}{3}\cdot\frac{d\alpha}{dP}\cdot\frac{dP}{dt}\right] \tag{a}$$

where

$$\alpha=\frac{\bar{M}_b}{\bar{M}_e}\cdot\frac{\bar{T}_e}{\bar{T}_b}\cdot\frac{P}{P_e}$$

The value of $\alpha$ is unity at the end of the process. Any error in the determination of $\bar{M}_b$, $\bar{T}_b$ and $P$ tends to be cancelled out. In fact, the authors have suggested that it is unnecessary to calculate the mean values of the burnt gas temperature and molecular weight. Values immediately behind the flame front, calculated thermodynamically, can be used in place of the mean values without causing a sensible error in $\alpha$. As the variations in the values of $\bar{M}_b$ and $\bar{T}_b$ are relatively small and $\alpha$ is for all practical purposes proportional to $P$, we may write

$$\alpha \simeq \frac{P}{P_e}$$

Therefore,

$$\frac{d\alpha}{dP}\simeq\frac{1}{P_e}$$

Equation (a) can be reduced to a simpler form if the approximation in density ratio $\alpha\simeq P/P_e$ is used

$$S_u=\frac{P_i}{P_e\,(P/P_i)^{1/\gamma_u}}\left[\frac{dr_b}{dt}+\frac{r_b}{3P}\,\frac{dP}{dt}\right]$$

This equation uses both $P$–$t$ and $r_b$–$t$ records and is applicable for the major part of the combustion process. Sharma, Agrawal, and Gupta[57] have modified the Rallis and Tremeer's equation to eliminate the use of the flame radius-time record for calculating the burning velocity. Table 10.1 shows the salient features of some of the burning velocity equations discussed in the foregoing paragraphs.

The bomb method which only uses the pressure record may prove to be the most accurate method for determining burning velocities. The values obtained using flame record will again need a correction because of the finite thickness of the flame. A correction factor for the methane-air mixtures as discussed in the soap bubble method will be 1.22.

The constant volume bomb method is one of the potential methods for the measurement of burning velocity and the study of the effects of various variables. Further improvements on this technique have been made to simplify the calculations and to bring the flame to an ideal one dimensional flame. Bradley and Hundy[28] have used the constant volume method by measuring the gas velocity $S_g$ with the help of a hot wire anemometer, and the flame speed $S_s$ by one of the following methods: (i) recording the flame position by the vertical knife edge schlieren system, (ii) reflection plate schlieren interferometry, and (iii) Gayhart-Prescott fine wire schlieren interferometry.

However, the flame speed $S_s$ (also referred to as the spatial velocity) is not a unique property of a combustible mixture. It can be shown to be the sum af two velocities, namely the burning or transformation velocity ($S_u$) and the unburned gas velocity immediately adjacent to the flame front ($S_g$), i.e.,

$$S_s = S_u + S_g$$

or the burning velocity is calculated by:

$$S_u = S_s - S_g \qquad (10.33)$$

The main drawback of this technique is that due to the high temperature of the flame, the wire of the hot wire anemometer probe is fused, and the preparation and calibration of the wire for each explosion is not only difficult but can also induce error. An error of 2% in the measurement of the gas velocity can cause an error of about 10% in the calculation of the burning velocity. This method is specially useful for mixtures which have low burning velocities as in the case of limit mixtures where the convection causes unsymmetrical development of the flame. No correction factor is necessary for this method.

### Double Flame Kernel Method

Flame kernels were used for the study of ignition and flame stabilization, but usually, because of their non-spherical shape, they were not used for



the calculation of burning velocities. Bolz and Burlage[27] tried to measure the burning velocity using flame kernels. The main disadvantage in this is that of the non-spherical flame shape. The advantage of the method is that the effect of the spark electrode is eliminated as the kernel is developed in a moving stream of the mixture. However, this is swept downstream as it grows. The necessary precaution is that the flow should remain laminar. During the growth of the kernel the gas cannot be said to be stationary with respect to the flame as the burned charge expands.

To overcome this difficulty, Raezer and Olsen[28] developed a unique process. They ignited the mixture simultaneously at two points and photographed the development of kernels. Since the gas velocity on the axis of centers must be zero, assuming the two kernels to be symmetrical, the speed along this axis tends to be equal to the burning velocity as the two kernels approach each other. The advantage of this method is that no auxiliary measurement is required, and the approaching flame assumes a shape quite near the ideal flat flame. It requires a small amount of the combustible mixture and the values of the burning velocity obtained agree well with the values obtained by other methods.

Andrews and Bradley[29] further improved upon the technique of Raezer and Olsen by developing double kernels in closed vessels. The ignition circuit was also improved, because the success of this technique largely depends upon the simultaneous ignition at two points. Even if the two sparks are ignited by a single circuit, the two spark gaps being placed in series can cause sufficient delay in the ignition timing between the two sparks. This action will produce two kernels which may not be symmetrical. For the methane-air mixture with a flame speed of 260 cm/s a time lag of 2 ms can produce a flame of 1.04 cm diameter when the second spark will pass. If the flame kernels are not symmetrical and are unequal in size, they will not produce a flame similar to the ideal flat

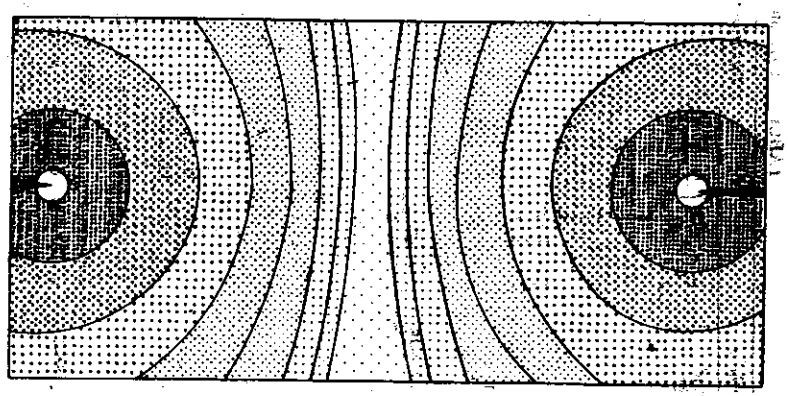

Fig. 10.7 Approaching flame front in a double kernel method.

**TABLE 10.1 Laminar Burning Velocity Equations for Combustion in a Spherical Bomb**

| *Authors* | *Equation* | *Experimental* | *Computed* | *Remarks* |
|---|---|---|---|---|
| Lewis and Von Elbe | $S_L=\frac{dr_f}{dt}\left(\frac{r_f}{r_b}\right)^3\left(\frac{P_f}{P}\right)^{1/\gamma_u}$<br>$r_f=R\left[\frac{P-P_i}{P'_e-P_i}\right]^{1/3}$<br>$r_b=R\left[1-\frac{P_i T_u P'_e-P}{PT_i P'_e-P_i}\right]^{1/3}$<br>$\frac{T_u}{T_i}=\left[\frac{P}{P_i}\right]^{(\gamma_u-1)/\gamma_u}$ | $p$–$t$ record | Thermodynamically computed equilibrium pressure $P_e'$ | Valid only in the initial range |
| Manton, Von Elbe and Lewis | $S_L=\frac{dr_b/dt}{1+\left[\frac{P'_e}{P}-1\right]/\gamma_u}$ | $r_b$–$t$ record | Thermodynamically computed equilibrium pressure $P_e'$ | Valid only when the mass fraction burned is less than 0.01 |
| Babkin, V'yun and Kozachenko | $S_L=\frac{dr_b/dt}{E_i}$<br>$E_i=0.85\ \frac{P_e}{P_i}$ | $r_b$–$t$ record | $E_i$ | Valid only in the initial range |
| Rallis | $S_L=\alpha\frac{\beta}{\beta'}\left[\frac{dr_b}{dt}+\frac{r_b\beta\,(1-\alpha)\,d\,(\alpha/\beta)}{3\alpha\,(\beta-\alpha)\,dt}\right]$<br>$\beta=\frac{\rho_u}{\rho_i},\ \beta'=\frac{\rho_u}{\rho_i}=\left[\frac{P}{P_i}\right]^{1/\gamma_u}$<br>$\alpha=\frac{\rho_b}{\rho_i}=\frac{M_b T_e P}{M_e T_b P_e},\ r_b=R\left[\frac{\beta-1}{\beta-\alpha}\right]^{1/3}$<br>Since $\alpha$ versus $P$ is linear, $\frac{d\alpha}{dP}=\frac{M_b T_e}{M_e T_b P_e}$<br>The equation in the simplified form, assuming uniform gas density distribution, i.e. $\beta=\beta'$, is<br>$S_L=\alpha\left[\frac{dr_b}{dt}+\frac{r_b}{3P}\left(\frac{\gamma_u-1}{\gamma_u}\right)\left(\frac{1-\alpha}{\beta-\alpha}\right)\frac{dP}{dt}\right]$ | $p$–$t$ and $r_b$–$t$ records | $\gamma_u$, $p_u$, $\alpha$ and $\beta$ | Valid for the major part of the combustion process |
| Rallis and Tremeer | $S_L=\frac{P}{P_e\,(P/P_i)^{1/\gamma_u}}\left[\frac{dr_b}{dt}+\frac{r_b}{3P}\frac{dp}{dt}\right]$<br>$\alpha=P/P_e$ | $p$–$t$ and $r_b$–$t$ records | $(\alpha=P/P_e)$, $\gamma_u$ | Valid for the major part of the combustion process |
| Sharma, Agrawal, and Gupta | $S_L=\frac{R\alpha}{3P\beta}\left[\frac{\beta\,(1-\alpha)/\gamma_u+\alpha\,(\beta-1)}{(\beta-\alpha)^2\,[(\beta-1)/(\beta-\alpha)]^{2/3}}+\left(\frac{\beta-1}{\beta-\alpha}\right)\right]^{1/3}\frac{dp}{dt}$<br>$\beta=\bar{\rho}_u/\rho_i;\ \beta'=\rho_u/\rho_i=(P/P_i)^{1/\gamma_u}$<br>$\alpha=\bar{\rho}_b/\rho_i=M_b\,\bar{T}_e\,P/M_e\,T_b\,P_e$<br>$r_b=R\,[(\beta-1)/(\beta-\alpha)]^{1/3}$ | $p$–$t$ record | $\alpha$, $\beta$, $\gamma_u$ | Valid for the major part of the combustion process from and above $P/P_i=1.01$<br>$\beta=\beta'$ assumed |

flame. Figure 10.7 shows the two flame kernels approaching each other.

The double flame kernel technique needs further development and may prove to be an accurate and easy method. It does not require any correction factor.

### Flame Thrust Method

So far, in our discussion of the various methods of measuring burning velocity, we have assumed that the pressure of the gas behind and ahead of the flame front remains the same, but this is not true. The pressure difference may be negligible for slow burning mixtures (about 0.01 cm of water for methane-air mixture), but is appreciable for fast burning mixtures. For the propane-oxygen mixture with burning velocity of the order of 200 cm/s, it comes out to be approximately 1.45 cm of water. For the acetylene-oxygen mixture it will be much higher. The pressure difference is set up because of the sudden heating, expansion, and acceleration of gases at the flame front. For a burner cone this difference between the unburned gas inside the cone and that of the burned gases outside is given as:

$$P_i - P_f = \rho_i S_u^2 (\rho_i/\rho_f - 1) \qquad (10.34)$$

where $i$ stands for the initial condition and $f$ for the final condition. To use this equation accurate values of the difference of pressure and densities are needed. The density calculation or measurement is not difficult, but the measurement of pressure is a bit difficult. In order to obtain a laminar flame for fast burning mixtures, small burners are required. In a small burner, the wall affects the burning velocity appreciably. Also, even a small pressure probe will disturb the flow pattern. The value of the pressure difference will give the average burning velocity, not accounting for the base or tip effects. With the development of any sensitive pressure measuring apparatus as the one developed by Payne and Weinberg[30] for studying electric wind effects in flames, which can measure pressure difference of the order of $10^{-3}$ cm of water, this technique can also be used for slow burning mixtures.

## COMPARISON OF BURNING VELOCITIES

The various methods used for the measurement of burning velocities have a few inherent defects which give rise to different values of burning velocities. Fortunately, most of the workers have preferred methane and propane as fuels for flame studies. This in turn has made it easy to compare the values of burning velocity obtained by different methods. Andrews and Bradley, in a critical review on the determination of burning velocities, have proposed a few correction factors. It is worthwhile to



reproduce the table given by them[2]. Table 10.2 shows the values of maximum burning velocities determined by different methods and the agreeable values obtained after applying the correction factors. They have also taken the values obtained by different workers working on the same type of apparatus so that the effect due to various measurement errors may be observed and the average of these may give an idea of the correct value.

**TABLE 10.2 Experimental and Corrected Values of Maximum Burning Velocity for Methane-Air Mixture (With Permission of the Combustion Institute, from *Combustion and Flame*, 1966, 10: 360)**

| *Authors* | *Method* | *Correction factor* | *Experimental $S_u$ at 298 K*, cm/s | *Corrected $S_u$ at 298 K*, cm/s |
|---|---|---|---|---|
| Gerstein et al. | Tube, orifices both ends | 1.16 | 33.8 | 39.2 |
| Egerton and Lefebvre | Tube, open ignition end | 1.17 | 37.5 | 43.9 |
| Henderson and Hill | Tube, orifice both ends | 1.16 | 37.8 | 43.9 |
| Manton et al. | Bomb | 1.22 | 37.0 | 45.2 |
| Manton and Milliken | —do— | 1.22 | 36.8 | 44.9 |
| Smith and Agnew | —do— | 1.22 | 37.5 | 45.8 |
| Agnew and Graiff | —do— | 1.22 | 34.5 | 42.1 |
| Karpov and Sokolik | —do— | 1.22 | 36.0 | 43.9 |
| Babkin | —do— | 1.22 | 32.0 | 39.1 |
| Straurs and Edse | Soap bubble | 1.22 | 34.0 | 41.5 |
| Bolz and Burlage | Flame kernel | 1.22 | 36.5 | 44.6 |
| Gerstein et al. | Burner, inner luminous total area | 1.21 | 33.3 | 40.3 |
| Dixon, Lewis and Wilson | —do— | 1.21 | 37.0 | 44.8 |
| Diederichsen and Wolfhard | —do— | 1.21 | 39.0 | 47.2 |
| Rosser et al. | —do— | 1.21 | 38.6 | 46.7 |
| Barassin et al. | —do— | 1.21 | 37.7 | 45.6 |
| Dugger | Burner inner shadow total area | 1.14 | 37.8 | 43.1 |
| Clingman et al. | —do— | 1.14 | 40.5 | 46.1 |
| Gilbert | —do— | 1.14 | 38.0 | 43.3 |
| Morgan and Kane | Nozzle burner, schlieren total area | 1.11 | 40.0 | 44.4 |
| National Bureau of Standards | —do— | 1.11 | 38.1 | 42.3 |
| Halpern | —do— | 1.11 | 37.4 | 41.5 |
| Fells and Rutherford | —do— | 1.11 | 39.6 | 44.0 |
| Lindow | Nozzle burner, schlieren particle track | — | 44.8 | 44.8 |
| Reed et al. | —do— | — | 44.7 | 44.7 |
| Andrews and Bradley | Bomb gas velocity by hot wire anemometry | — | 46.0 | 46.0 |

The observed change of burning velocity with the flame from curvature has been accounted for quantitatively by Fristrom[55] who has shown that when properly defined, the burning velocity (rather normalized burning velocity $S_u^*$ proposed by Fristrom) is independent of the flame front curvature, and depends only on the initial state of the gas mixture, viz., pressure, temperature, and composition.

The normalised burning velocity, $S_u^*$ is expressed as

$$S_u^* = S_u A_o \tag{10.35}$$

where $S_u$ is the measured burning velocity. $A_o$ is the stream tube area ratio, a geometric factor which is the ratio of the stream tube area at the inlet temperature to that at the point of the initial reaction. This is a parameter which depends on the flame geometry and can be determined by the direct detailed measurement of the flame front microstructure. $S_u^*$ corresponds to an ideal one dimensional flat flame ($A_o=1$). Table 10.3 shows the relationship between the measured and normalised burning velocity for flames of different geometry.

**TABLE 10.3 Some Examples of Measured and Normalized Burning Velocity**
(From R.M. Fristrom, *Physics of Fluids*, 1965, 8:274)

| *Flame* | *Geometry* | *P* atm | $A_o$ | $S_u$ (*T*) cm/s | $S_u^*$(300K) cm/s |
|---|---|---|---|---|---|
| 0.078 $CH_4$–0.92 $O_2$ | Flat | 0.1 | 0.971 | 62(315) | 52 |
| 0.078 $CH_4$–0.92 $O_2$ | Spherical | 0.1 | 0.713 | 92(375) | 52.5 |
| 0.078 $CH_4$–0.92 $O_2$ | Flat | 0.05 | 0.935 | 93(400) | 65 |
| 0.078 $CH_4$–0.92 $O_2$ | Spherical | 0.05 | 0.718 | 93(372) | 54 |
| 0.04 $C_3H_8$–0.96 Air | Conical | 0.25 | 0.878 | 52(315) | 44 |
| 0.04 $C_3H_8$–0.96 Air | Button | 0.25 | 0.878 | 52(315) | 44 |
| 0.031 $C_2H_2$–0.97 $O_2$ | Flat | 0.1 | 0.961 | 71(300) | 68 |
| 0.039 $C_2H_4$–0.96 $O_2$ | Flat | 0.1 | 0.952 | 71(300) | 68 |
| 0.043 $C_2H_6$–0.96 $O_2$ | Flat | 0.1 | 0.961 | 71(300) | 68 |

## 10.5 FACTORS AFFECTING BURNING VELOCITY

Various physical and chemical factors are known to affect the laminar burning velocity. The physical variables are: temperature, pressure, electric field, acoustical, and mechanical disturbance. The chemical variables are: fuel–oxidant ratio, inert admixtures, chemical additives, and the effect of the hydrocarbon structure.

### Temperature Dependence of Burning Velocity

The effect of the initial temperature, i.e., preheating of the gas mixture was studied by many workers. The burning velocity was found to increase



appreciably with temperature for the entire range of composition and for all hydrocarbons. Passauer[31] gave burning velocity for various initial temperatures and compositions. In his experiment the highest initial temperature for the methane–air mixture was 680°C. From the data obtained he proposed an empirical law:

$$S_u = aT_i^2 \tag{10.36}$$

which when written in terms of the mass burning velocity $m$ defined as the amount of substance in grams ignited per unit surface area of the flame per unit time (gm/cm² s), can be expressed as

$$m = bT_i \tag{10.37}$$

where $m = S_u \frac{P_i}{RT_i} aT_i^2 \frac{P_i}{RT_i} = bT_i$

When Passauer drew the graph between $m$ and initial temperature, he found a set of straight lines with different slopes for each hydrocarbon, which when extrapolated converged at approximately the same point near −273°C intersecting the abscissa as shown in Fig. 10.8. But these results

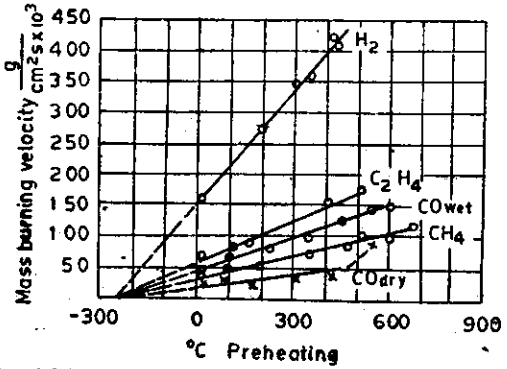


**Fig. 10.8 Mass burning velocity of various fuel-air mixtures as a function of degree of preheating.**

for simple hydrocarbons, gave the exponent of $T$ for heavier hydrocarbons to be lower. Heimel and Weast[32] expressed their observations in the form:

$$S_u = B + CT_i^n \tag{10.38}$$

where $B$, $C$ and $n$ are empirical constants, the value of $n$ lying between 2 and 3.

Assuming the burning velocity relative to an arbitrary value of 100 at 25°C and 1 atm pressure, Dugger[33] proposed the following relations:

For methane-air mixtures in the temperature range of 141–615 K

$$S_u = 24 + 0.47 \times 10^{-3}\, T^{2.11} \tag{10.39}$$

For methane-air mixtures in the temperature range of 200 to 617 K

$$S_u = 16 + 4.05\, T^{1.74} \tag{10.40}$$

and for propane-air mixtures in the temperature range of 200 to 617 K

$$S_u = 25 + 0.85T^2 \tag{10.41}$$

Andrews and Bradley[47] have suggested the following relation for the methane-air mixtures at 1 atm pressure:

$$S_u = 10 + 0.000371\ T_u^2 \text{ cm/s} \tag{10.42}$$

If a hydrocarbon-air mixture is preheated over 800 K, the preflame reactions may occur which reduce the burning velocity. Kuehl[34] observed that the point of maximum burning velocity shifts to less rich mixtures with increasing temperatures. Dugger, Weast and Heimel[35] reported that if the gas is kept preheated for a longer time the burning velocity is decreased.

### Pressure Dependence of Burning Velocity

Considerably more work appears to have been done on the pressure than on the temperature dependence of burning velocity. Much controversy apparently exists regarding the dependence of burning velocity on pressure, particularly with fuel–air mixtures. In general, however, the results indicate an increase of burning velocity with reduction in pressure. The existence of a maximum burning velocity at a pressure of approximately 300 mmHg has also been reported on more than one occasion. On the other hand, Manton and Milliken[36] suggest pressure dependence to be a function of the absolute value of the burning velocity, and indicate the existence of a critical burning velocity, above which the pressure dependence is positive and below which it is negative.

Ubbelohde and Koelliker[37] appear to have been the first to provide experimental evidence of the dependence of burning velocity on pressure. Using a burner with various mixtures over the pressure range of 1 to 4 atm, they found the burning velocity to increase with a reduction in pressure. Hydrogen-oxygen mixtures proved to be an exception to this rule. Carbon monoxide-air mixtures appeared to have a maximum burning velocity at 300 mmHg. Wolfhard[38] measured the burning velocity of acetylene-oxygen mixtures by the total area method between 10 and 760 mmHg. In the range for which the measurements are reliable, $S_u$ was found to be constant with a decrease in pressure up to 10 mmHg. Gilbert's[39] results for both acetylene-oxygen and propane-oxygen at lower pressures (down to 3 mmHg) are affected by the flame shape and depend on burner size, but do not indicate any appreciable variation in burning velocity with pressure for these flames.

For methane-oxygen mixtures, Smith and Agnew[40] found a positive dependence of burning velocity on pressure with $S_u$ values of 5.64 m/s at 1 atm and 3.86 m/s at 0.1 atm using the spherical bomb method. Strauss and Edse[41] found positive pressure dependence of burning velocity for hydrogen-oxygen and methane-oxygen flames between 1 and 90 atm. This finding is in general agreement with Agnew and Graiff[42].



For hydrocarbon-air flames, Gilbert's results for methane, ethylene, propane, and isobutylene with air using a burner method, all show some increase at low pressure, while Smith and Agnew's spherical bomb experiments on methane-air show a definite negative dependence over a quite large range of 0.1 to 20 atm. Diederichsen and Wolfhard[43], using a burner method, also found that the burning velocity of methane-air mixtures decreases to a value as low as 6 cm/s at 40 atm. Rallis[44] et al. for acetylene-air stoichiometric mixtures, using the spherical bomb method, concluded that the pressure dependence is such that when, at 300 K, the pressure is increased from 0.3 to 2.0 atm, then the burning velocity first increases from 1.14 to 1.31 m/s at 0.75 atm, where it reaches a maximum. It then decreases to the minimum value of 1.2 m/s at 1.15 atm, after which it again rises to 1.275 m/s at 2.0 atm. The burning velocity tends to become independent of pressure for very high values of pressures and temperatures.

Manton and Milliken[36], using the bomb method, found that the pressure dependence of methane, ethylene, and propane-oxygen mixtures with various amounts of nitrogen, helium and argon as diluents could be expressed by

$$S_u \propto P_i^m \tag{10.43}$$

where the pressure exponent $m$ is a function of burning velocity. Below 0.5 m/s, $m$ is negative whilst above 1 m/s, it is positive.

Lewis[54] has reported the pressure dependence of burning velocity for a large number of flames using the spherical bomb method. The pressure dependence can be expressed as a simple power law:

$$S_{u(a)}/S_{u(b)} = (P_a/P_b)^n \tag{10.44}$$

where $S_{u(a)}$ and $S_{u(b)}$ are burning velocities at pressures $P_a$ and $P_b$ respectively. The values of pressure exponent $n$ in the empirical Eq. (10.44) are shown in Fig. 10.9. Bradley and Hundy[26] found the pressure exponent for methane-air mixtures using hot wire anemometres in closed vessels as

$$S_u \propto P^{-0.5} \tag{10.45}$$

Egerton and Lefebvre[45] expressed the effect of pressure on the burning velocity for methane-air mixtures over a pressure range of 1 to 9 atm as

$$S_u \propto P_i^{-0.46} \text{ for } 9\% \text{ mixture} \tag{10.46}$$

and

$$S_u \propto P_i^{-0.5} \text{ for } 11\% \text{ mixture} \tag{10.47}$$

Babkin et al.[46] suggested the pressure dependence on $S_u$ for methane-air mixtures over a pressure range of 3 to 60 atm as

$$S_u = 37.4\ P_i^{-0.5} \tag{10.48}$$

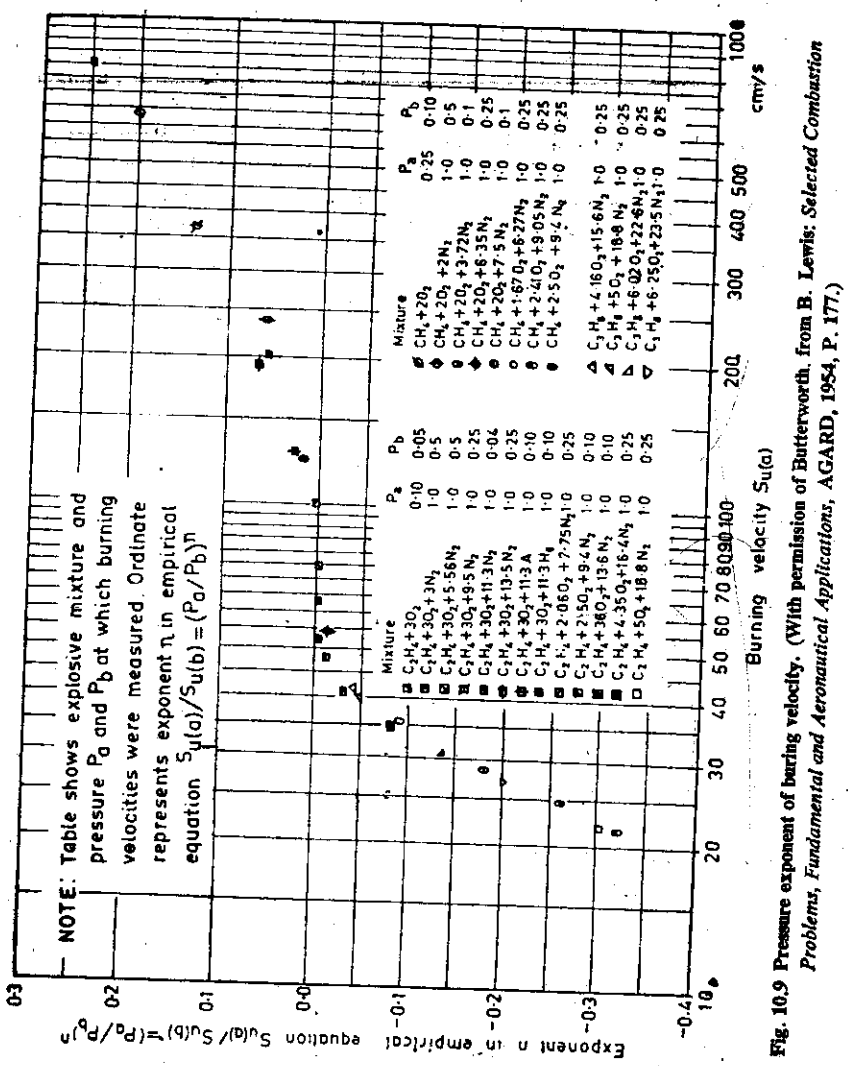


Fig. 10.9 Pressure exponent of burning velocity. (With permission of Butterworth, from B. Lewis: *Selected Combustion Problems, Fundamental and Aeronautical Applications*, AGARD, 1954, P. 177.)



Andrews and Bradley, using the constant volume method and hot wire anemometer for the measurement of gas velocity, reported the pressure dependence of burning velocity for methane-air mixtures for pressures above 5 atm to be given by the equation

$$S_u = 43\ P_i^{-0.5} \text{ cm/s} \tag{10.49}$$

The same authors, using the constant volume method with double ignition, reported the effect of pressure on burning velocity for 10% methane-air mixtures and pressures below 5 atm to be given by the equation:

$$S_u = 45\ P_i^{-0.5} \text{ cm/s} \tag{10.50}$$

where $P_i$ is the initial pressure in atmospheres.

In view of the above discussion it appears that the constant volume bomb method is a very reliable method for the determination of burning velocity and its pressure dependence even at very high pressures. However, the observations are likely to be affected by heat losses for low pressures and slow burning mixtures.

### Effect of Electric Field

Earlier reports on the effect of an electric field on the burning velocity were quite hetrogeneous and confusing. Some reports indicated an increase in the burning velocity, while others reported a decrease or even extinguishment of the flame, and yet others indicated that the electric field had no effect on flame propagation. This is because the electric field has different effects on different fuels. The effect also depends upon the type, magnitude, and frequency of the field applied.

In general, we may say that hydrocarbon flames are greatly affected by an electric field, while carbon-monoxide or hydrogen flames are least affected. It has also been observed that the application of a D.C. field has maximum effect on the flame propagation velocity in a tube while the high frequency A.C. field has minimum effect. The electric field affects the flame propagation rate in two different ways: (i) by changing the shape or size of the flame, and (ii) by increasing the electron activity, thus changing the chemical reaction rate.

Fowler and Corrigan[48] reported that a D.C. electric field increased the flame propagation velocity of the methane-air mixture by about 50% in a tube, while the low frequency 60 Hz A.C. field of the same strength increased it by about 30% only. Jaggers and Von Engel[49] observed for town gas (20% $CH_4$, 55% $H_2$, and 20% CO)-air mixtures that a field up to 1 kV/cm D.C. or 50 Hz had no measurable effect on the flame propagation velocity in a tube. However, for methane-air mixtures they found that the flame propagation velocity increased; the increase was more pronounced in the case of the ethylene-air mixture. They attributed the effect of change in shape and area of the flame for this increase. They also

confirmed the observation of Fowler and Corrigan that the D.C. field is more effective than the A.C. field. Their observations have shown that the effect of the high frequency field is less on the flame propagation velocity as compared to the low frequency A.C. field, but suggested that the high frequency field increases the value of the burning velocity. They attributed this increase in the burning velocity to the increase in the vibrational level of electrons.

### Effect of Mixture Composition

The effect of mixture composition is quite marked on the burning velocity. At a very low percentage of fuel, the mixture will not ignite or the flame will not propagate. The flame will only start propagating at a particular concentration of the fuel-oxidant mixture. This concentration of fuel is known as the lower limit of inflammability, sometimes called the limit of inflammability, and the burning velocity at this limit is known as the limit velocity. The concentration of fuel is generally expressed in terms of the equivalence ratio, $\phi$ defined as the actual fuel-oxidant ratio divided by the stoichiometric fuel-oxidant ratio. Generally the lower inflammability limit is 0.5 to 0.6 times the equivalence ratio and the lower limit velocity for the hydrocarbon-air mixture is about 15 to 20 cm/s. As the mixture strength is raised, the burning velocity increases to a maximum value at a slightly richer side of the stoichiometric ratio. The equivalence ratio for the maximum burning velocity, $\phi_m$ varies approximately from 1.1 to 1.35. A few empirical relations are available to calculate the burning velocity at different values of $\phi$, if the value of maximum burning velocity and $\phi_m$ are known, but there is no general formula.

Sometimes the fuel-oxidant ratio is expressed in terms of the mixture strength $\lambda$, which is the reciprocal of $\phi$, i.e., it equals the ratio of the actual amount of oxidant to the stoichiometric amount of oxidant required. After acquiring a maximum value, the burning velocity starts decreasing, as the mixture strength is further increased. Thus a bell-shaped curve is obtained which is symmetrical about the axis giving $\phi_m$. Again, at another value of $\phi$ known as the upper limit of inflammability, the flame fails to propagate itself. At this equivalence ratio, the burning velocity will be referred to as the upper limit velocity. It should be noted that, at the inflammability limits, the burning velocity is not zero, but has a finite value which is about one-third to one-fourth of the maximum burning velocity. Figure 10.10 shows a set of curves for burning velocity at different values of per cent fuel in air. This bell-shaped behaviour of $S_u$ versus per cent fuel in oxidant (or equivalence ratio $\phi$) is almost universal with each fuel.

Sharma, Agrawal and Gupta[57] have presented various correlations showing the dependence of laminar burning velocity on mixture composition, initial temperature and initial pressure. An equation for predicting the laminar burning velocity of methane-air mixtures for initial pressures



of 1-8 atm, temperatures of 300–600 K, and equivalence ratios of 0.8 to 1.2 in a constant-volume spherical combustion vessel is:

$$S_u = C\,(T_u/300)^{1.68/\sqrt{\phi}} \quad \text{for } \phi \leqslant 1.0$$

$$S_u = C\,(T_u/300)^{1.68\sqrt{\phi}} \quad \text{for } \phi \geqslant 1.0$$

where $C = -418 + 1287/\phi - 1196/\phi^2 + 360/\phi^3 - 15\,\phi\,(\log_{10} P)$.

The values obtained by this equation compare with the values determined experimentally by the authors to within 9 per cent.

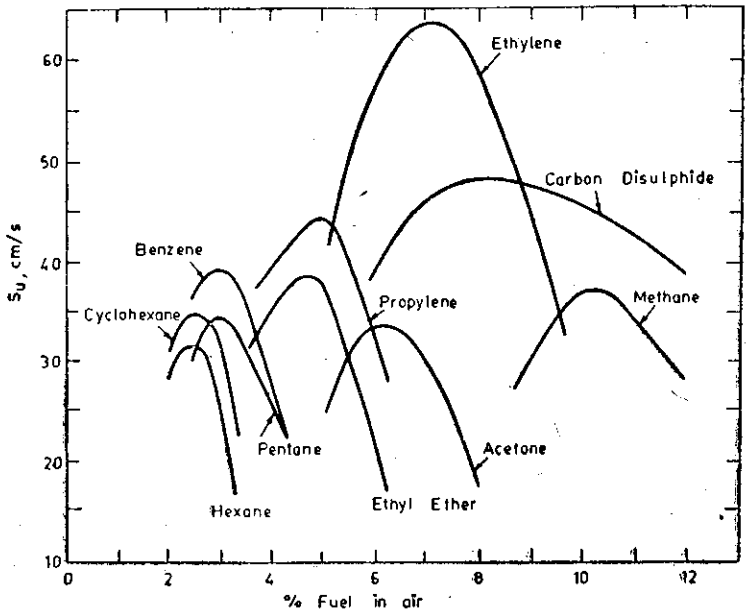


**Fig. 10.10 Effect of per cent fuel on the burning velocity.**

### Effect of Admixtures

The effect of admixtures on burning velocity is quite pronounced and of great practical importance. Admixtures may be classified as inert and active admixtures. For inert admixtures the oxidant is usually replaced by some inert gas, e.g., A, He, $N_2$, $CO_2$; etc. It is observed that the effect of the inert component is the dilution of the mixture, thus the burning velocity is always reduced and the ignition zone narrowed, i.e., the lower inflammability limit is increased while the upper limit is reduced.

Stevens[16] found that for the above four inert gases, the effectiveness was in the order: $CO_2 > N_2 > He > A$. The influence of an inert gas depends upon the heat capacity, diffusion constant, and thermal conductivity of the

gas. Besides the dilution effect, these factors affect the reaction rate and flame temperature thus reducing the burning velocity.

Figure 10.11 shows the burning velocities of methane-oxygen mixtures diluted by different proportions of nitrogen. It is observed that with an increasing percentage of inert gas, the peak of the burning velocity curve is regularly shifted to the left. This phenomenon is observable with each type of inert gas.

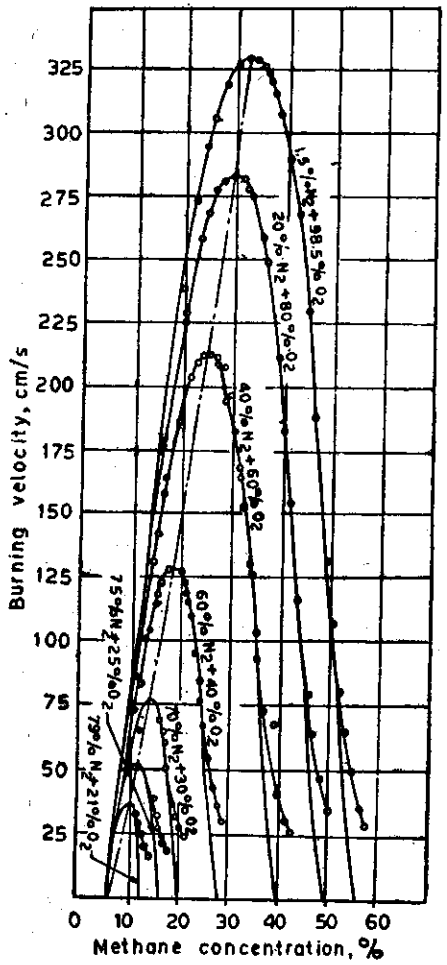


**Fig. 10.11 Effect of nitrogen admixture on the burning velocity of methane-oxygen mixtures (Based on the data of G. Jahn).**

The burning velocity of a combustible mixture containing $N_2$ and $CO_2$ as diluents may be written as:



$$S_u = S_{u,p}\,(1 - 0.01\ N_2 - 0.012\ CO_2) \qquad (10.51)$$

where $S_{u,p}$ is the burning velocity of the pure combustible mixture, and $N_2$ and $CO_2$ are the percentage concentrations of $N_2$ and $CO_2$.

The active admixtures are those admixtures which chemically affect the burning of a fuel. The admixtures may be formed by mixing another fuel, any catalytic agent, or any inhibitor. The study of the effect of active admixtures is very important because, in practice, many mixed fuels are used. Catalyzing effects are sometimes required for increasing the rate of the combustion reaction and the inhibitors are usefulfor extinguishing fire.

The burning velocity of different mixed fuels does not obey a simple mixing rule, specially when the nature of two or more fuels is quite different or one has a catalyzing or inhibitive effect on the other. However, for many fuel admixtures, Payman and Wheeler[50] gave the law of velocities. It has three provisions:

1. If two or three mixtures with equal burning velocities are mixed in any proportion, the burning velocity in the resulting mixture will remain unchanged. This law, however, will not hold good if two mixtures with the same velocities, one with excess of oxidant (lean mixture) and the other with excess of fuel (rich mixture), are mixed. From this law, two further provisions can be made.
2. Mixtures of limit mixtures are themselves limit mixtures, i.e., if two lean limit mixtures are mixed, the resulting mixture will be a limit mixture. Similarly, a mixture of two rich limit mixtures will also be a limit mixture.
3. Mixtures of maximum mixtures are themselves maximum mixtures. By a maximum mixture we mean a mixture which gives maximum burning velocity.

The above two laws can be written mathematically by the simple mixing rules as

$$L = \frac{a+b+c}{\frac{a}{L_a}+\frac{b}{L_b}+\frac{c}{L_c}}\,\% \qquad (10.52)$$

where $L$ is the required limit of flammability or the composition required for maximum mixture, $a$, $b$, and $c$, are the per cent compositions of simple gases in the complex mixture; $a+b+c=100\%$. $L_a$, $L_b$ and $L_c$ are compositions corresponding to the "limits" or "maximum mixtures" of the simple gases.

From this formula the value of maximum burning velocity of the mixture can be written as:

$$S_{u,\max} = \frac{mS_{u,a}+nS_{u,b}+pS_{u,c}+\ldots}{m+n+p+\ldots} \qquad (10.53)$$

where $m$, $n$, $p$, etc. are the per cent concentrations of simple mixtures in the maximum velocity complex mixture.

It should be noted that these laws will not hold true for a mixture of fuel with hydrogen or carbon monoxide, but are quite useful for mixtures of simple hydrocarbons.

The effect of $H_2$, $H_2O$ and $CH_4$ is sometimes catalytic, e.g., a small amount of $H_2$ or $H_2O$ appreciably increases the burning velocity of CO–air mixtures. Garner and Johnson[51] found that only 0.23% of $H_2$ in the carbon monoxide-oxygen mixture increased the burning velocity from 100 to 760 cm/s. This effect can be well explained by reviewing the mechanism of carbon monoxide oxidation with or without the presence of $H_2$ or $H_2O$ as discussed in Chapter seven. The effect of ethyl nitrate, ethyl iodide, and chloroform was found to be similar, while carbon tetrachloride reduced the burning velocity, thus showing an inhibition effect.

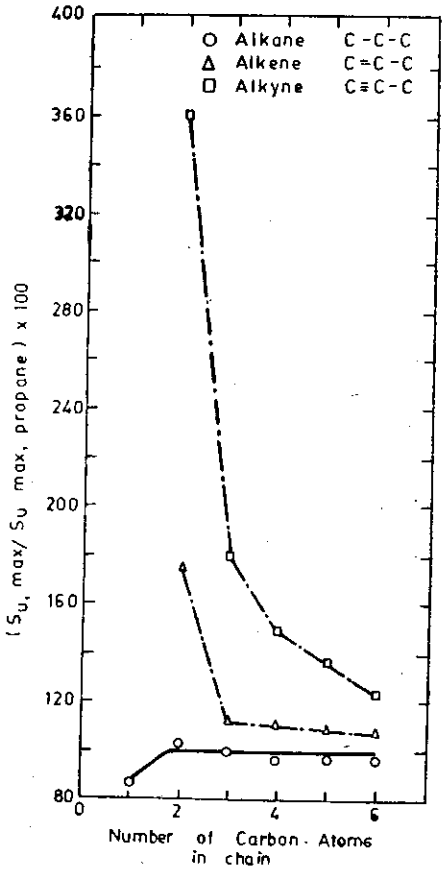


**Fig. 10.12 Effect of chain length and saturation on relative burning velocities of straight chain hydrocarbons at 25°C and 1 atm.**



For hydrocarbon-air mixtures, it is found that organic halides and metallic salts have a pronounced inhibition effect. Zentler Gordon[52] found that 0.13% by volume of n-octyl bromide reduces the flame speed of town gas by 50% and 1% of it reduces the flame speed to 1/5. He observed that the effect of heavier organic halides is more and bromides are more effective than chlorides or iodides.

Hydrocarbons are found to be good inhibitors for hydrogen-air flames, e.g., 3½% of butane reduces the flame speed from 275 to 15 cm/s. Similarly, 0.5% by volume of $Fe(CO)_5$ reduces it to 65 cm/s. Rosser, Inami, and Wise[53] found that $1 \times 10^{-5}$ g/cm³ of $Na_2CO_3$ reduces the burning velocity of methane–air mixture from 65 to 15 cm/s.

### Effect of Fuel Structure

Figure 10.12 shows the effect of the number of carbon atoms in the fuel on the maximum burning velocity for alkanes, alkenes, and alkynes. The burning velocity increases in the order: alkanes<alkenes<alkynes. For alkanes (saturated hydrocarbons such as propane, butane, hexane, etc.), the burning velocity is nearly independent of the number of carbon atoms in the fuel molecule. The effect of increased chain length decreases the burning velocity of alkenes and alkynes.

**Example 10.1**

Calculate the limits of inflammability of a liquefied petroleum gas (LPG) mixture which has the following volumetric analysis:

$CH_4$: 1.6%, $C_2H_6$: 14.0%; $C_3H_8$: 53.4%, $C_4H_{10}$ (iso+normal): 31.0%

*Solution:*

From Table A.6 the lower and upper limits of inflammability of the constituents gases are given below:

| *Gas* | *Limit of inflammability (% by volume)* | |
|---|---|---|
| | *Lower* | *Upper* |
| $CH_4$ | 5.3 | 15.0 |
| $C_2H_6$ | 3.0 | 12.5 |
| $C_3H_8$ | 2.12 | 9.35 |
| $C_4H_{10}$ (iso+$n$) | 1.83 | 8.43 |

The required limit of inflammability can be calculated by employing the simple rule of mixing:

$$L = \frac{a+b+c+d}{\frac{a}{L_a}+\frac{b}{L_b}+\frac{c}{L_c}+\frac{d}{L_d}}$$

where $a$, $b$, $c$ and $d$ are the percentage proportions of the gases present in the LPG mixture.

The lower limit of inflammability is:

$$L_1=\frac{100}{\frac{1.6}{5.3}+\frac{14.0}{3.0}+\frac{53.4}{2.12}+\frac{31.0}{1.83}}=2.12\%$$

The upper limit of inflammability is:

$$L_2=\frac{100}{\frac{1.6}{15.0}+\frac{14.0}{12.5}+\frac{53.4}{9.35}+\frac{31.0}{8.43}}=9.42\%$$

**Example 10.2**

Calculate the composition required for the maximum mixture and the value of maximum burning velocity of a liquefied petroleum gas mixture which has the same volumetric analysis as given in Example 10.1. The following data may be used:

| *Fuel gas* | *Maximum burning velocity of fuel-air mixture* | |
|---|---|---|
| | *% Fuel in mixture (by vol.)* | $S_{u,max}$ (cm/s) |
| $CH_4$ | 10.05 | 39 |
| $C_2H_6$ | 6.30 | 46 |
| $C_3H_8$ | 4.59 | 45 |
| $C_4H_{10}$ | 3.52 | 44 |

*Solution:*

The required composition for the maximum mixture is given by:

$$L=\frac{a+b+c+d}{\frac{a}{L_a}+\frac{b}{L_b}+\frac{c}{L_c}+\frac{d}{L_d}}=\frac{100}{\frac{1.6}{10.05}+\frac{14.0}{6.30}+\frac{53.4}{4.59}+\frac{31.0}{3.52}}$$

$=4.4\%$

The maximum burning velocity of the complex mixture is calculated from the equation:

$$S_{u,max}=\frac{m(S_{u,a})+n(S_{u,b})+p(S_{u,c})+q(S_{u,d})}{m+n+p+q}$$

where $m$, $n$, $p$ and $q$ are the percentage proportions of the gases present in the LPG mixture. Therefore,

$$S_{u,max}=\frac{1.6(39)+14.0(46)+53.4(45)+31.0(44)}{100}$$

$=44.73$ cm/s

**Example 10.3**

The burning velocity of a combustible mixture was determined by employing the nozzle burner–total area method. The data recorded were as follows:



Volumetric flow rate of the combustible mixture $=220$ cm$^3$

Height of the mean cone of the flame $=3.83$ cm

Diameter of the nozzle-burner port $=8.3$ mm

Calculate the value of the burning velocity.

*Solution:*

Assuming the flame cone to be right circular with the base diameter equal to the nozzle-burner port diameter, the burning velocity is expressed as:

$$S_u=\frac{V_{f1}}{A_F}$$

where $A_F$ = flame cone surface area

$$=\pi r\sqrt{r^2+h^2}$$

$$=\pi\left(\frac{0.83}{2}\right)\sqrt{\left(\frac{0.83}{2}\right)^2+(3.83)^2}$$

$=5$ cm$^2$

$$\therefore \quad S_u=\frac{220}{5}$$

$=44$ cm/s

**Example 10.4**

A gaseous combustible mixture is contained in a long cylindrical glass tube open at one end and closed at the other end. The internal diameter of the tube is 5.5 cm. The speed of the uniform movement of the flame front was determined to be 84 cm/s by igniting the combustible mixture at the open end. From the snapshots of the flame front, the flame shape was found to be nearly hemispherical. Calculate the burning velocity of the mixture.

*Solution:*

As the unburned gas is stationary, the equation for the burning velocity may be written as:

$$S_u=\frac{a_o}{A_F}(S_s)$$

where $a_o$ = cross-sectional area of the tube $=\frac{\pi}{4}d_o^2$

$A_F$ = flame front surface area (hemispherical) $=\frac{\pi}{2}d_o^2$

$S_s$ = spatial velocity of the flame.

The above equation is derived from the consideration that the volume of the unburned mixture consumed per unit time equals the product of the flame front surface area and the burning velocity.

Substituting the values of $a_o$ and $A_F$ in the above expression, we have

$$S_u=\frac{\pi}{4}d_o^2\left(\frac{2}{\pi d_o^2}\right)S_s$$

or $$S_u = \frac{S_s}{2}$$

$$= \frac{84}{2}$$

$$= 42 \text{ cm/s}$$

**Example 10.5**

Consider that a homogeneous combustible mixture is spark-ignited at the centre of a soap-bubble and the flame growth is recorded by a rotating drum camera. The change in the radius of the flame sphere with time after spark is given below:

| Time after spark, $t$, ms | 1.12 | 2.23 | 3.34 | 4.46 | 5.20 | 7.80 | 9.66 | 11.50 |
|---|---|---|---|---|---|---|---|---|
| Flame radius, $r_b$, cm | 1.07 | 2.22 | 3.51 | 4.76 | 5.60 | 6.94 | 7.05 | 7.05 |

The initial diameter of the soap bubble is 7 cm. Determine:

(a) The spatial velocity of the flame in cm/s

(b) The expansion ratio of the soap bubble

(c) The burning velocity of the combustible mixture.

*Solution*:

Plot the flame radius (in cm) versus time (in ms) graph. The linear portion represents the smooth travel of the flame, the curved portion results when the flame front nears the end of the combustible mixture and begins to slow down.

The spatial velocity of the flame is given by $S_s = dr_b/dt$. On measuring the slope of the $r_b$–$t$ curve over the linear portion, we get

$$S_s = \frac{dr_b}{dt} = 1052 \text{ cm/s}$$

In order to determine the final radius of the sphere of the burned mixture from the plot of flame radius vs time, the portion representing the slow expansion of the sphere is extrapolated back to the intersection with the rapidly expanding portion. The intersection of the two linear segments is used as the final diameter. The expansion ratio of the soap bubble is calculated from the relation:

$$E = \left(\frac{r_{\text{final}}}{r_{\text{initial}}}\right)^3 = 7.81$$

The burning velocity is determined from the equation:

$$S_u = \frac{S_s}{E} = \frac{1052}{7.81} = 134.8 \text{ cm/s}$$

**Example 10.6**

In an experimental study to determine the burning velocity of a hydrocarbon fuel-air mixture by the constant volume bomb method, simultaneous records of flame growth and pressure rise with time were obtained by igniting the mixture centrally in a spherical vessel of 14 cm internal diameter. The initial pressure and temperature of the combustible mixture were 1 atm and 300 K. The values of pressure and flame radius measured from $P$–$t$ and $r_b$–$t$ records at regular intervals of time in the early stages of combustion up to $P/P_i \simeq 1.2$ are given below:



| *Time after spark* $t$ (ms) | *Observed flame* $r_b$ (cm) | *Observed pressure* $p$ (atm) |
|---|---|---|
| 0 | 0.0 | 1.0 |
| 2 | 0.23 | 1.0 |
| 4 | 0.65 | 1.0005 |
| 6 | 1.07 | 1.0015 |
| 8 | 1.48 | 1.008 |
| 10 | 1.89 | 1.0225 |
| 12 | 2.3 | 1.0452 |
| 14 | 2.7 | 1.074 |
| 16 | 3.08 | 1.1018 |
| 18 | 3.44 | 1.1468 |
| 20 | 3.78 | 1.2071 |

The thermodynamically computed value of the equilibrium pressure $P_e'$ following constant volume combustion is 8.75 atm.

Compute the value of burning velocity by the use of

(i) Lewis and Von Elbe equation requiring pressure-time record alone and $P_e'$, and

(ii) Manton and Von Elbe equation requiring flame radius-time record alone and $P_e'$.

Take the value of $\gamma_u$ for the unburned mixture as 1.39.

*Hints for Solution*:

(i) The Lewis and Von Elbe equation is:

$$S_u = \frac{dr_i}{dt}\left(\frac{r_i}{r_b}\right)^2 \left(\frac{P_i}{P}\right)^{1/\gamma_u}$$

where $$r_i = R\left[\frac{P - P_i}{P_e' - P_i}\right]^{1/3}$$

$$r_b = R\left[1 - \frac{P_i}{P} \cdot \frac{T_u}{T_i} \cdot \frac{P_e' - P}{P_e' - P_i}\right]^{1/3}$$

and $$\frac{T_u}{T_i} = \left(\frac{P}{P_i}\right)^{(\gamma_u - 1)/\gamma_u}$$

Since $R$, $P_i$, $T_i$, $\gamma_u$ and $P_e'$ are known, $r_i$, $r_b$, $T_u$ can be calculated corresponding to different values of $P$ and $t$ from the $P$–$t$ record in the initial range up to $P/P_i \simeq 1.1$. The calculated value of $r_b$ can be compared with the observed value of $r_b$ from $r_b$–$t$ records. To obtain burning velocities it is necessary to plot values of $r_i$ obtained from the above equation as a function of time and to determine the slopes $dr_i/dt$.

(ii) The Manton and Von Elbe equation (originally derived by Dery) using the experimental slope $dr_b/dt$ is:

$$S_u = \frac{dr_b/dt}{1+\{(P_e'/P)-1\}/\gamma_u}$$

This equation is valid only when the mass fraction burned $\left( n=\frac{P-P_i}{P_e'-P_i} \right)$ is less than 0.01.

Since $R$, $P_i$, $P_e'$ and $\gamma_u$ are known and $r_b$ is measured at a given interval of time $t$, the corresponding instantaneous value of $P$ can be calculated from the relation between $r_b$ and $P$.

The value of $S_u$ determined from the above two equations at $P/P_i=1$ and $T_i=300$ K are: 33.3 cm/s and 32 cm/s respectively. These values are obtained by extrapolating the values of $S_u$ determined from each equation, from the graphs of $S_u$ versus $P/P_i$.

## REFERENCES


1. J. W. Linnett, *Fourth Symposium (International) on Combustion*, Williams and Wilkins, Baltimore, 1953, pp. 20-35.
2. G.E. Andrews, and D. Bradley, *Combustion and Flame*, 1972, **18**: 133-53.
3. A.C. Egerton, and S.K. Thabet, *Proc. Roy. Soc.*, 1952, **A211**: 445-71, J. Powling, *Fuel*, London, 1949, **28**: 25-28.
4. W. Michelson, *Ann. Physik*, 1889, **37**: 1.
5. B. Lewis, and G. Von Elbe, *J. Chem. Phys.*, 1943, **11**: 75.
6. V.S. Babkin, A.V. V'yun, and L.S. Kozachenko, Fiz. Goreniya Vzryva, 1966, **2**: 52-60. English Trans: Effect of pressure on normal flame velocity investigated by the initial-section method in a constant volume method, *Combustion, Explosion and Shock Waves*, 1966, **2**: 32.
7. M. S. Uberoi, A. M. Kuethe, and H. R. Menkes, *Phys. Fluids*, 1958, **1** : 159.
8. R.A. Gross, *Interim Tech. Rep. No. 2, Div. Appl. Sci.*, Harvard Univ., 1952 (Contract No. DA-19-020-ORD-1029, Army Ord. Dept.).
9. R.M. Fristrom, *J. Chem. Phys.*, 1956, 24 : 888.
   ———, *Phys. Fluids*, 1965, **8**: 273.
10. E. Mallard, and H.Le Chatelier, *Ann. Mines*, 1883, **8**: 274.
11. H.F. Coward, and F.J. Hartwell, *J. Chem. Soc.*, 1932.
12. M. Gerstein, Q. Levine, and E.L. Wong, *J. Am. Chem. Soc.*, 1951, **73**: 418.
13. H. Guenoche, N. Manson, and G. Mannot, *Compt. Rend.*, 1948, **226**: 163.
14. H.T. Henderson, and G.R. Hill, *J. Phy. Chem.*, 1956, 60: 874.
15. P. Laffitte, and J. Combouriu, *Journees International de La Combustion et de La Conversion de l Energie*, p. 55.
16. E.W. Stevens, *NACA Report Nos.* 1923 (176), 1927 (280), 1929 (305), 1929 (337), 1930 (372), *J. Am. Chem. Soc.*, 1928, **50**: 3244.
17. E.F. Fiock, and C.H. Roeder, *NACA Report*, 1935 (532).
18. G. Dixon-Lewis, and M.J.G. Wilson, *Trans. Faraday Soc.*, 1951, **47**: 1106.
19. B. Lewis, and G. Von Elbe, *J. Chem. Phys.*, 1934, **2**: 283-90.
20. E.F. Fiock, and C.F. Marvin, *Chem. Rev.*, 1937, **21**: 367-87.
21. J. Manton, G. Von Elbe, and B. Lewis, *Fourth Symposium (International) on Combustion*, Williams and Wilkins, Baltimore, 1953, 358-63.
22. R.C. Eschenbach, and J.T. Agnew, *Combustion and Flame*, 1958, **2** : 273-85.
23. J. Grumer, E.B. Cook, and T.A. Kubala, *Combustion and Flame*, 1959, **3**: 437-46.





24. K.H. O' Donovan, and C.J. Rallis, *Combustion and Flame*, 1959, **3**: 201-14.
25. C.J. Rallis, University of Witwatersrand, Deptt. of Mech. Engg., *Research Report No.* 20, 1964.
26. D. Bradley, and G.F. Hundy, *Thirteenth Symposium (International) on Combustion*, The Combustion Institute, Pennsylvania, 1971, 575-83.
27. R.E. Bolz, and H. Burlage, *NASA Tech. Note*, D-551, 1960, Jet Propulsion, 1955, **25**: 265.
28. S.D. Raezer, and H.L. Olsen, *Combustion and Flame*, 1962, **6**: 227.
29. G.E. Andrews, and D. Bradley, *Combustion and Flame*, 1973, **20**: 77-89.
30. K.G. Payne, and F.J. Weinberg, *Eighth Symposium (International) on Combustion*, Williams and Wilkins, Baltimore, 1962, p. 207.
31. H.E. Passauer, *Das Gas-und Wasserfach, Jahrg*, 73, *Heft* 17, Apr. 26, 1930, 393-397
32. S. Heimel, and R.C. Weast, *Sixth Symposium (International) on Combustion*, Reinhold, New York, 1957, p. 296.
33. G.L. Dugger, *NACA Report No.* 1061, 1952.
34. D.K. Kuehl, *Eighth Symposium (International) on Combustion*, Williams and Wilkins, Baltimore, 1962, p. 510.
35. G.L. Dugger, R.C. Weast, and S. Heimel, *Fifth Symposium (International) on Combustion*, Reinhold, New York, 1955, p. 589.
36. J. Manton, and B.B. Milliken, *Proc. Gas Dynamics Symposium on Aerothermochemistry*, Northwestern University, Evanston, Illinois, 1956, p. 151.
37. L. Ubbelohde, and E. Koelliker, *J. Fur Gasbeleucht*, 1916, **59**: 49.
38. H.G. Wolfhard, *Z. Tech. Phys.*, 1943, **24**: 206.
39. M. Gilbert, *Sixth Symposium (International) on Combustion*, Reinhold, New York, 1957, p. 74.
40. D. Smith, and J.T. Agnew, *Sixth Symposium (International) on Combustion*, Reinhold, New York, 1957, p. 83.
41. W.A. Strauss, and R. Edse, *Seventh Symposium (International) on Combustion*, Butterworth, London, 1959, p. 377.
42. J.T. Agnew, and L.B. Graiff, *Combustion and Flame*, 1961, **5**: 209-19.
43. J. Diederichsen, and H.G. Wolfhard, *Trans. Faraday Soc.*, 1956, **52**: 1102.
44. C.J. Rallis, A.M. Garforth, and J.A. Steinz, *Research Report No.* 26, March 1965, Deptt. of Mech. Engg., University of Witwatersrand.
45. A.C. Egerton, and A.H. Lefebvre, *Proc. Roy. Soc. London*, 1954, **A222**: 206-23.
46. V.S. Babkin, L.S. Kozachenko, and I.L. Kuznetsov, *Zh. Prikl Mekhan, i Teklin Fiz.*, 1964, **3**: 145. English translation: TT 66-61882 (1966).
47. G.E. Andrew, and D. Bradley, *Combustion and Flame*, 1972, **19**: 275-88.
48. R.G. Fowler, and S.J.B. Corrigan, *Physics of Fluids*, 1966, **9**: 2073.
49. H.C. Jaggers, and A. Von Engel, *Combustion and Flame*, 1971, **16**: (1-3) 275.
50. L.N. Khitrin, *The Physics of Combustion and Explosion* (Translated from Russian), Israel Program for Scientific Translations, Jerusalem, 1962, p. 163.
51. W.E. Garuer, and C.H. Johnson, *J. Chem. Soc.*, 1928, p. 280.
52. H.E. Zentler-Gordon, *Ph. D. Thesis*, London, 1940.
53. W.A. Rosser, S.H. Inami, and H. Wise, *Combustion and Flame*, 1963, **7**: 107.
54. B. Lewis, *Selected Combustion Problems: Fundamentals and Aerodynamics Applications*, Butterworth, London, 1954.
55. R.M. Fristrom, *The Physics of Fluids*, Feb. 1965, **8**: (2).
56. C.J. Rallis, and G.E.B. Tremeer, "Equations for the determination of burning velocity in a spherical constant volume vessel", *Combustion and Flame*, 1963, **7**: 51-61.
57. S.P. Sharma, D.D. Agrawal, and C.P. Gupta, "The pressure and temperature dependence of burning velocity in a spherical combustion bomb, *Eighteenth Symposum (International) on Combustion*, The Combustion Institute, Pennsylvania, 1981, pp. 493-501.

# 11

# TURBULENT FLAME PROPAGATION

The effect of turbulence on flame propagation has long been known. Mallard and Le Chatelier attributed the high velocity of flame propagation, obtained under certain circumstances, to the effect of turbulence. Similarly, the fact that the charge inside the cylinder of an internal combustion engine could be burned in a very short period of time was due to the effect of turbulence. Although it was known that turbulence could increase the burning velocity by 10 to 100 times, the mechanism of flame propagation under turbulent conditions was not known till 1941. Turbulent flames usually exist in most engineering applications, e.g., I.C. engines including jet and rocket engines, welding torches, furnaces, etc., but the theoretical and experimental work done on turbulent flames does not still lead to any definite laws or the concept of turbulent flame propagation.

As stated earlier, a flame propagates in a stream at a velo city which is the vector sum of the burning velocity and stream velocity. In laminar flow, the flame is usually a thin smooth surface. The shape of the flame is governed by the gas flow geometry in a burner and by the shape of the vessel in a stationary mixture. For a laminar flame, it is possible to define the burning velocity, independent of the measuring apparatus within reasonable limits. This is not yet possible for a turbulent flame. Values of turbulent burning velocity depend not only on the apparatus used, but also on the concept of the turbulent flame assumed. In turbulent flow, the stream velocity fluctuates at random and, consequently, the flame in such a stream is continuously subjected to random distortions as it conforms to the fluctuations of the stream.

Figure 11.1 shows a turbulent flame on a burner, illustrating the boundaries of the flame brush and mean flame surface about which the instantaneous flame front oscillates. A turbulent flame would consume greater quantities of the fuel-air mixture than a laminar flame of the same height. The mean flame height and width of the burner port can be used



to estimate the lower limit to the flame volume required under a particular set of conditions. Any reduction in the available space would lead to inefficient burning. The distance between the inner and outer boundaries of the flame brush at the tip of the flame is called "brush width".

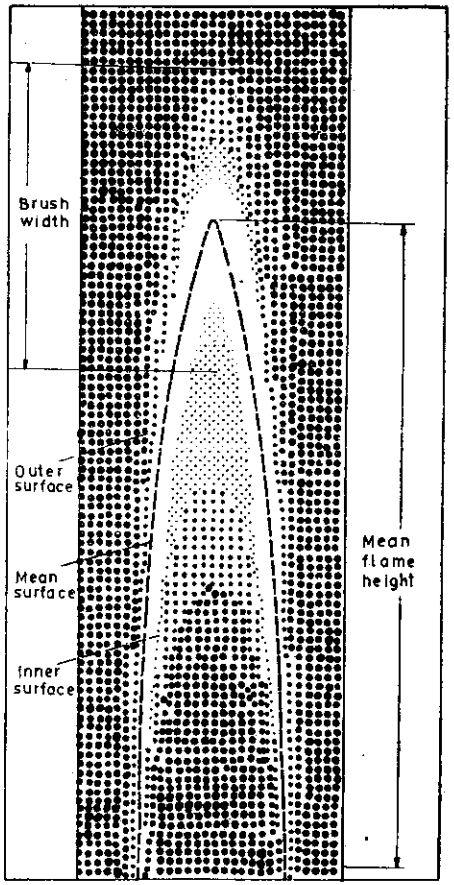


**Fig. 11.1 Turbulent flame model showing flame brush and mean surface**

## 11.1 TURBULENT BURNING VELOCITY

In early attempts to measure the turbulent burning velocity, Gouy's definition of burning velocity was employed. Initially it was assumed that the visible inner cone of the flame corresponds to the turbulent burning velocity and the outer cone corresponds to the laminar

burning velocity. With this concept, the turbulent burning velocities were calculated for various mixtures. Damkohler[1], using Gouy's formula and the above concept of turbulent and laminar burning velocity, studied the effect of Reynolds number on the ratio of turbulent to laminar burning velocity, $S_T/S_u$ as calculated from visible flame area ratio, $A_{outer}/A_{inner}$. Later, Bollinger and Williams[2] used the average position of the flame front instead of the inner edge as the latter is not so well defined. Karlovitz[3] used the locus of maximum light intensity measured by the densitometer from the brightest portion of the flame on a long-time exposed photograph. Assuming the flame surface as a paraboloid of revolution, the flame surface area may be calculated from the equation:

$$A_T=\frac{2\pi}{3}\left(\frac{r_t^2}{2h}\right)^{1/2}\left\{\left(2h+\frac{r_t^2}{2h}\right)^{3/2}-\left(\frac{r_t^2}{2h}\right)^{3/2}\right\} \tag{11.1}$$

When $\frac{r_t^2}{2h} << 2h$, the equation reduces to

$$A_T=\frac{4\pi}{3} r_t\, h \tag{11.2}$$

where $A_T$ is the flame surface area under turbulent conditions, $h$ is the height of the flame and $r_t$ is the radius of the burner tube.

Even when $h=2r_t$, Eq. (11.2) gives an error of only about 2% over Eq. (11.1).

Karlovitz used the angle method for calculating the local turbulent as burning velocity from the equation:

$$S_T=U \sin \alpha \tag{11.3}$$

where $U$ is the local mean flow velocity and $\alpha$ is the angle included by the average turbulent flame front and direction of the approach velocity. Hottel et al.[4] attempted to estimate the total surface area of a wrinkled flame from the height and diameter of the wrinkles visible on a spark photograph. Each wrinkle was assumed to be a cone. It was observed that the base diameter of the cone was related to the state of turbulence as

$$d_b=5.0\ d_\varepsilon \tag{11.4}$$

where $d_\varepsilon$ is the eddy diameter obtained from the turbulence scale ($d_\varepsilon$ at $R_y=0.5$), $R_y$ is the correction factor perpendicular to the $x$-direction. The height of wrinkles is related to the intensity of turbulence $\sqrt{\overline{u^2}_x}$ by the equation

$$h_p=\frac{0.266\sqrt{\overline{u^2}_x}}{S_u} \tag{11.5}$$

Another method adopted to calculate the flame area is to measure the intensity of light at a fixed air/fuel ratio through a given filter. For laminar flames at various flow rates, the light intensity at the same air/fuel ratio is measured. As the intensity of light is found to be a linear function of the flow rate, so the light intensity is used to measure the flame area by using a calibration curve obtained with laminar flames. The basic assumption in this method is that the laminar and turbulent flame structures are same, only the area of flame surface is increased in turbulent flames.



Apart from the burner method, the tube and spherical bomb methods have also been employed to calculate turbulent burning velocities. The turbulence is generated by injecting the gas through a nozzle or by a rotating or reciprocating blade or by a diaphragm. Mickelsen[5] produced a spherical flame in a turbulent mixture flowing through a 10 cm × 10 cm duct. The flame kernel obtained by centrally igniting the mixture was used to calculate $S_T$. Scurlock[6] used the V-shape flame obtained by supporting it on a rod to calculate the value of $S_T$. Summerfield[7] observed that the wrinkled flame model of Damkohler did not explain his experimental observations. He was of the view that the turbulent flame brush should be treated as a combustion zone in depth, i.e., the ignition and combustion should take place throughout the volume homogenously as a result of turbulent mixing. Spalding's[8] and Longwell's[9] experimental observations also corroborate Summerfield's model. However, further work by other investigators favours the wrinkled flame model.

## 11.2 FACTORS AFFECTING TURBULENT BURNING VELOCITY

### Effect of Fuel Concentration

Damkohler[1] studied the effect of fuel concentration on the turbulent burning velocities of propane-oxygen mixtures. The results were obtained from the measurements based on the outer and inner boundaries of the flame brush, which represent the laminar and turbulent burning velocities respectively. He was unable to study unstable lean flames, but turbulent flames showed a rapidly increasing velocity from rich mixtures toward stoichiometric. Higher values of burning velocities were obtained with higher flow velocities. This increase in the burning velocity was not due to changes in the fuel/oxidant ratio alone. Williams, Hottel, and Scurlock[10] observed that with low flow velocities (<125 cm/s), $S_T$ varies with air/fuel ratio, but becomes independent of it, if the flow velocities exceed 250 cm/s. They conducted experiments using propane and city gas. Bollinger and Williams[2] obtained bell-shaped curves similar to the laminar burning velocity curves at various Reynolds numbers. With increasing Reynolds numbers, the curves move higher. They observed that the maxima of the curves lie slightly on the richer side of the stoichiometric; maxima

not shifting appreciably with Reynolds number. Whol et al. also obtained a similar shape, but the maxima shifting slightly towards the richer side with increase in turbulence. The maximum of the turbulent burning velocity curve is found to be quite near the concentration for the maximum value of the laminar burning velocity curve. All these results, except those of Williams et al. at higher velocities, support the wrinkled flame model. Williams' observations indicate that the turbulent burning velocity is characteristic of flow only and independent of laminar burning velocity, type of fuel, or fuel-air ratio. Figure 11.2 shows the results obtained by Lefebvre and Reid[12] for propane-air mixtures.

### Effect of Fuel Type

Bollinger and Williams reported turbulent burning velocities for three fuels, viz., acetylene, ethylene, and propane under similar conditions with air as the oxidant. They obtained a common empirical equation

$$S_T = 0.18\ S_u\ d^{0.26}\ Re^{0.24}\ \text{cm/s} \qquad (11.6)$$

where $d$ is the diameter of the burner in cm. It is obvious from Eq. (11.6) that the turbulent burning velocity is directly proportional to the laminar burning velocity.

### Effect of Initial Temperature

Hoiligenstaedt[13] measured the effect of the initial temperature on the turbulent burning velocity of coke-oven gas-air mixtures. The turbulent

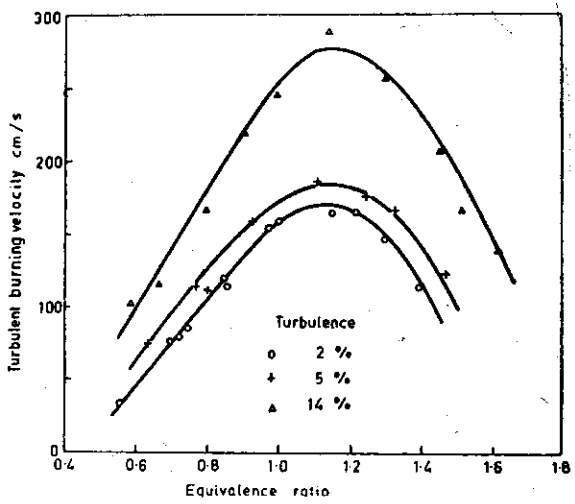


**Fig. 11.2 Effect of air--fuel ratio on turbulent burning velocity (With permission of the Combusion Institute, from *Combusion and Flame*, 1966, 10: 360.)**



burning velocity was measured by taking the inner visible cone area. He proposed that $S_T$ varies with absolute initial temperature as:

$$S_T \propto T^{1.6} \qquad (11.7)$$

Similar results were reported by Delbourg[13] on town gas-air flames. It was observed that the ratio of turbulent to laminar burning velocity is nearly independent of the initial temperature.

### Effect of Pressure

Goldenberg and Pelevin[14] reported the effect of pressure on turbulent burning velocities. They studied the effect on a burner where the flame was stabilized with the help of a pilot flame. The experiments were carried out in a pressure range of 100 to 760 mm of Hg. No screens were used to generate turbulence. The intensity of turbulence varied between 4 and 5%. Two sets of data were obtained, one by keeping the Reynolds number constant, and the other with constant flow velocity. At constant Reynolds number, they obtained the following relation

$$S_T = \frac{S_{T_0}}{(P/P_0)^{0.25}}$$

or

$$S_T \propto P^{-0.25} \qquad (11.8)$$

where $P_0$ and $S_{T_0}$ correspond to atmospheric conditions. Similar results were obtained for the Reynolds number varying from 4000 to 16 000. These results are similar to those for the effect of pressure on $S_u$. Keeping the flow velocity constant they obtained the following relation

$$S_T = AP^n \qquad (11.9)$$

where $n$=0.455 and the coefficient $A$ is a function of the fuel concentration

or

$$S_T \propto P^{0.455} \qquad (11.10)$$

Depending upon the experimental results and hydrodynamic considerations, they predicted that for the isotropic turbulence generated by the screens, $S_T$ is expressed as

$$S_T \propto P^{\frac{1}{2}} \qquad (11.11)$$

They suggested that the factor influencing the turbulent burning velocity on changing the pressure is the change in density and hence the kinematic viscosity.

## 11.3 CONCEPT OF TURBULENT FLOW

In laminar flow of fluids, the streamlines remain parallel to one another. If the velocity of flow is increased or a disturbance is introduced in the

stream flow, it is found that eddies are formed. In the case of flames, turbulence is generally recognized by a hissing sound and a thickening of the flame front. In the case of a flow through a tube or a pipe, turbulence is generally characterized by the Reynolds number. For the open tube burner the flame is always laminar for Re $<$ 2300, and is always turbulent for Re $>$ 3200. In the transition range, i.e., Re between 2300 and 3200, the fluctuations tend to damp out. But by inserting a grid in the tube, turbulence can be generated at a low Reynolds number. Similarly, for flow through a nozzle, it is possible to get laminar flow at even Re = 40000.

To get the exact characteristics of flow, it is desirable to study the flow through open tube burners. But as this requires a very long tube and the atmospheric air also changes the composition of the mixture, most turbulent flame studies are carried out in an enclosed space. Turbulence is generated by inserting grids of different mesh numbers in flames stabilized by bluff bodies at very high flow rates. Turbulent motion may be considered similar to molecular motion. In turbulent flow, small masses of fluids move in a random fashion in all directions superimposed on the main flow. In molecular motion, the size of the molecules is constant but in turbulent flow, these eddies or small masses vary in size, shape, and velocity in a wide range. Mathematically, turbulent flow is expressed in terms of the mean flow velocity and its fluctuating component.

In one-dimensional flow, the instantaneous value of the velocity of a fluid particle $U$ is given as the sum of the time-average velocity, $\bar{U}$ and a fluctuating component $u$. Thus

$$U = \bar{U} + u \tag{11.12}$$

$u$ is the instantaneous deviation from the mean and obviously $\bar{u}=0$.

The fluctuating component is characterized by its root mean square value $u'$. Thus

$$u' = \sqrt{\overline{u^2}} \tag{11.13}$$

Two characteristics of the turbulent flow generally referred to in a combustion process, are the intensity and scale of turbulence. The intensity of turbulence is the ratio of the fluctuating component to the flow velocity component. It is expressed as a percentage and is defined as $(u'/U)$ 100.

There are two descriptions of turbulent flow. In the Lagrangian description of flow, the point of reference moves with the stream, and a correlation coefficient $R_t$ is defined by the equation

$$R_t = \frac{\overline{u_0 u_t}}{\sqrt{\overline{u_0^2}}\sqrt{\overline{u_t^2}}} \tag{11.14}$$

where $u_0$ and $u_t$ refer to the values of $u$ at time zero and at a later time $t$



respectively. For $t \to 0$, $R_t \to 1$ and for $t \to \infty$, $R_t \to 0$. The scale of turbulence in the Lagrangian description is defined as

$$l_1 = \sqrt{\overline{u^2}} \int_0^\infty R_t \, dt \tag{11.15}$$

In the Eulerian description of flow in which the stream passes by a fixed point of reference, two points at a distance $y$ in the $y$-direction are considered and the correlation coefficient, $R_y$ is defined as

$$R_y = \overline{u_{y_0} u_y} \Big/ \sqrt{\overline{u^2}_{y_0}} \sqrt{\overline{u^2}_y} \tag{11.16}$$

For the two points quite near each other, $y \to 0$, $R_y \to 1$ and for $y \to \infty$, $R_y \to 0$. In the Eulerian description, the scale of turbulence is

$$l_2 = \int_0^\infty R_y \, dy \tag{11.17}$$

The scale $l_2$ may be regarded as proportional to the average size of the fluid elements or eddies.

It is difficult to measure $l_1$. But the scale of turbulence can be easily measured with the help of a hot wire anemometer in terms of $l_1$ at two places. Similar to the molecular diffusivity $D$, the eddy diffusivity $\varepsilon$ is defined as

$$\varepsilon = l\,u' \tag{11.18}$$

where $l$ is the mixing length which is roughly equal to the diameter of turbulence balls. Taylor suggests measurement of eddy diffusivity $\varepsilon$ by introducing a concentrated source of heat in a turbulent stream and measuring the spread of heat downstream. From the experiment on turbulence behind a grid or honeycomb in a wind tunnel, Taylor[15] found that $l_1$ has approximately half the value of $l_2$, although no theoretical relation exists between $l_1$ and $l_2$. If the gas flows through a wire mesh or perforated plate, the distance required to obtain isotropic turbulence after the mesh is about 80 times the diameter of the wire forming the mesh. The intensity of turbulence attains a value of about 5% behind the grid. The eulerian scale of turbulence $l_2$ is of the order of the wire diameter. In the case of pipe flow without any grid, it is found that after the turbulent flow is fully developed, the intensity of turbulence is about 3% and the scale $l_2$ is about 0.17 times the radius of the pipe. The scale of turbulence is maximum at the centre of the pipe and continuously decreases to zero towards the wall. The intensity of turbulence increases from the centre towards the wall, reaches a maximum quite near the wall, and again decreases to zero at the wall.

## Structure of Turbulence

Turbulent eddies have both translational and rotational motion. The turbulent mass of the eddies and mixing length are more than the molecular mass and mean free path and hence far more effective in the transport process. The large eddies which are produced when the streams first interact are very anisotropic. The large eddies initially formed due to turbulence generating grids or baffles have a low wave number, and are of the order of a few hundred Hz frequency as shown in Fig. 11.3. By a process of vortex stretching and through a spectrum of eddies the fluid is made isotropic. The stretching of vortex elements in any one direction leads to a reduction in length scales with an increase in velocity and vorticity components in the other two directions. Vortex stretching plays an important role in the break-up of eddies into smaller sizes and the process continues till the eddies become so small that they are eliminated by viscous friction. The small scale eddies have a larger wave number and a higher frequency of the order of $10^4$ to $10^5$ Hz. In this region of the turbulence spectrum the motion is highly isotropic (no preference to any direction).

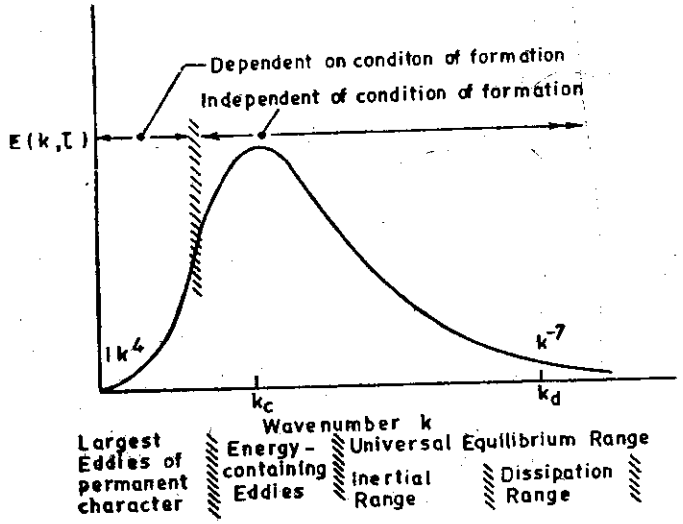


**Fig. 11.3 Turbulent energy spectrum.**

It is possible to obtain the maximum kinetic energy of turbulence with energy balance without the necessity of finding the local turbulent stresses (Reynolds stresses), eddy viscosities of various elements of the fluid involved, etc.



Taylor using the theory of statistics and Fourier transformation has shown that for isotropic turbulence the rate of energy dissipation is given by

$$e=15\,\nu\left(\frac{\partial \bar{u}}{\partial x}\right)^2$$

He defined a length scale $\lambda$ called the Taylor microscale such that

$$\left(\frac{\partial \bar{u}}{\partial x}\right)^2=(u'^2/\lambda^2)$$

where $u'$ is the r.m.s. fluctuating velocity. He also introduced a Turbulent Reynolds number $R_\lambda$ based on $\lambda$ (Taylor microscale) and defined $R_\lambda=u'\lambda/\nu$ where $\nu$ is the kinematic viscosity of the fluid.

Kolmogoroff has proposed that for a large Turbulent Reynolds number the fluid has a universal character, and the local small scale eddies of turbulent motion are isotropic whether the large scale eddies are isotropic or not. The motion at very small scales is chiefly governed by the viscous forces and the amount of energy handed down to them for the larger eddies. He derived from the universal equilibrium theory microscale values of length $\eta$, velocity $U_\eta$ and time $\tau_\eta$ based on $e$ and $\nu$ only.

The Kolmogoroff scales as shown in Fig. 11.4. are defined as

$$\eta=\left(\frac{\nu^3}{e}\right)^{1/4}=\lambda 15^{-1/4}\,R_\lambda^{-1/2}$$

$$U_\eta=(e\nu)^{1/3}=\frac{\nu}{\eta}=15^{1/4}\frac{u'}{R_\lambda^{1/2}}$$

$$\tau_\eta=\left(\frac{\nu}{e}\right)^{1/2}=\frac{\eta}{U_\eta}=\frac{\lambda}{15^{1/2}\,u'}$$

## Effect of Flow Velocity and Turbulence on Turbulent Burning Velocity

Turbulent flame propagation parameters used for the correlation of turbulent burning velocity, as proposed in the literature by various investigators, are different in different cases and they either contain apparatus dependent terms (duct diameter, bar width of the turbulence generating screen, and mesh size) or mixed chemical and turbulence parameters ($S_u$, $u'$, and $l$).

Figure 11.5 shows the effect of the intensity of turbulence on the turbulent burning velocity using equations as indicated besides the curves (for equations, see flame theories). It is seen that with an increase in the intensity of turbulence, there is a substantial increase in the turbulent burning velocity.

Figure 11.6 shows the effect of an increase in flow velocity at various intensities of turbulence. It is observed that the turbulent burning velocity

increases linearly with an increase in the inlet flow velocity. The slope of the line increases with an increase in the intensity of turbulence. At zero

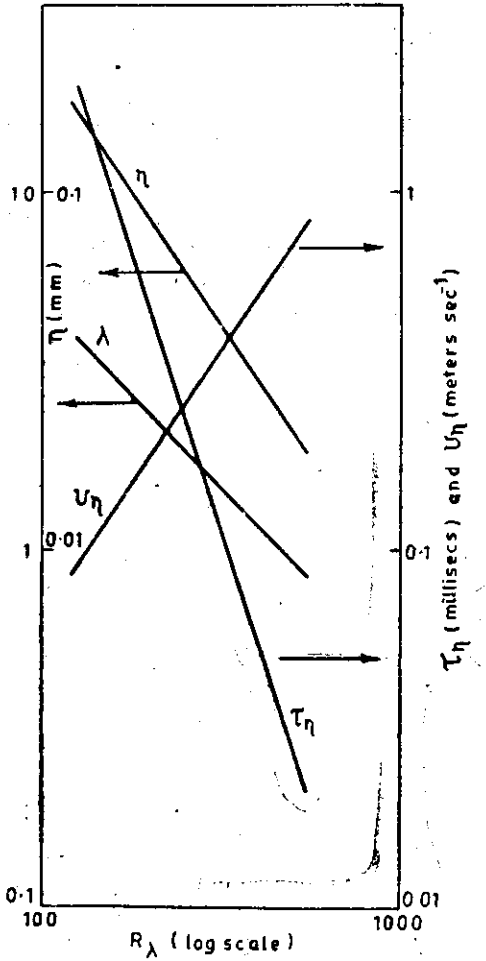


**Fig. 11.4 Variation of Kolmogoroff scale with $R_\lambda$, $l$=10 mm, $\upsilon$=1.56×13$^{-6}$ m$^2$s$^{-1}$.**

inlet flow velocity, all lines converge at a single point corresponding to the laminar burning velocity. Figure 11.5 shows the effect of Reynolds number on $S_T$ for three fuels—acetylene, ethylene and propane—and four different diameters of burners.

Bollinger and Williams[2] derived an empirical relation (Eq. (11.6)) which gives the effect of the diameter of the burner and Reynolds number on the turbulent burning velocity. Wohl et al.[11] proposed the following



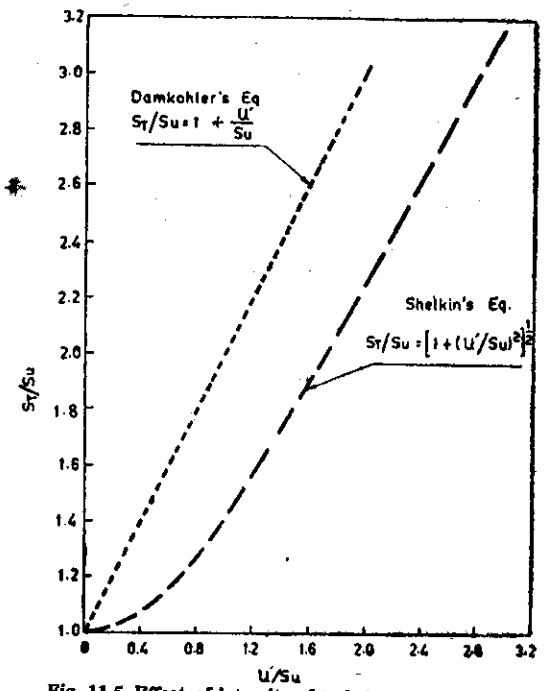


**Fig. 11.5 Effect of intensity of turbulence on $S_T/S_U$.**

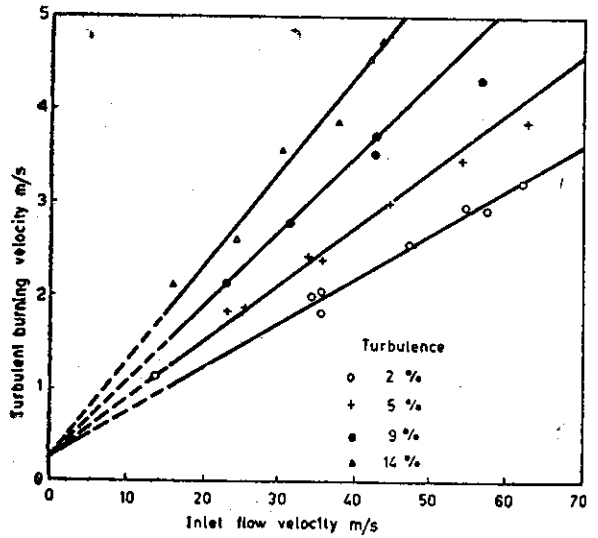


**Fig. 11.6 Effect of inlet flow velocity on turbulent burning velocity (With permission of Combustion Institute, from *Combustion and Flame*, Vol. 10 p. 364, 1966.)**

empirical relation representing the effect of inlet flow velocity and intensity of turbulence on the ratio $\frac{S_T}{S_u}$:

$$\frac{S_T}{S_u} = 1 + 26.2\,\frac{u'}{U} + 1.4\left(\frac{U}{24}\right)^{1.12} \qquad (11.19)$$

where $U$ is the inlet flow velocity in ft/s.

Lefebvre and Reid[12] proposed the empirical equation

$$\frac{S_T}{S_u} = 1 + 0.43\,u' + 0.04\,U \qquad (11.20)$$

where $U$ and $u'$ are in ft/s. Both these experimental results were obtained using propane-air mixtures on enclosed flames in a horizontal duct, the flames supported by the bluff body and pilot burner respectively.

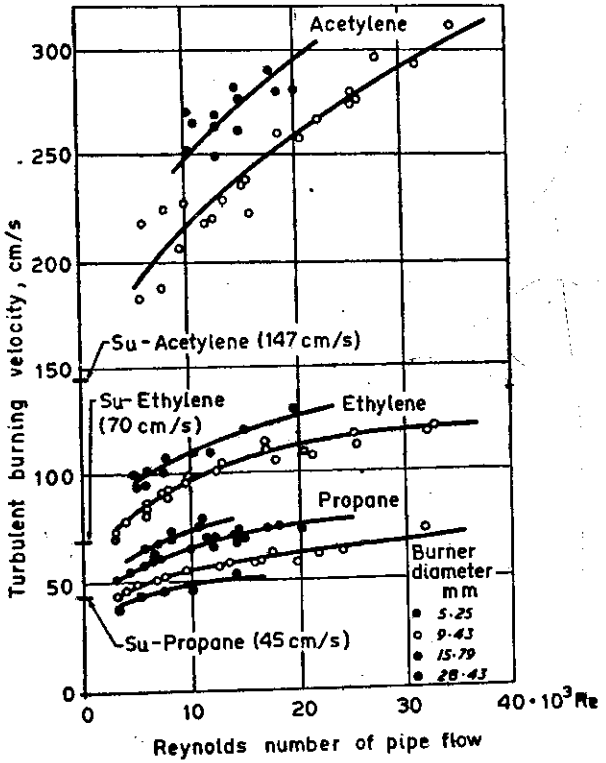


**Fig. 11.7 Variation of turbulent burning velocity with Reynolds number. (After Bollinger and Williams.)**

## 11.4 STRUCTURE OF A TURBULENT FLAME

In the case of a laminar flame most of the fuel is burned in a very thin reaction zone, hardly 10 to 20% of the heat is liberated in the preheat



zone and after the luminous flame front. Figure 9.1 representing the structure of a laminar flame is enlarged to show the exact concentration and temperature profiles, otherwise the gradients of concentration and temperature curves at the ignition point are very steep. However, in the case of a turbulent flame a thick brushy flame is obtained. Most of the reaction takes place between the visible inner and outer cones. Approximately 2 to 3% of the reaction takes place before the visible inner cone and about 80 to 90% of the fuel is consumed before the outer visible cone. Inside the thick visible flame the reaction proceeds smoothly. Figure 11.8 shows the concentration profile of a turbulent flame in a burner. At the bottom of the curve two visible cones are drawn. The curve

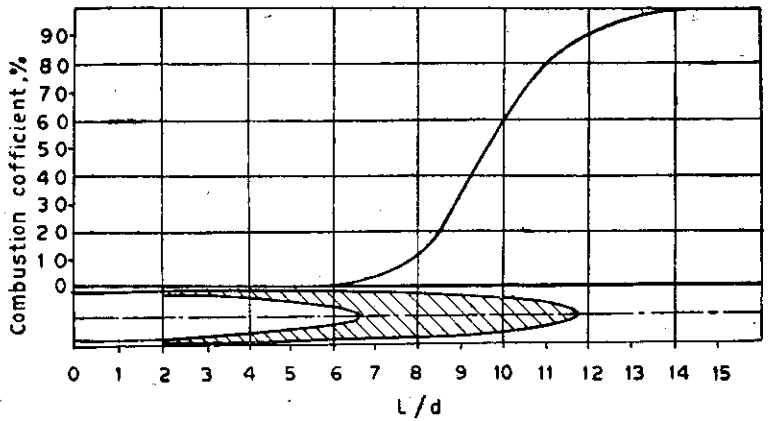


**Fig. 11.8 Structure of a turbulent flame.**

represents the time average value of the concentration. Assuming the visible flame model, the concentration profile at a particular plane and at any instant resembles a laminar flame profile. The position of the reaction zone keeps shifting between the inner and outer cones with respect to time and location. The above picture is essentially for large scale turbulence.

## 11.5 TURBULENT FLAME THEORIES

No rigorous mathematical description of a turbulent flame is yet available nor does it seem likely that it will be available in the near future. The theoretical considerations are regarding the physical picture of a turbulent flame and enable the prediction of the effect of turbulence on burning velocity. There are two models of a turbulent flame: the first was proposed by Damköhler[1] who suggested a wrinkled flame, the mixture

burning at the surface only, and the second by Summerfield[7] based on the theory that the gas burns throughout the volume due to turbulence.

Damköhler's model of the wrinkled flame is still considered better and is in accord with the experimental observations made by most workers. He separately considered the effect of large-scale and small-scale turbulence. For large-scale (greater than flame thickness) turbulence, Damköhler suggested that due to velocity fluctuations the plane flame front is distorted at different points. At some places, the local flow velocity exceeds the laminar burning velocity resulting in a conical bunsen type flame. If, at some other places, the local flow velocity is less than the laminar burning velocity, there will be a tendency for the flame to flash again, resulting in a conical shape. Both the effects increase the flame area. The concept can be well understood by Fig. 11.9.

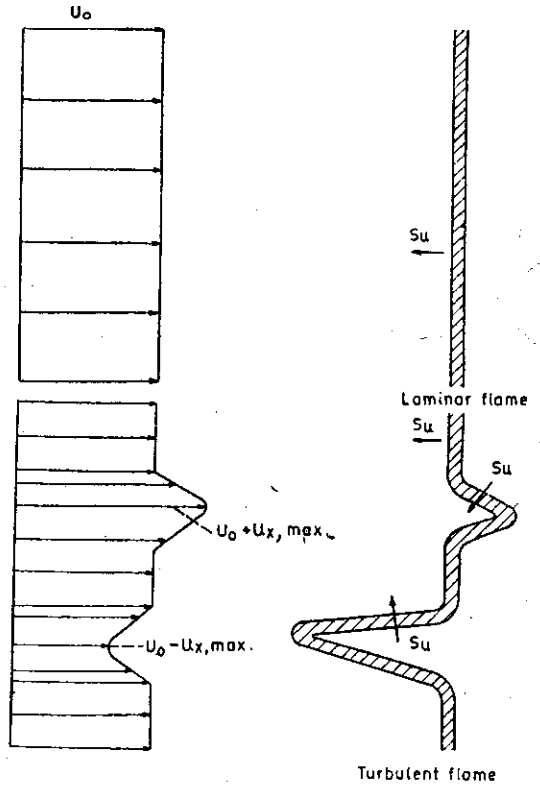


**Fig. 11.9 Model of combustion wave in turbulent flow. (After Damkohler.)**

Damköhler suggested that the structure of the flame front remains essentially the same and the increase in the burning velocity is attributed



to the increase in the flame surface only. For the constant value of $S_u$ the increase in flame area will be proportional to the flow velocity. Hence for the mean flow through the turbulent flame

$$S_T \propto \sqrt{\overline{u_x^2}} \tag{11.21}$$

and if the scale of turbulence or mixing length is constant, then

$$S_T \propto \varepsilon \tag{11.22}$$

and since $\varepsilon \propto \mathrm{Re}$

therefore, $S_T \propto \mathrm{Re}$ (11.23)

for large-scale low intensity turbulent flame. However, experimentally Damköhler found

$$S_T \propto \sqrt{\mathrm{Re}} \tag{11.24}$$

for low Reynolds numbers

and $$S_T = a\,\mathrm{Re} + b \tag{11.25}$$

for higher Reynolds numbers. He attributed the constant $b$ for small-scale turbulence.

In case of small-scale turbulence, the flame is not wrinkled, but the diffusion and heat transfer rates are increased. From Semenov's equation for a laminar flame it may be written as

$$S \propto \sqrt{\frac{K_{\text{laminar}}}{c_p\,\rho_0}} \tag{11.26}$$

Since $\frac{k_{\text{laminar}}}{c_p \rho_0}$ = kinematic viscosity, therefore, $S_u \propto \sqrt{\nu}$ (11.27)

In turbulent flow, the eddy diffusivity $\varepsilon$ determines the turbulent heat transfer coefficient so that

$$\varepsilon = \frac{k_{\text{turbulent}}}{c_p\,\rho_0} \tag{11.28}$$

Therefore, it may be written

$$\frac{S_T}{S_u} = \sqrt{\frac{k_{\text{turbulent}}}{k_{\text{laminar}}}} = \sqrt{\frac{\varepsilon}{\nu}} \tag{11.29}$$

The above equation describes the effect of small-scale turbulence. However, the value of $\varepsilon$ changes across the burner. Therefore, Damköhler calculated the average turbulent burning velocity from a hypothetical flame shape. Theoretical values of $S_T$ were found to be higher than experimental values which he attributed to the mixing length being not so small as to be negligible.

Shchelkin[16] extended the mechanism proposed by Damköhler. He

considered the effect of molecular transport also apart from the diffusion in case of fine scale turbulence, and proposed

$$S_T = S_u \sqrt{\frac{l+\varepsilon}{D}} \tag{11.30}$$

where $D$ is the molecular diffusivity.

For large-scale turbulence, Shchelkin agreed with Damköhler's model, but took the height of the turbulent flame cone to be proportional to the intensity of turbulence, equal to $l\sqrt{\overline{u^2}}/S_u$. The expression for the ratio $S_T/S_u$ is written as

$$\frac{S_T}{S_u}\sqrt{1+\left(\frac{B\sqrt{\overline{u^2}}}{S_u}\right)^2} \tag{11.31}$$

where $B=2$ for a cone. The equation reduces to Damköhler's equation for

$$\left(B\sqrt{\overline{u^2}}/S_u\right)^2 >> 1$$

or for

$$\sqrt{\overline{u^2}}\, S_u \tag{11.32}$$

For large intensities of turbulence, Shchelkin suggested

$$S_T \propto \sqrt{\overline{u^2}} \tag{11.33}$$

and is independent of $S_u$, i.e., it is only dependent on the intensity of turbulence and is independent of the fuel type, air/fuel ratio, etc. Shchelkin proposed that for very high intensities the wrinkled flame front breaks up into small balls burning independently, their size reduces as they move downstream and as the mixture inside burns up (Fig. 11.10). Karlovitz[3] also supported Damköhler's wrinkled flame model but argued that the turbulent burning velocities measured by the angle method on burners gave much higher values than the theoretically

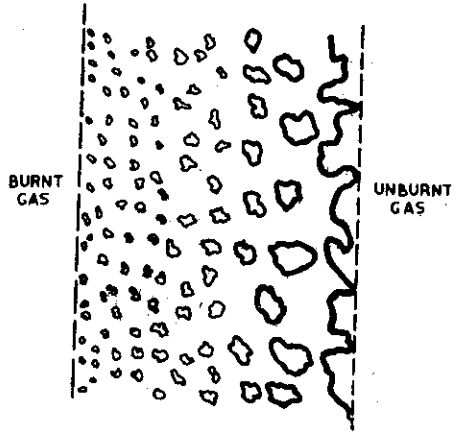


**Fig. 11.10 Structure of combustion wave in a highly turbulent flow. (After Shchelkin.)**



computed values of $S_T$ which he attributed to the flame generated turbulence. He found that for weak turbulence

$$S_T = S_u + u' \tag{11.34}$$

and for strong turbulence

$$S_T = S_u + (2\, S_u\, u')^{0.5} \tag{11.35}$$

He suggested that the value of $S_T$ is much more dependent on $S_u$ rather than on the intensity of turbulence even at the highest level of turbulence.

Scurlock and Grover[17] considered the wrinkled flame model for large-scale turbulence. They also emphasized the effect of flame generated turbulence, and assumed that the passage of an eddy through a plane flame front produces wrinkling. The effect of passage of a single eddy of different intensity from a plane flame front is shown in Fig. 11.11. Figures 11.11(a), 11.11(b) and 11.11(c) represent the intensities $u'/S_u =$

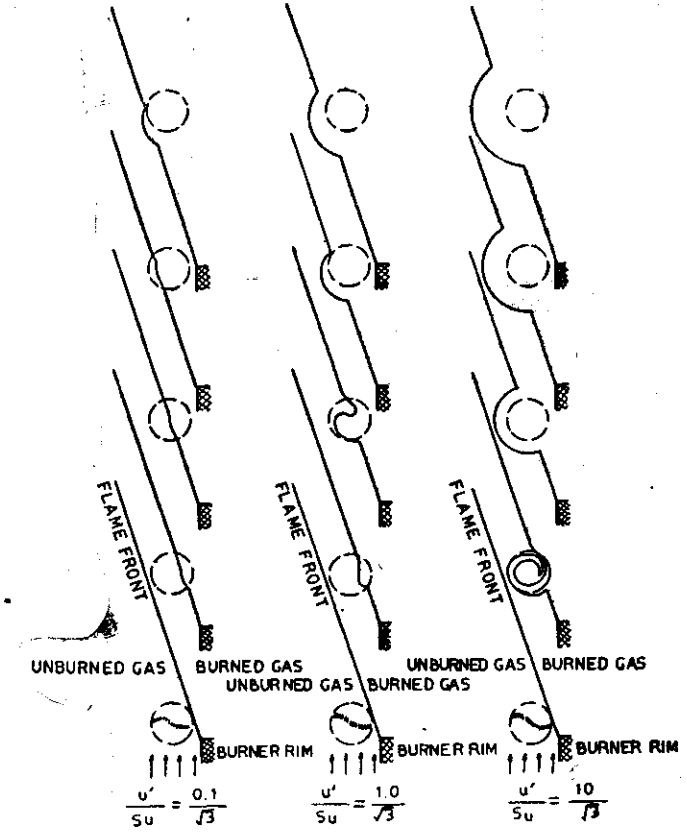


**Fig. 11.11 Effect of passage of single eddies of different intensity across a flame front. (With permission of the Combustion Institute from *Fourth Symposium International) on Combustion*, 1953, p. 646.)**

0.1 $\sqrt{3}$, 1.0/$\sqrt{3}$, and 10/$\sqrt{3}$ respectively. The two-dimensional eddy is assumed to have a rotary motion, with the velocity components superimposed on the mean flow along any diameter corresponding to a sine wave. The effect of intensity on the degree of distortion with time, the motion of the disturbed flame element up along the flame front after some time, and the degree of distortion after the passage of the eddy are shown clearly. Figure 11.12 shows the flame fronts at the initial condition after

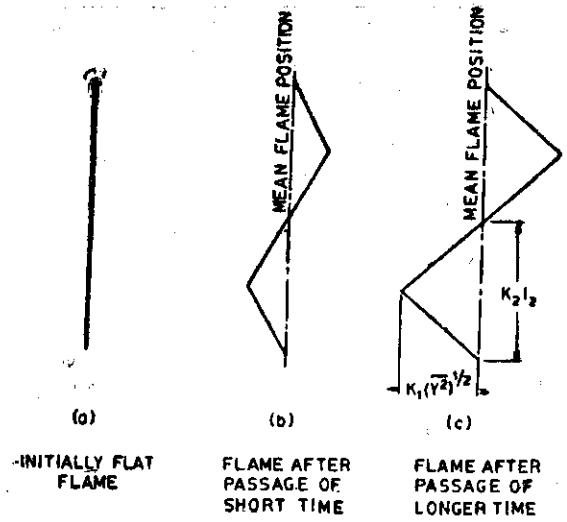


**Fig. 11.12 Diagram showing wrinkling of flame front with passage of time. (With permission of the Combustion Institute from *Fourth Symposium (International) on Combustion*, 1953, p. 651.)**

a short time has elapsed and after the passage of a longer period of time. Scurlock and Grover assumed that the average height of the wrinkles is proportional to the root mean square displacement $\sqrt{\overline{y^2}}$ of the flame element from the mean flame front position and the average base width of these wrinkles is proportional to the eulerian scale $l_2$, or the average height$=K_1\sqrt{\overline{y^2}}$ and the average base width$=K_2 l_2$, where $K_1$ and $K_2$ are the proportionality constants. Scurlock and Grover suggested the following equation:

$$\frac{S_T}{S_u}=\frac{A_T}{A_L}=\left\{1+C_1\left(\frac{\overline{y^2}}{l_2}\right)\right\}^{1/2} \tag{11.36}$$

where $C_1=4\ K_1^2/K_2^2$

They suggested three effects to be of importance in determining $\overline{y^2}$, and thus in determining the area of the wrinkled flame. These are:

(1) Eddy diffusion, associated with turbulence in the unburned gases, which tends to increase $\overline{y^2}$.



2. Propagation of the flame into the unburned gases which tends to reduce $\overline{y^2}$.
3. Instability, shear, and eddy diffusion, resulting from flame generated velocity gradients produced by the pressure drop across the combustion zone, associated with the density decrease of the gases, upon passage through the flame front, which tends to increase $\overline{y^2}$.

Scurlock and Grover have given mathematical expressions to show the effect of the above three factors on $\overline{y^2}$, or we can say, on the turbulent burning velocity. They concluded that eddy diffusion tends to increase $\overline{y^2}$, the rate of area increase being made greater by increasing $u'$, by decreasing $S_u$ and by decreasing $l_2$. Flame propagation causes $A_T/A_L$ to approach a maximum limiting value which is a direct function of $u'/S_u$. However, in most cases, turbulent elements do not reach this asymptote because of the short time available. The maximum flame generated turbulence $u'_m$, increases approximately as the three halves power of $\rho_u/\rho_b$ and the first power of the unburned gas velocity $U$. For confined flames (generally $U \gg S_T$), $u'_m$ is much higher than $u'$ and is expected to control $S_T$ for unconfined flames ($U = S_T$), often $u' = u'_m$.

The effect of flame generated turbulence was not considered by early workers like Damköhler, while Scurlock[6] first gave the effect of flame generated turbulence for enclosed flames. Because of the increased flow velocity of the burned gas due to expansion, a shear force between the unburned gas and burned gas is produced, creating a highly turbulent flow. Figure 11.13 shows the shear regions which are responsible for

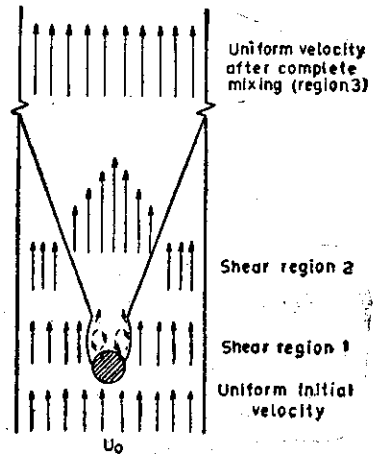


**Fig. 11.13 Shear regions generating turbulence in a rod stabilized flame. (After Scurlock.)**

generating turbulence. In the case of open burner flames, the burned gases are free to expand. Karlovitz suggested that in open flames, the expansion of the burned gas from the flame which is oriented at random

angles, produces random fluctuations in the unburned gas, thus increasing the turbulence intensity. The turbulence increases as the burning proceeds from the base to the tip of the flame. Karlovitz, based on the expansion ratio, computed the flame generated turbulence as

$$\sqrt{\overline{u^2}}=(1/\sqrt{3})(\rho_u/\rho_b-1)\,S_u \qquad (11.37)$$

However, many experimental results still conform to the simple model of Damköhler, without exhibiting any important generation of additional turbulence by the flame.

Summerfield first suggested that the turbulent flame is not a surface phenomenon. He considered the turbulent flame to be a deep zone of chemical reactions as suggested by Shchelkin for high intensity turbulence. Spalding also suggested that instead of the wrinkled flame, flame propagation in turbulent flow is determined by the rate of entrainment of cold mixture by hot gases. He did not give any specific equation for $S_T$ but suggested that $S_T$ is independent of the scale of turbulence or intensity of turbulence, but is directly proportional to the inlet velocity of the mixture. He further suggested that the turbulent burning velocity is independent of the laminar burning velocity, except indirectly through a relation between $S_u$ and the density ratio $\rho_u/\rho_b$. Shetinkov[18] assumed that both surface and homogeneous burning may take place in a turbulent flame. However, he suggested that most fuels burn in microvolumes homogeneously.

From the above review of turbulent flame theories it is observed that most of the investigators have focussed attention on the influence of intensity of turbulence on the turbulent burning velocity, although Damköhler did introduce the mixing length concept and the macroscale of turbulence for the effects of small-scale turbulence. Efforts are presently in progress to determine the influence of scale independently at various levels of intensity of turbulence.

Ballal and Lefebvre[19,20] conducted experiments on enclosed flames using premixed propane-air mixtures at atmospheric pressure in a duct 31 cm long and 10×10 cm cross-section. By suitable modifications to grid geometry and flow velocity, the scale and intensity of turbulence were varied independently in such a manner that their influence on burning velocity and flame structure could be studied. They identified three distinct regions, each having different characteristics in regard to the effect of scale on turbulent buring velocity. This 3-region model is supported by the experimental data briefly presented below.

**Region 1** $u' < 2S_u$ This is generally a region of low turbulence intensity and low inlet velocity. Fig. 11.14 shows that $S_T/S_u$ increases linearly with an increase in the integral scale of turbulence $L$. From examination of the schlieren photographs and with burning velocity measurements this region was identified to depict low turbulence. The authors suggested that the buring velocity is increased due to the effect of turbulence by



the wrinkling of the flame and thus extending its surface area. The experimental data can be correlated by the expression:

$$\left(\frac{S_T}{S_u}\right)^2=1+0.125\left(\frac{u'L}{S_u\delta_1}\right)^2$$

when $u' \ll 2S_u$ and $\eta > \delta_1$.

$\eta$ is the Kolmogoroff scale which can loosely be said to represent the smallest eddy size of dissipation as shown in Fig. 11.15.

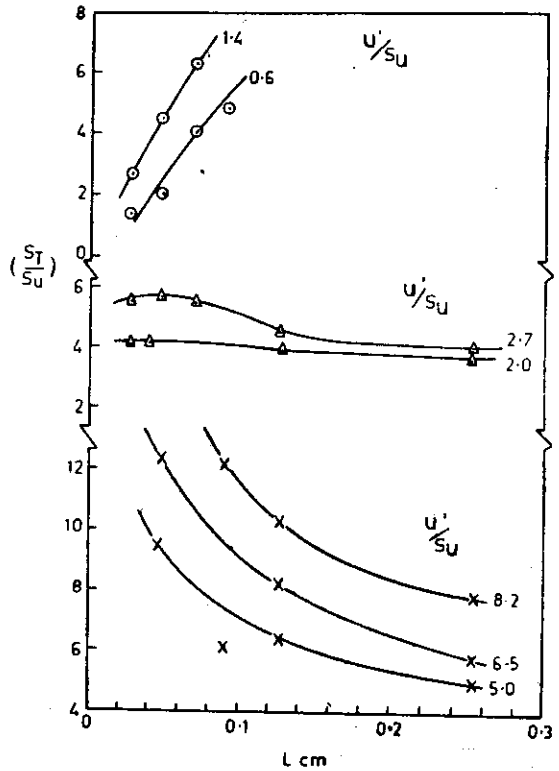


**Fig. 11.14 Influence of turbulence scale on the ratio of turbulent to laminar burning velocity.**

**Region 2:** $u' \simeq 2S_u$ In this region of transition the turbulent burning velocity is virtually independent of the integral scale $L$ and laminar burning velocity or the physico-chemical factor. Figures 11,14 and 11.15 show clearly that $S_T/S_u$ becomes independent of the scale when $u' \simeq 2S_u$.

**Region 3:** $u' > 2S_u$ The increase in intensity of turbulence is usually accompanied by a decrease in scale. This region of strong turbulence indicates that the turbulent burning velocity depends on the laminar burning velocity and tends to decrease with the increase of scale. As

$\eta < \delta_l$, the effect of strong turbulence is such that the eddies entering the reaction zone are too small to produce appreciable wrinkling of the flame surface. It is suggested that in this region high burning rates are observed

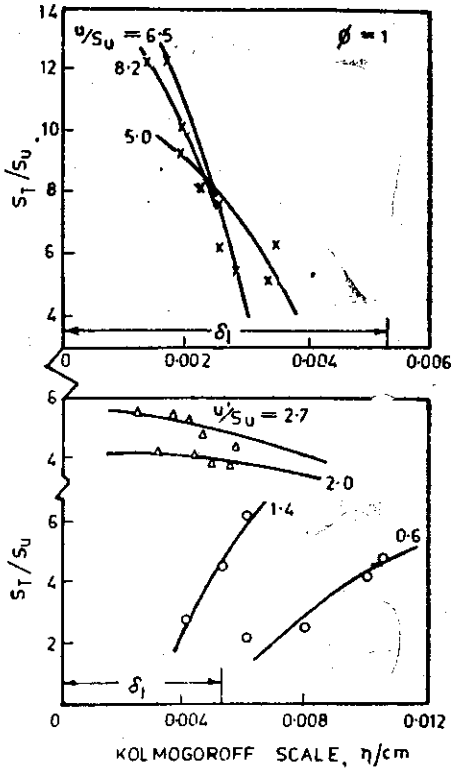


**Fig. 11.15 Influence of Kolmogoroff scale on turbulent burning velocity.**

and combustion in depth takes place. The increase in the level of noise noticed in this region may be due to the laceration of the flame surface into small pieces, and the entrainment of pockets of the unburned mixture in the products of combustion of the extended reaction zone. The experimental values of turbulent burning velocity are predicted satisfactorily by the correlation:

$$\left(\frac{S_T}{S_u}\right)^2 = 10^{-4}\left(\frac{u'^2}{L}\right)$$

The effect of the integral scale on turbulent burning velocity may be summarized as follows:

1. $u' \ll 2S_u$, $\dfrac{S_T}{S_u} \propto L$



2. $u' \cong 2S_u$, $\dfrac{S_T}{S_u}$ independent of $L$, and

3. $u' > 2S_u$, $\dfrac{S_T}{S} \propto \dfrac{1}{\sqrt{L}}$.

Andrews et al. [21,22] measured turbulent burning velocities of methane-air and ethylene-air mixtures at 1 atm pressure in an explosion vessel equipped with four fans driven by air turbines. The authors suggest a rational basis for the correlation of burning velocity data by plotting the ratio $S_T/T_u$ against turbulent Reynolds number $R_\lambda = \dfrac{u'\lambda}{\nu}$ in which $u'$ is the r.m.s. turbulent velocity, $\lambda$ is the Taylor microscale and $\nu$ is the kinematic viscosity. No equations or correlations are proposed by them but they conclude that the wrinkled laminar flame can exist at low values of $R_\lambda$ ($<100$) and its impossibility at higher values of $R_\lambda$. Their graphical correlation as shown in Fig. 11.16, does not substantiate the above results very clearly to indicate the change in the structure of the flame.

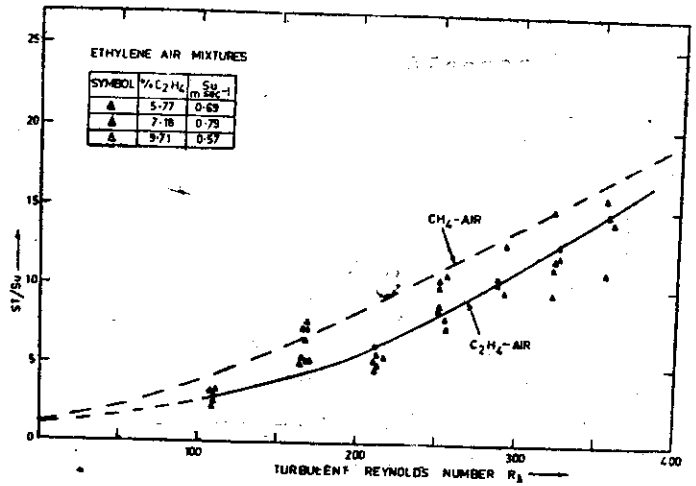


**Fig. 11.16 Variation of $S_T/S_u$ with $R_\lambda$ for different $C_2H_4$-air mixtures. Broken curve is for $CH_4$-air mixtures.**

Abdel-Gayed and Bradley[23] have proposed another correlation involving $R_l = \dfrac{u'l}{\nu}$ where $l$ is the length scale of turbulence, $u'$ is the r.m.s. turbulence velocity, and $\nu$ is the kinematic viscosity. It is suggested that when $\dfrac{S_u}{u'} > 1$, a wrinkled flame regime is possible to the right of the broken line as shown in Fig. 11.17. A summary of the important models on turbulent flame propagation is given in Table 11.1.

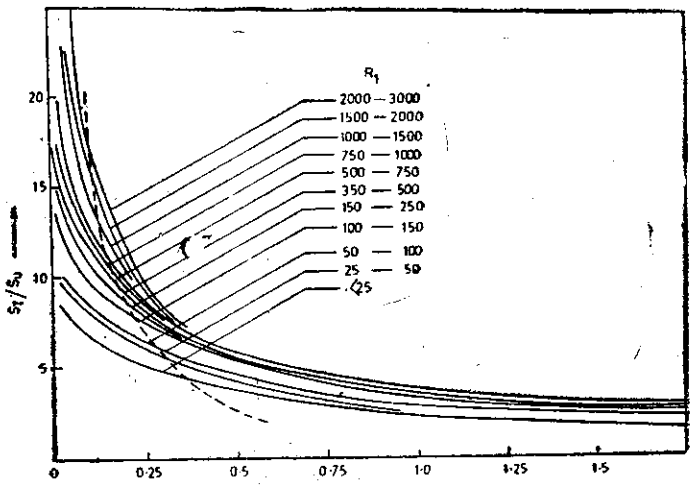


**Fig. 11.17** Variation of $S_T/S_u$ with $S_u/u'$ for different values of Re.

**TABLE 11.1**

**Summary of the Important Models on Turbulent Flame Propagation**

| *Authors and Reference* | *Postulated Flame Structure/ Assumptions* | *Equations/Criteria* | *Conclusions/Remarks* |
|---|---|---|---|
| 1 | 2 | 3 | 4 |
| Damköhler[1] | Wrinkled laminar flame | $\frac{S_T}{S_u}=1+\frac{u'}{S_u}$ | $S_T$ independent of the scale of turbulence |
| | (a) Large-scale turbulence $l_2 \gg \delta_1$ | $S_T = u'$ when $u' \gg S_u$<br>$S_T \propto$ Re | |
| | (b) Small-scale turbulence $l_2 < \delta_1$<br>$\delta_1$=thickness of laminar reaction zone | $\frac{S_T}{S_u}=\sqrt{\frac{\varepsilon}{\nu}}$ where $\varepsilon$ = Eddy diffusivity | $S_T$ increases due to rate of transport processes |
| Shchelkin[17] | (a) Wrinkled conical laminar flame | | |
| | (i) $u' \leqslant S_u$, $l_2 >> \delta_1$ | $\frac{S_T}{S_u}\left[\ 1+B\,(u'/S_u)^2\ \right]^{1/2}$<br>where $B$=constant | $S_T$ independent of scale of turbulence |
| | (ii) $u' \gg S_u$, $l_2 \gg \delta_1$<br>Surface split into separate eddies (islands) | $S_T \leqslant u'$ | |
| | (b) Small scale | $\frac{S_T}{S_u}=\sqrt{1+\frac{\varepsilon}{\nu}}$ | |

(contd)

**TABLE 11.1 (contd)**

| 1 | 2 | 3 | 4 |
|---|---|---|---|
| Frank-Kamenetsky[24] | Surface split into separate islands burning with $S_n$ | $S_T \simeq (S_n\, u')^{1/2}$ | |
| Leason[25] | Turbulent flow composed of eddies (dia $= l$)<br>Sinusoidal velocity distribution through each eddy when $lu'/2S_u > 1$ | $\frac{S_T}{S_u} = \left[1 + \left(\frac{2u'}{S_u}\right)^2\right]^{1/2}$ | (i) Turbulence increases flame area<br>(ii) Turbulence increases rate of diffusion of active species or heat |
| Karlovitz[3] | Wrinkled laminar flame: additional turbulence generated by flame | | (i) $S_u$ remains a more important factor than turbulence intensity, even for $u' \gg S_u$ |
| | (i) $l_2 \gg \delta_1$ without flame generated turbulence $u' << S_u$ | $S_T = S_u + u'$ | |
| | (ii) $u' \gg S_u$ for strong turbulence.<br>$u'$ is increased by $u''$<br>$u'' = \frac{S_u}{\sqrt{3}}\left(\frac{\rho_u}{\rho_b}\right)$ | $S_T = S_u + (2S_u\, u')^{1/2}$ | (ii) Flame generated turbulence intensity is much greater than $u'$ for strong turbulent flow |
| Scurlock and Groves[17] | Wrinkled laminar flame with generated turbulence | $\frac{S_T}{S_u} = \left[1 + C\left(\frac{Y}{l_2}\right)^2\right]^{1/2}$<br>$C$ = constant<br>$\sqrt{\overline{Y^2}}$ = r.m.s. displacement dependent on eddy diffusion, flame propagation and flame generated turbulence. | (i) $S_T$ dependent on turbulence scale<br>(ii) For high velocity confined flames, flame generated turbulence far outweighs initial turbulence |

| 1 | 2 | 3 | 4 |
|---|---|---|---|
| Wohl et. al.[11] | Wrinkled laminar flame $l_2 \gg \delta_1$ | $\frac{S_T}{S_u} = 1 + 26.2\,\frac{u'}{U} + 1.4\left(\frac{U}{24}\right)^{1.18}$ | $S_T$ independent of $l_2$ |
| Sokolik[26] | Model of small eddies gradually burning up in laminar flames | $S_T = 1/2u\left(1 + \frac{\rho_u}{\rho_b}\right)$<br>where $u$ = eddy velocity | |
| Summerfield[7] et al. | Thermal theory: model applies irrespective of scales | $S_T/S_u = \frac{\varepsilon}{\nu}\,\frac{\delta_1}{\delta_T}$<br>$\delta_T$ = thickness of turbulent reaction zone | $\frac{S_T\,\delta_T}{\varepsilon}$ is a function of air-fuel ratio only |
| Kovasznay[27] | Combination of wrinkled and distributed reaction zone model | $D = \frac{u'\delta_1}{S_u\lambda}$ | (i) L <1 Wrinkled laminar flame model<br>(ii) L >1 Distributed extended reaction zone |
| Povinelli and Fuhs[28] | Large-scale turbulence wrinkles flame surface, small-scale influences transport rates | $\frac{S_T}{S_u} = \left[1 + \frac{u'}{S_u}\right]\int_0^{n_0} F(n)dn + \left[1 + \frac{\varepsilon}{\nu}\right]\int_{n_0}^{\infty} F(n)\,dn$ | |
| Bhaduri[29] | Combination of wrinkled and distributed reaction zone models | $\frac{S_T}{S_u} = \frac{u'\,l_2}{U\,d}$ | Gradual transition from wrinkled laminar structure to distributed reaction zone |

(contd)

Table 11.1 (contd)

| 1 | 2 | 3 | 4 |
|---|---|---|---|
| Kozachenko[20] | Wrinkled laminar flame with additional turblence generated by flame | $S_T = S_u'' + u'' + u''$<br>$\frac{S_T}{S_u} = 1 + \frac{u'}{S_u} + \left[\frac{\rho_u/\rho_b - 1}{\sqrt{3}}\right] \left[1 - \left(\frac{S_u}{S_u + u'}\right)^2\right]^{0.5}$<br>$\frac{u'}{S_u} \gg 1$<br>$\frac{S_T}{S_u} = \frac{u'}{S_u} + \left[\frac{\rho_u/\rho_b - 1}{\sqrt{3}} + 1\right]$ | |
| Ballal and Lefebvre[19,20] | Combination of wrinkled laminar and distributed reaction zone | | (i) Wrinkled laminar flame |
| | (ii) $\frac{S_T}{S_u} \propto L$ when $\frac{u'}{S_u} < 2.0$<br>$\eta > \delta_1 L = \frac{U}{8} \underset{n \to 0}{\text{Lim}} E(n)$<br>$\eta$ = Kolmogoroff scale | $\left(\frac{S_T}{S_h}\right)^2 = 1 + 0.125 \left(\frac{u' L}{\delta_1 S_u}\right)^2$ | |
| | (ii) $S_T/S_u$ independent of scale when $u'/S_u \geq 2.0$ | | (ii) Transition |
| | (iii) $S_T/S_u \propto 1/\sqrt{L}$ when $u'/S_u > 2.0$, $\eta < \delta_1$ | $(S_T/S_u)^2 = 10^{-4} (u'/L)^2$ or $S_T/S_u = 0.5\ u'\ S_l/S_u\ \eta$ | (iii) Distributed reaction zone |

| 1 | 2 | 3 | 4 |
|---|---|---|---|
| Andrews[22,23] et al. | Combination of wrinkled laminar and distributed reaction zone models | $R_\lambda = u'\lambda/\nu$ | $R_\lambda < 100$ perhaps wrinkled laminar flame |
| Spalding[8] | Flame propagation depends on entrainment of cold mixture by hot gas | None applicable | (i) $S_T$ independent of scale of turbulence and % turbulence<br>(ii) Proportional to inlet velocity |
| Wright and Zukoski[21] | Flame propagation dependent on inlet flow velocity | None applicable | Rate of flame spreading from a bluff body was found to be remarkably independent of approach stream speed, temperature fuel-air ratio, fuel type, as long as flame is turbulent and flow subsonic everywhere |
| Lefebvre and Reid | Wrinkled laminar flame model | $S_T/S_u = 1 + 0.43u' + 0.04\ U$ | Flame spreading rate varied with % turbulence and fuel-air ratio at all velocities |
| Sanematsu[23] | Wrinkled laminar flame model | $S_T/S_u = \frac{u'}{S_u} \cdot \frac{l}{b} \cdot n \cdot \phi^n$<br>$b$ = screen mesh diameter<br>$\phi$ = equivalence ratio<br>$n$ = constant | |

## REFERENCES


1. G. Damkohler, "The effect of turbulence on the flame velocity in gas mixtures," *NACA TM*, 1947 (1112).
2. L.M. Bollinger, and D.T. Williams, *NACA Report*, 1949 (932), (*Supercedes NACA TN 1707*).
3. B. Karlovitz, D.W. Denniston, Jr., and F.E. Wells, *J. Chem. Phys.*, 1951, 19: 541.
4. Hottel, H.C., Williams, G.C., and Levine, R.S., *'Fourth Symposium (International) on Combustion'*, Williams and Wilkins, Baltimore, 1953, 636-644.
5. W.R. Mickelsen, *M.S. Thesis*, Case Inst. of Tech., 1953.
6. A.C. Scurlock, *Meteor Rept Mass. Inst. Technol.*, No. 19, 1948.
7. M. Summerfield, S.H. Reiter, V. Kebely, and R.W. Mascolo, *Jet Propulsion*, 1955, 25 : 377.
8. D.B. Spalding, *Seventh Symposium (International) on Combustion*, Butterworths, London, 1959.
9. J.P. Longwell, *Fourth Symposium (International) on Combustion*, Williams and Wilkins, Baltimore, 1953, p. 90.
10. G.C. Williams, H.C. Hottel, and A.C. Scurlock, *Third Symposium on Combustion and Flame and Explosion Phenomena*, Williams and Wilkins, Baltimore, 1949, p. 21.
11. K. Wohl, L. Shore, H. Von Rosenberg, and C.W. Weil, *Fourth Symposium (International) on Combustion*, Williams and Wilkins, Baltimore, 1953, 620-635.
12. A.H. Lefebvre, and R. Reid, *Combustion and Flame*, 1966, 10: 355-366.
13. G.W. Culshaw, and J.E. Garside, *Recent Studies of Aerated Burner Flames*, Inst. Gas. Eng. (London), Inst. Gas Res. Fellowship Rep. 1946-47 (Review papers from period 1943-46 including those of Delbourg, Heiligenstaedt, and Vasilesco).
14. S.A. Goldenberg, and V.S. Pelevin, *Seventh Symposium (International) on Combustion*, Butterworths, London, 1959, p. 590.
15. G.I. Taylor, *Proc. Roy. Soc. London*, 1935 A 151 : 421.
16. Shchelkin, K.I., *J. Tech. Phys.* (USSR), 1913, 13: (9-10), 520-30, English Translation, *NACA Tech. Memo.* 1947. (1110).
17. A.C. Scurlock, and J.H. Grover, *"Fourth Symposium (International) on Combustion*, Williams and Wilkins, Baltimore, 1953, 645-658.
18. E.S. Shetinkov, *Seventh Symposium (International) on Combustion*, Butterworths, London, 1959, p. 583.
19. Ballal, D.R. and Lefebvre, A.H., "Turbulence effects on enclosed flames", *Acta Astronautica*, 1(n 3-4): 471-483, March-April 1974, Pergamon Press, New York.
20. Ballal, D.R. and Lefebvre, A.H., "The structure and propagation of turbulent flames", *Proc. of the Royal Society of London*, 1975, A 344 : 217-234.
21. Andrews, G.E., Bradley, D. and Lwakabamba, S.B., *Fifteenth Symposium (International) on Combustion*, The Combustion Institute, 1974, 655-664.
22. Andrews, G.E., Bradley, D. and Lwakabamba, S.B., *Combustion and Flame*, 1975, 24: 285.
23. Abdel-Gayed, R.G. and Bradley, D., *Sixteenth Symposium (International) on Combustion*, The Combustion Institute, 1976, p. 1725.
24. Frank Kamenetskii, D.A., "Contribution to the Theory of Microdiffusive Turbulent Combustion", *Trudy Nauchno-Issledovatel's Kogo Instituta (7) Oboronglz*, 1946.
25. Leason, D.B., *Fuel*, 1951, 30: 233.





26. Sokolik, A.S., *The Experimental Basis of the Theory of Turbulent Combustion in Turbulent Flow*, L.N. Khitrin Ed., Moscow 1959, English Translation IPST 1963, p. 54.
27. Kovasznay, L.S.G., *Jet Propulsion*, 1956, 26: 485.
28. Povinelli, L.A. and Fuhs, A.E., *Eighth Symposium (International) on Combustion*, Williams and Wilkins, Baltimore, 1962, p. 554.
29. Bhaduri, D., *Effect of Turbulence on Premixed Gaseous Flames—CMERI Report*, 1968, B6.
30. Kozachenko, L.S., *Eighth Symposium (International) on Combustion*, Williams and Wilkins, Baltimore, 1962, p. 567.
31. Wright, F. H. and Zukoskii, E. E., *Eighth Symposium (International) on Combustion*, Williams and Wilkins, Baltimore, 1962, p. 933
32. Sanematsu, H., *Combustion and Flame*, 1969, 13: 1.

# 12

# FLAME STABILITY

Flame stabilization is accomplished by the interaction of the flame and flow in a burner. In order to understand this interaction, an analysis of open or confined flames on bunsen-type burners will be helpful. In ramjet type combustion chambers, flame stability is achieved by attaching the flame to a simple device known as a bluff body, e.g., a rod or a plate placed normal to the flow. The discussion of flame stabilization presented in this chapter is limited to open burner flames with secondary (ambient) air, which have been studied by a number of investigators. The mechanism of stabilization of combustion waves supported on wires or rods, stabilization by eddies, and the concept of flame stretch are also briefly discussed.

## 12.1 FLAME STABILIZATION ON OPEN BURNERS

Since a laminar combustion wave propagates with a characteristic burning velocity $S_u$, a stationary flame may be obtained by moving the mixture, as in the case of a bunsen burner. The condition for getting a stable stationary flame is that at any point the velocity of the mixture should be equal to the burning velocity. The burning velocity depends upon a number of parameters, e.g., mixture composition, initial temperature, pressure, etc. The burning velocity near a solid surface is reduced due to the quenching effect. The velocity of the mixture depends upon the type of flow and the distance from the wall. For a premixed laminar flame, the flow velocity is very low near the walls and above the rim, but increases towards the centre of the burner giving an approximately parabolic profile.

The phenomenon of stability in a laminar flow can be best understood by the study of flame stabilization on a bunsen burner. Flame stability is



the first and foremost fundamental design requirement of any burner. The flame is always stabilized near a solid surface, near the rim in the case of a bunsen burner. At all other points, the flow velocity exceeds the burning velocity. If the flow velocity at every point near the rim exceeds the burning velocity, "blow-off" will occur, i.e., the flame will be carried away downstream. For a very rich mixture a lifted flame may be available. On the other hand, if the flow velocity is reduced to an extent where at any point the flow velocity is less than the burning velocity, "flashback" or "lightback" will occur, i.e., the flame will travel upstream into the burner. This flashback may cause a serious explosion if the flame travels up to the container which has a large volume of the premixed mixture.

## 12.2 CHARACTERISTIC STABILITY DIAGRAM

The characteristic stability diagram, as shown in Fig. 12.1, may be drawn for any fuel-oxidant mixture giving the limits of flashback, blow-off, and blow-out. In the diagram, the unshaded area under the curve ABC gives the zone of flashback. Points A and C correspond to the

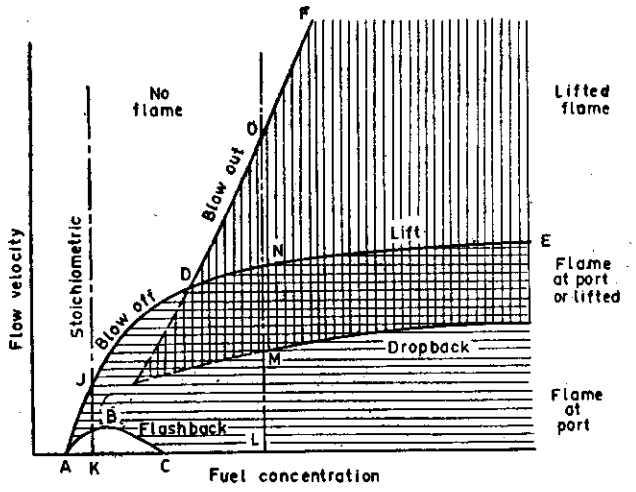


**Fig. 12.1 Characteristic stability diagram for open flames. [With permission of the Combustion Institute, from *Third Symposium (International) on Combustion*, 1949, p. 16.]**

lower and upper limits of flammability. After point C, a stable flame at the burner port is available because of the diffusion of air from the atmosphere. If we study the nature of flame at point K, which corresponds to the stoichiometric mixture, from point K to point B, the burning velocity exceeds the flow velocity, and hence flashback occurs. A stable

flame will be available at the burner port for flow velocities between points B and J. Above point J, the flow velocity exceeds the burning velocity and the blow-off of the flame occurs.

For rich mixtures, indicated by point L, a stable flame is obtained which may resemble a diffusion flame. At point N, the flame stabilizes at some distance above the burner port. This is because the rich mixture, due to mixing of ambient air, becomes less rich, resulting in an increased burning velocity, and because of expansion of the streamlines, the flow velocity is also slightly reduced. Such flames are referred to as lifted flames.

If the flow velocity is high, the streamlines, at a distance above the rim, break into a turbulent stream. The turbulent burning velocity is always much higher than the laminar burning velocity, therefore, a stable lifted flame is obtained where the laminar stream breaks into a turbulent one. If the flow velocity is further increased, blow-out will occur, say, at a point O. Between points M and N, the flame may occupy either a lifted position or may stabilize at the port. Point M corresponds to the flow velocity at which a lifted flame will return back to the burner port. In this range a lifted flame can also be brought to the burner port by a momentary interruption of the mixture flow. Limits M and N are quite well defined reproducible limits. The lift curve DNE is a continuation of the blow-off curve. It can be seen that the blow-out curve DOF is quite steep, indicating that the blow-out of a very rich mixture is difficult. For very rich mixtures, a stable flame either at the port, or in a lifted condition, will always be available. The dashed curve, between the points D and G, is a continuation of the blow-out curve. If the mixture composition is intermediate between D and G, the combustion wave may be removed from the stream by either blow-out or blow-off. If accomplished by blow-out, the gas velocity is raised above the drop back limits, and by a suitable manipulation a lifted flame is formed. The gas velocity is then increased to the blow-out limit. If accomplished by blow-off, care is taken that the combustion wave remains seated on the rim when the drop-back limit is exceeded, and the gas velocity is raised beyond the blow-out limit to the blow-off limit. With small burner tubes, point D of the diagram may be well within the region of laminar flow in the burner tube. In this case, the jet persists as a laminar stream to a considerable height above the rim before it breaks into a turbulent one and a lifted flame appears, sometimes, far above the rim.

## 12.3 MECHANISM OF FLAME STABILIZATION

The study of the mechanism of flame stabilization is important as it can predict the critical parameters for the blow-off and flashback of flames. Lewis and von Elbe[1] proposed the concept of boundary velocity



gradient. According to them, the stabilization of a flame at the burner rim is aerodynamic and depends on the existence of a region where the gas-flow balances the burning velocity. If the burning velocity decreases less rapidly than the gas velocity as the wall is approached, the flame will be stabilized. If the reverse is true, no balance is possible. This developed a relation between the critical boundary velocity gradient and the blow-off.

To understand the stability of a flame, consider a bunsen burner issuing a premixed combustible mixture such that the flow is laminar and of a poiseuille type. The gas velocity at the rim of the burner wall is zero, increasing to a maximum value at the centre. We assume that the streamlines are parallel to the axis of the tube and the gas velocity increases linearly, in the boundary layer near the wall, from zero to a particular value. We shall confine our observation to a very small region near the fringe of flame at the rim of the burner. The zone of observation is usually very small, about 1 to 2 mm.

Figure 12.2 shows a premixed fuel-air mixture flowing through a burner. Only a small portion near the tip of the burner is shown magnified, to give a clear idea about the shape and position of the wave profile. As stated earlier, the gas velocity profile is assumed to be linear. The

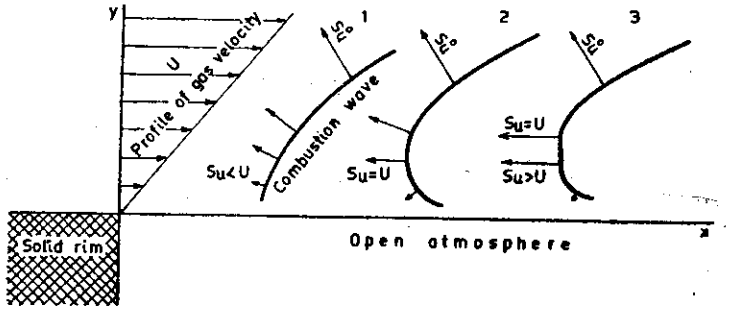


**Fig. 12.2 Stabilization of a combustion wave near the burner tip. The burning velocity is represented by vectors. (With permission of Academic Press, from B. Lewis and G. von Elbe : *Combustion, Flames and Explosions of Gases*.)**

vectors shown in the figure give the magnitude and direction of the gas velocity which is zero at the burner wall, and increasing with the increased distance from the wall. The profile shown is within the boundary layer. Three positions of the flame fringe are shown. The arrows on these fringes give the magnitude and direction of the burning velocity. As the wave front moves downwards, i.e., near the burner rim, the burning velocity is reduced due to the loss of heat and chain carriers. Similarly, as the distance from the rim increases, either in the vertical direction or towards the axis of the burner, the burning velocity increases.

Assuming that the gas velocity profile is the same at all the three flame front positions, we find at position 1, i.e., near the burner rim, the value of the burning velocity, $S_u$ at every point is less than that of the gas velocity. Therefore, the combustion wave will be driven back downstream by the gas flow. As the wave moves away from the burner rim, the burning velocity at different points increases. At position 2, the burning velocity at a point may become equal to the gas velocity. At all other points the gas velocity may exceed the burning velocity. If at any point the gas velocity equals the burning velocity, the wave will stabilize and stay at position 2. At position 3, i.e., further away from the rim, the buring velocity at any point exceeds the gas velocity, which will push the flame back to position 2. Thus, it is clear that there will be only one position where the wave front will stabilize. With the change of gas flow, the gas velocity profile will change. A reduction in gas velocity will bring the combustion wave closer to the rim, while an increase in gas velocity will push the wave front slightly away from the burner rim. For any stable flame, the gas velocity equals the burning velocity only at one point, at all other points the gas velocity exceeds the burning velocity. Therefore, the flame front is inclined against the direction of flow.

The actual shape of a flame may vary from burner to burner depending upon its design but the basic principle of stabilization remains the same. Unless the burner diameter is very small the gas velocity may be expressed by the equation

$$U = gy \qquad (12.1)$$

where $y$ is the distance from the stream boundary and $g$ is a constant known as the boundary velocity gradient. If the gas flow is reduced, $g$ decreases and the combustion wave shifts nearer to the solid rim of the burner. If we go on reducing the gas velocity, a condition will be reached when flashback occurs. At such a stage, the value of $g$ is called the critical boundary velocity gradient for flashback ($g_f$). Similarly, if the gas flow is increased, the combustion wave moves away. Again, at any instant, a position will come when blow off will occur. This value of $g$ is called the critical boundary velocity gradient for blow-off ($g_b$). It should be noted that as the distance of combustion wave from the burner increases, the burning velocity starts decreasing near the flame fringe due to the mixing of ambient air in a lean stoichiometric mixture. Thus, after some distance, the decrease in burning velocity due to dilution may exceed the increase in burning velocity due to the reducing loss of chain carriers.

As the combustion wave moves up, the flame fringe moves near the stream boundary. Figure 12.3(c) shows how the flame position shifts with the increasing flow. Three flame positions A, B, and C are shown. With increasing gas flow, the flame moves up and the fringe of the flame comes closer to the stream boundary. Figure 12.3 (b) shows the variation of



burning velocity with distance from the stream boundary for the three positions of the flame. Curves A, B and C in Figure 12.3 (b) show how,

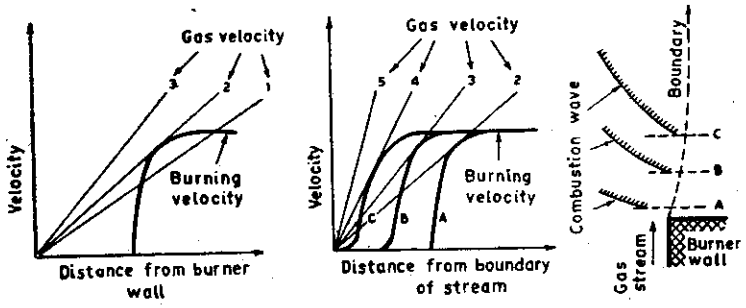


**Fig. 12.3 Illustration of burning velocity and critical boundary velocity gradient.**

for a particular position of the flame, the value of the burning velocity increases with increasing distance of the fringe from the stream boundary. It can be observed that the burning velocity for position A is zero up to certain distance because of the loss of heat and chain carriers. It then increases rapidly acquiring a constant maximum value. As the position of the flame moves up, the loss of heat and chain carriers reduces, thus bringing the flame near the stream boundary. Again, with the increasing height for a lean or stoichiometric mixture, the dilution of mixture by ambient air reduces the burning velocity near the stream boundary. Therefore, the burning velocity curve C may represent the limit of approach of the flame fringe towards the stream boundary. Similarly, curve A may represent the nearest point to which a stable flame can approach the burner. For the rich mixture, however, a lifted flame may occur instead of blow-off after position C. In Fig. 12.3 (a), the straight lines 1, 2, 3. etc. represent the value of gas velocity with respect to the distance from the burner wall. Thus, the slope of these lines gives the value of the boundary velocity gradient. With increasing gas flow, the gradient increases. Now, for any burning velocity curve between the limiting curves A and C, there will be a gas flow for which the straight line representing the velocity gradient is tangent to the burning velocity curve. Any line, such as 1, which has a gradient less than 2, will intersect the curve A. This means that for the gas velocity corresponding to 1, there is a region where the burning velocity exceeds the gas velocity resulting in flashback. On the other hand, any gas velocity greater than that corresponding to 4 will not intersect even the curve C. Thus, for such a flow everywhere, the gas velocity exceeds the burning velocity, resulting in blow-off. The critical boundary velocity gradients for flashback ($g_f$) and blow-off ($g_b$) are given by the slopes of the lines 2 and 4 respectively.

The critical boundary velocity gradient for an open tube burner can be calculated from the equation for frictional drag. For laminar flow the velocity distribution is given by Poiseuille's equation:-

$$U = n(R^2 - r^2)$$

where $R$ is the distance from the centre to the boundary of the stream, $r$ is the distance of any flow line from the stream centre and

$$n = (-\Delta p/l)/4\mu$$

in which $\Delta p$ is the pressure drop over the pipe length $l$, and $\mu$ is the viscosity of the gas. Differentiation of the Poiseuille's equation with respect to $r$ and setting $r = R$, the boundary velocity gradient is found to be $g = -2nR$. For a cylindrical tube, the volumetric flow rate

$$V = \int_0^R 2\pi\, Ur\, dr$$

Introducing the value of $U$ and integrating, we have

$$V = (\pi/2)\, nR^4$$

Combining the equation for $g$ and $V$, we have

$$g = \left(\frac{4}{\pi}\right)\frac{V}{R^3}$$

or

$$g = \frac{8\, U_{av}}{d_{tube}} \tag{12.2}$$

A general equation which holds for both laminar and turbulent flows is

$$g = \frac{f \rho\, U^2_{av}}{2\, \mu} = \frac{f\, U_{av}\, \mathrm{Re}}{2\, d_{tube}} \tag{12.3}$$

where $f$ is the friction factor from the empirical Fanning equation and is given by:

For laminar flow

$$f = \frac{16}{\mathrm{Re}} \tag{12.4}$$

For turbulent flow

$$f = \frac{0.046}{\mathrm{Re}^{0.2}} \tag{12.5}$$

For laminar flow through short circular ports and orifices

$$f = \frac{8.5}{\mathrm{Re}^{0.85}} \tag{12.6}$$

Similarly, the values of the friction factor for various shapes, e.g., long rectangular channel, long square channel, and long triangular channel are, respectively

$$f = \frac{40.2}{\mathrm{Re}^{1.27}} \tag{12.7}$$



$$f = \frac{1.89}{\mathrm{Re}^{1.11}} \tag{12.8}$$

$$f = \frac{29.8}{\mathrm{Re}^{1.29}} \tag{12.9}$$

No reliable equation is available for the transition region, i.e., for $2100 < \mathrm{Re} < 4000$. An arbitrary interpolation may be used for calculating the value in this range.

The blow-off data for open burner flames on tubes of different diameters are correlated by a single curve of critical boundary velocity gradient against fuel concentration for both laminar and turbulent flows. Ordinarily, flashback is not encountered in the case of turbulent flow, but it may occur with very fast burning mixtures such as hydrogen-oxygen flames in large size burners or at high pressures. The critical boundary velocity gradient for flashback ($g_f$) is always greater for turbulent flames than that for laminar flames of the same mixture. This is because of the reduced thickness of the laminar boundary layer at the wall within which stabilization occurs.

## 12.4 FLAME STRETCH THEORY

The boundary velocity gradient theory of Lewis and von Elbe gives good results and is in agreement with experimental values. However, it fails to explain a few experimental facts. For example, in some cases the dead space does not increase with an increase in gas flow, as it should before blow-off. Similarly, in some cases, the dead space changes without a change in the boundary velocity gradient. For blow-off of flames, dilution by the secondary air also plays a major role, but in the case of flames supported on an axially mounted wire, the dilution of flame near the stabilization zone does not take place. There are many such anomalies which are not explained by the boundary velocity gradient theory, though it may be again pointed out that the data obtained experimentally for blow-off of various sizes and shapes of the burner agree quite well with the theoretical explanation of the gradient theory.

Karlovitz[2] was the first to give the concept of flame stretch. While studying turbulent flames, he observed that flame propagation ceased in steep flow velocity gradients. He attributed this to the stretching of the flame front by shear flow. He observed that when a flame propagates in a velocity gradient, the flame becomes curved and presents a convex surface to the approaching unburned gas. For a uniform flow a flat flame surface will conduct some energy to the unburnt gas which is again convected back. Thus for such a case, the flame temperature will remain constant, near to the adiabatic flame temperature. For a flow field having a velocity gradient, a convex flame surface is formed, which will radiate and conduct some energy, but all this energy will not flow back to the surface from which it originated. This will result in the lowering of the flame tempera-

ture at the convex surface of the flame. This process of lowering of the flame temperature will continue and will lead to the extinction of the flame.

Figure 12.4 shows the flow field with a velocity gradient. Over a distance $y$, the gas velocity increases from $U_1$ to $U_2$. Now if we assume $S_u$ to be constant, the vector parallel to the flame front associated with $U_1$ will be much less than that with $U_2$, i.e., A will be much less than $B$. This increase in the flow component, parallel to the flame front, represents an energy flux, along the flame, away from the low velocity region. Thus, a part of the energy conducted to the preheat zone from the low velocity region is convected back to the high velocity region.

Karlovitz showed, analytically, the effect of flame stretch on the burning velocity. Consider a streamline, as shown in Fig. 12.5 with a velocity $U$. The two temperature surfaces $T_u$ and $T_i$ which are shown at a distance $\eta_0$. $T_u$ represents the unburnt surface and $T_I$ the reaction zone. Let the velocity vector $U$ intersect the $T_I$ surface at point A. The mass flow rate per unit area in the direction normal to $T_I$ surface at this point will be $\rho_u U \cos \alpha$. At a distance $\eta_0$ along the normal from the point A, the flow velocity would be $U + \frac{dU}{dy} \eta_0 \sin \alpha$, and the corresponding mass flow per unit area in the normal direction would be:

$$\rho_u \left(U + \frac{dU}{dy} \eta_0 \sin \alpha\right) \cos \alpha$$

The ratio of two mass flow rates is, therefore,

$$1 + \frac{dU}{dy} \frac{\eta_0}{U} \sin \alpha$$

In a flow which substantially exceeds the burning velocity, sin $\alpha$ is close to 1, so that the second term may be written as:

$$\frac{dU}{dy} \frac{\eta_0}{U} = K \tag{12.10}$$

This $K$ is a measure of the increase in area or stretching of the wave. This is called the "flame stretch factor" or "Karlovitz number". It is a dimensionless number, representing the degree of quenching, and is very useful in correlating the blow-off data pertaining to several combustible mixtures, including those inhibited by inert gases or inhibitors. Lewis and von Elbe[3] have shown that $\eta_0$ is a measure of the preheat zone thickness and can be calculated by the equation:

$$\eta_0 = \frac{K}{C_p \rho_u S_u} \tag{12.11}$$

According to the boundary velocity gradient theory, blow-off is a function of the boundary velocity gradient only. But according to the flame



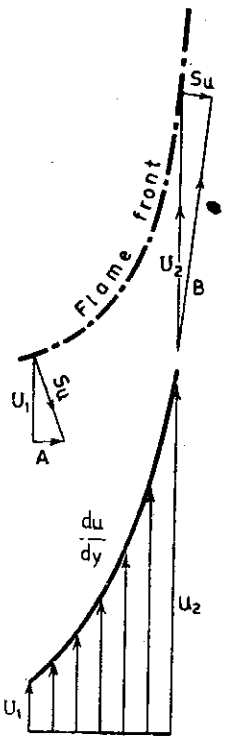


Fig. 12.4 Flame propagation in a velocity gradient. (With permission of the Institution of Gas Engineers, from the *Institution of Gas Engineers Journal*, March, 1978, p. 160.)

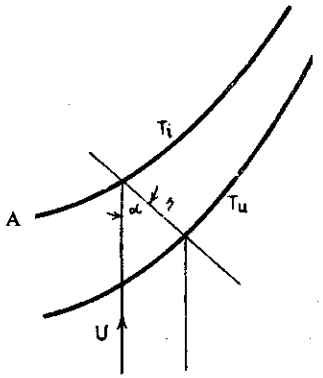


Fig. 12.5 Scheme of stretch of a combustion wave.

stretch theory, blow-off occurs because of aerodynamic quenching of the flame due to stretching, and is a function of the Karlovitz number. In other words, we may say that it depends upon the velocity gradient, preheat zone thickness, and local flow velocity. The degree of quenching is directly proportional to the velocity gradient $\frac{dU}{dy}$ and $\eta_0$, and inversely proportional to the local velocity $U$. As the value of $K$ increases, a point will come at which the reduction in the burning velocity will lead to a significantly thicker preheat zone, because the preheat zone thickness is inversely proportional to the burning velocity. The increased thickness accentuates the effect of the velocity gradient and so the thickness increases still further. Thus, once a critical value of $K$ is reached, an auto-accelerating process starts and a part of the flame is extinguished.

To test the validity of the flame stretch theory of blow-off, Reed[4] calculated the value of the Karlovitz number $K$ for a large number of

cases for which reliable data on blow-off flow rates, and corresponding burning velocities were available. We may write

$$K = \frac{\eta_0}{U}\frac{dU}{dy} = \frac{\eta_0}{S_u} g_b \tag{12.12}$$

because near the fringe where the flame is stabilized, the flame velocity equals the flow velocity i.e., $U = S_u$. Therefore, for blow-off, a Karlovitz similarity factor is written in the following form after substituting the value of $\eta_0$ from Eq. (12.11) in Eq. (12.12)

$$K = \frac{g_b K}{\rho_u C_p S_u^2} \tag{12.13}$$

Taking $g_b$ as the boundary velocity gradient at blow-off, the value of $K$ can be calculated.

Reed[4] argued that if the blow-off is due to excessive aerodynamic quenching or flame stretch, the Karlovitz number $K$ should be expected to have a constant value at the blow-off condition, irrespective of the change in fuel gas, the mixture composition, temperature, pressure, etc. As such, since $K = g_b\eta_0/S_u$, the plot of $g_b\eta_0$ against $S_u$ should give a straight line.

Figure 12.6 shows a plot between $g_b\ \eta_0$ versus $S_u$ on a logarithmic scale. The data are for mixture with only the primary reaction zone. The scatter of points is attributed by Reed to the variation in the value of $S_u$ reported by different workers A 20% error in $S_u$ may give an error of above 60% in the value of $K$. An expected straight line with a slope of unity, confirms that blow-off is due to excessive flame stretch. The equation of this straight line is written as:

$$0.23 = \frac{g_b\eta_0}{S_u} = \frac{g_b K}{\rho_u C_p S_u^2} \tag{12.14}$$

The value of $K = 0.23$ was obtained by Reed for various fuels such as methane, propane, natural gas, etc. But for fast burning mixtures, e.g., hydrogen-air, methane-oxygen, etc., a marked deviation was observed, which was attributed to the preferential diffusion of one component in the mixture, if the diffusion coefficient of the component in the mixture varies much from the other component. This result is also valid for flames which only have a primary reaction zone, e.g., flames of lean mixtures, or of rich mixtures burning in inert atmospheres.

Edmondson and Heap[5] confirmed Reed's observations for rich mixtures. They were unable to establish the flame stretch concept on cylindrical burner flames. But they obtained a constant value of $K$ in case of flames stabilized over very thin plates for mixture compositions up to 1.9 times the stoichiometric one. The value of $K$ obtained by them was $0.95 \pm 0.15$. They have tried to justify that the difference in their value of $K$, as compared to that of Reed, was due to the unreliable burning velocity data used by Reed. Though not fully established, the flame stretch concept gives better agreement between the theoretical and experimental



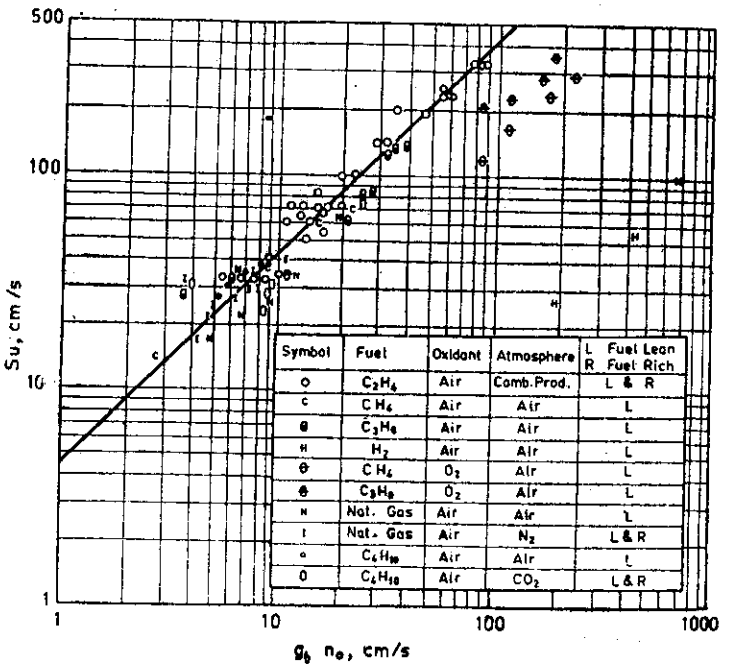


**Fig. 12.6 Correlation of blow-off data on a flame stretch basis. (With permission of the Institution of Gas Engineers, from the *Institution of Gas Engineers Journal*, March 1968, p. 168.)**

values for many cases of blow-off. It is expected that with a better understanding of parameters related to stability, the flame stretch concept will be established in the near future.

## 12.5 FLAMES SUPPORTED BY INSERTING A SOLID OBJECT IN A GAS STREAM

If a solid object is inserted in a combustible gas stream, the flow near the solid surface is retarded because of frictional drag. Thus a flame can be attached to this surface instead of the burner rim. For example, if a wire or rod is inserted axially along the axis of the burner, an inverted V-shaped flame will be obtained above the wire tip.

The mechanism of flame stabilization by a wire is shown in Fig. 12.7 (a) and 12.7 (b). Figure 12.7 (a) shows the stream flow along the wire. Just above the wire there is a region of zero flow. Three planes, A, B, and C give the possible positions of the flame. Figure 12.7 (b) shows that the burning velocity will be zero over a distance from the wire corresponding

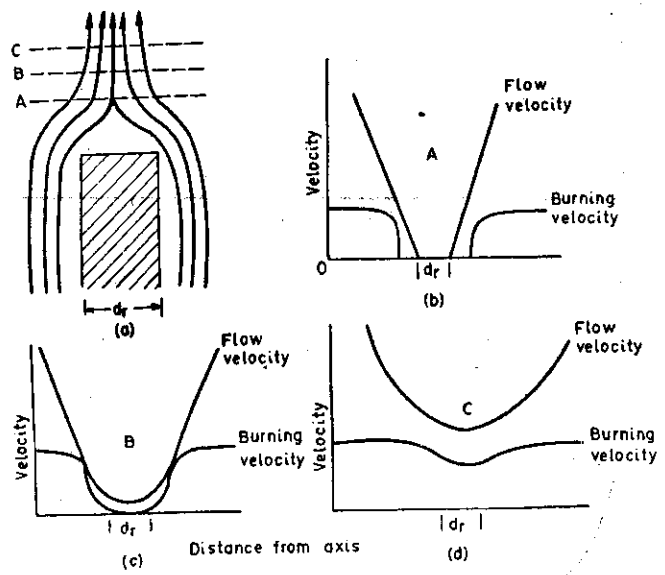


**Fig. 12.7 Stabilization of combustion wave by rod:**
**(a) Flow lines around rod. (c) Burning and flow velocity in plane B.**
**(b) Burning and flow velocity in plane A. (d) Burning and flow velocity in plane C.**
**(With permission of Academic Press from B. Lewis and G. von Elbe: *Combustion, Flames and Explosion of Cases*, 1951, p 246.)**

to the quenching distance, the gas velocity is zero at the wire surface and increases outwards. In this position, the burning velocity is lower than the gas velocity at all places, so the flame will be pushed downstream, i.e., upwards. On moving up, both the burning velocity and gas velocity increase. The burning velocity increases more rapidly than the gas velocity. Therefore, at a position B, the burning velocity curve meets the gas velocity and a point of tangency exists. Thus a stable flame is obtained at position B. Further up, the burning velocity increases to its maximum value because of the absence of the quenching effect. The velocity curve at position C is shown for a condition where the burning velocity has an almost constant maximum value and the gas flow is increased, so that the gas velocity exceeds the burning velocity at all places, thus blowing off the flame.

The quenching effect of the wire can be reduced by heating the wire. This will bring the flame slightly near the wire. For small diameter wires or rods, the critical boundary velocity gradient is found to be independent of the wire diameter. The blow-off of flames supported on such wire cannot be explained as simply as in the case of the open tube burner. For large diameter wires, a higher flow velocity and a higher boundary velocity gradient are needed for blow-off.



A flame can also be supported by inserting a wire ring concentrica lly at a considerable height above the burner port. The diameter of the ring is smaller than the inner diameter of the burner tube and it is thus placed within the undiluted mixture. By igniting this mixture above the ring a conical flame is stabilized at the ring as on an open burner tube. This is because near the ring the gas velocity is very small and a velocity gradient exists near the surface. The flame cannot be made to travel upstream because at all places below the ring, the gas velocity exceeds the burning velocity. Similarly, a flame can be supported on a wire gauze as in the Meker burner.

## 12.6 FLAME STABILIZATION BY EDDIES

The mechanism of flame stabilization proposed by Lewis and von Elbe is reasonable for the burner as well as for supported flames. However, some of the characteristics of supported flames are not so well described. According to the theory, supported flames do not always blow off. It has been found that a small residual flame often remains in the wake of the

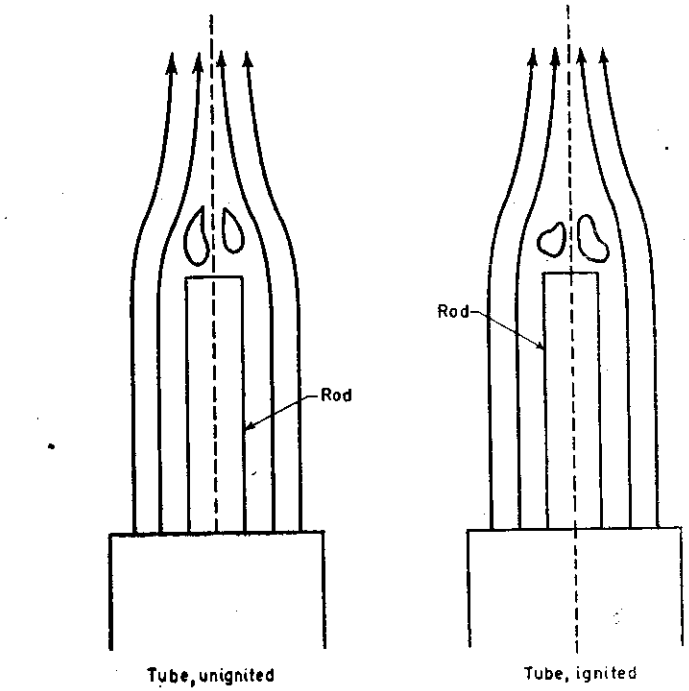


**Fig. 12.8 Stabilization by eddies. (With permission of Academic Press from B. Lewis and G. von Elbe: *Combustion, Flames and Explosion Gases*, 1951, p. 269.)**

support. The velocity gradient in this region is not linear and eddies are formed just after the support as shown in Fig. 12.8. The eddies are apparently stabilized by the flame, as for a given flow, the eddy is smaller in size with a flame than without. These eddies provide a constant source of ignition to stabilize the flame, and, therefore, act as a source of heat and active radicals. The blow-off of the flame is governed by the nature of the eddies and the flow around them, as the equilibrium is set up between heat production in the eddies, heat transfer to the surrounding flow, and ignition requirements.

## 12.7 QUENCHING DISTANCE, PENETRATION DISTANCE AND DEAD SPACE

Flame stabilization depends upon quenching near a solid surface. But the quenching of a flame is independent of the nature of the solid surface because of its high heat capacity as compared to that of the gases. However, quenching depends upon the burner diameter, pressure, and composition of the mixture. For a particular pressure and mixture composition, the flame cannot be supported on a burner below a certain diameter. This diameter is known as the "quenching diameter". The quenching diameter is approximately proportional to the reciprocal of the pressure. The flow velocity limits for flashback and blow-off coincide when quenching occurs. If, instead of a circular burner, the flame is passed between two parallel plates, the distance below which the flashback does not occur for a particular mixture is called the "quenching distance". The quenching distance is not equal to, but is smaller than, the quenching diameter.

The quenching property of a solid surface is quite important and is used in the design of flame traps. The flame trap is nothing but a fine wire gauze which has mesh width less than the quenching distance. The miner's safety lamp is another example of the utilization of the quenching effect.

Another quantity which indicates the quenching effect is the depth of penetration or the penetration distance $d_p$, and is defined as:

$$d_p = \frac{S_u}{g} \tag{12.15}$$

i.e., the ratio of the fundamental burning velocity to the critical boundary velocity gradient. Since, near the boundary

$$U = gy$$

$$\therefore \quad d_p = \frac{S_u \cdot y}{U} \tag{12.16}$$

or we may define the penetration distance as the distance at which the gas velocity equals the fundamental burning velocity $S_u'$. At a distance less than $d_p$, the value of burning velocity $S_u'$ will be less than $S_u$ indicating that the effect of quenching is present.



Another term used quite commonly is the dead space, defined as that distance above the burner rim or near the wall where the quenching is complete and the luminous zone assumes a position parallel to the gas flow lines. Figure 12.9 shows the difference between the penetration

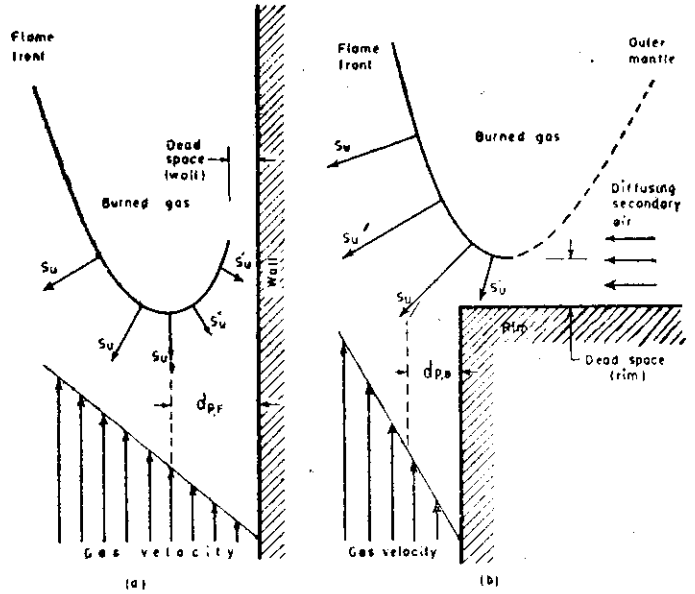


**Fig. 12.9 Penetration distance and dead space.** (With permission of the American Chemical Society from *Industrial and Engineering Chemistry*, 1955, 47: (1) 110.)

distance and the dead space near a vertical wall and above the burner rim.

The quenching distance, dead space, and penetration distance are reduced with an increase in the burning velocity. Therefore, quenching a flame with high burning velocity is more difficult than for a slow burning flame.

### REFERENCES

1. B. Lewis, and G. von Elbe, *J. Chem. Phys.* 1943, 11: 75, *Trans. Am. Soc. Mech. Engrs*, 1948, 70: 307.
2. B. Karlovitz, D.W. Denniston, Jr., D.H. Knapschaefer, and F.E. Wells, *Fourth Symposium (International) on Combustion*, Williams and Wilkins, Baltimore, 1953, p. 613.
3. B. Lewis, and G. von Elbe, *Combustion, Flames and Explosions of Gases*, Academic Press, New York, 1961, p. 226.
4. S.B. Reed, *Inst. of Gas Engrs. J.*, 1968, p. 162.
5. H. Edmondson, and M.P. Heap, *Combustion and Flame*, 1970, 15: (2), 179-187.